

Supporting Information

Diversifying fluoroalkanes: light-driven fluoroalkyl transfer via vinylboronate esters

*Kaushik Chakrabarti,^{#a} Chandana Sunil,^{#a} Benjamin M. Farris,^a Simon Berritt,^b Kyle Cassaidy,^c Jisun Lee^b and Nathaniel K. Szymczak^{*a}*

^a*Department of Chemistry, University of Michigan, 930 N. University, Ann Arbor, Michigan 48109, United States*

^b*Medicine Design, Pfizer Inc., Eastern Point Rd., Groton, CT. 06340 (USA)*

^c*Chemical Research and Development, Pfizer Inc., Eastern Point Rd., Groton, CT. 06340 (USA)*

Table of Contents

A) General considerations.....	3
B) Procedure for the synthesis of [RBPIn-CF ₂ Ph] ⁻ adducts.....	3
C) Experimental procedures	9
D) Optimization tables	10
E) Representative calculations for the conversion of a reaction	13
F) Procedure for the control experiments	15
G) Procedure for estrone derivative synthesis	19
H) Procedure for derivatization reaction using KHF ₂	20
I) List of unreactive substrates.....	20
J) Characterization data of compounds	21
K) Computational Details	28
L) Quantum Yield Measurement.....	32
M) Tolerance test to common functional groups.....	34
N) Spectroscopic data of the products	34
O) References.....	78

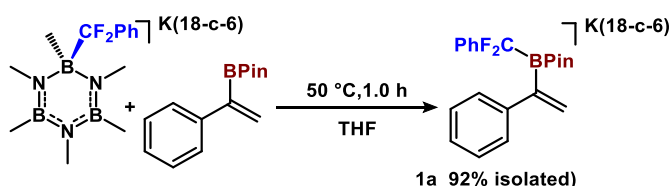
A) General considerations

Hexamethylborazine- CF_2Ph ; $[\text{Me}_6\text{B}_3\text{N}_3\text{CF}_2\text{Ph}]\text{K}(18\text{-c-}6)^1$, hexamethylborazine- CF_2H ; $[\text{Me}_6\text{B}_3\text{N}_3\text{CF}_2\text{H}]\text{K}(18\text{-c-}6)^2$ and Hexamethylborazine- CF_3 ; $[\text{Me}_6\text{B}_3\text{N}_3\text{CF}_3]\text{K}(18\text{-c-}6)^3$ were synthesized using previously described methods. THF, pentane, dimethoxyethane (DME), acetonitrile and benzene were purified using a Glass Contour solvent purification system through percolation through a Cu catalyst, molecular sieves, and alumina and finally stored over activated molecular sieves for a minimum of 48 hours. (Trifluoromethoxy)benzene $[\text{PhOCF}_3]$ and liquid difluoromethyl arenes (ArCF_2H) were dried over calcium hydride, distilled, and freeze-pump-thawed. Toluene was dried over sodium metal, then distilled, and freeze-pump-thawed. Methanol was dried over calcium hydride and then distilled and freeze-pump-thawed. All other reagents were used from commercial sources without further purification. Unless otherwise noted, all manipulations were performed under an inert nitrogen atmosphere.

NMR spectra were recorded on Varian Vnmrs 500, Varian MR400 and Bruker Advance Neo 500 spectrometer. ^1H , ^{13}C , ^{11}B and ^{19}F shifts are reported in parts per million (ppm) relative to TMS, with the residual solvent peak used as an internal reference. ^{19}F NMR spectra are referenced to (trifluoromethoxy)benzene or, in spectra lacking internal standard, on a unified scale, where the single primary reference is the frequency of the residual solvent peak in the ^1H NMR spectrum. Peaks not listed in the peak assignment correspond to residual solvent. Multiplicities are reported as follows: singlet (s), doublet (d), triplet (t), double triplet (dt), triple doublet (td), quartet (q), pentet (p), septet (sp), and multiplet (m). Carbon atoms attached to boron are not observed due to quadrupolar relaxation. Linear prediction (LP) was applied for processing the ^{11}B NMR spectra in the mestrenova software for minimizing the borosilicate glass peak. Mass spectra were obtained on an electrospray a Micromass AutoSpec Ultima Magnetic Sector Mass Spectrometer electron ionization mass spectrometer, Shimadzu QP-2010 GCMS, Agilent 1290 Infinity II UPLC with Agilent 6230 LC/TOF for ESI or an Agilent GC 8860 with an Agilent mass spectrometer 5977B GC/MSD. UV-vis absorbance measurements were performed using a Cary 50 Bio spectrophotometer. The standard photochemical procedure utilizes a 440 nm LED lamp available from Kessil (PR160-440nm; https://www.kessil.com/products/science_PR160L.php). Alternative wavelengths tested were chosen from the remaining Kessil PR160 series. Safety hazards of irradiation with Kessil lamps: Blue light (400nm to 500nm are particularly high-energy visible light) exposure can cause photochemical reactions in the eye's tissues, especially the retina, lens, and cornea, which can lead to temporary or permanent damage. A UVEX safety eye glass is essential for working with Kessil lamps. In addition to this the reaction area was covered with safety shields coated with UV protected glass material. The Kessil lamps were kept 4 cm apart from the reaction vials for optimum and reproducible reactivity.

B) Procedure for the synthesis of $[\text{RBPin-CF}_2\text{Ph}]^-$ adducts

1) Synthesis of 1a:



In a 20 mL vial, [K(18-c-6)(B₃N₃Me₆-CF₂Ph)] (200 mg, 0.34 mmol) and vinyl-BPin (77.3 mg, 0.34 mmol) were mixed with 5 mL THF and heated for 1.0 h at 50 °C and the conversion was assessed by ¹⁹F NMR (PhOCF₃ was added as internal standard). The THF was removed in vacuo, and the residue was washed with pentane (3 x 6 mL) to afford the title compound **1a** as an off-white solid (92%, 206 mg). ¹H NMR (600 MHz, THF-d₈, ppm) δ 7.41 (d, *J* = 6.9 Hz, 2H), 7.28 (d, *J* = 7.4 Hz, 2H), 6.97-6.91 (m, 3H), 6.86 (t, *J* = 7.5 Hz, 2H), 6.76 (t, *J* = 7.3 Hz, 1H), 5.15 (d, *J* = 6.1 Hz, 1H), 4.94 (d, *J* = 6.0 Hz, 1H), 3.57 (s, 24H), 1.09 (s, 6H), 1.05 (s, 6H). ¹³C NMR (125 MHz, CDCl₃, ppm) δ 150.98, 144.62 (t, *J*_{C-F} = 22.5 Hz), 127.80, 126.39 (t, *J*_{C-F} = 8.8 Hz), 125.67, 125.39, 125.03 (t, *J*_{C-F} = 2.5 Hz), 122.54, 116.61, 77.78, 69.82, 26.59, 26.41. ¹⁹F NMR (564 MHz, THF-d₈, ppm) δ -105.88 (s, 2F). ¹¹B NMR (192 MHz, CDCl₃, ppm) δ 3.90 (bs, 1B). ESI-MS: calcd for C₂₁H₂₄BF₂O₂ (M-K(18-c-6)): 357.1837, found: 357.2065.

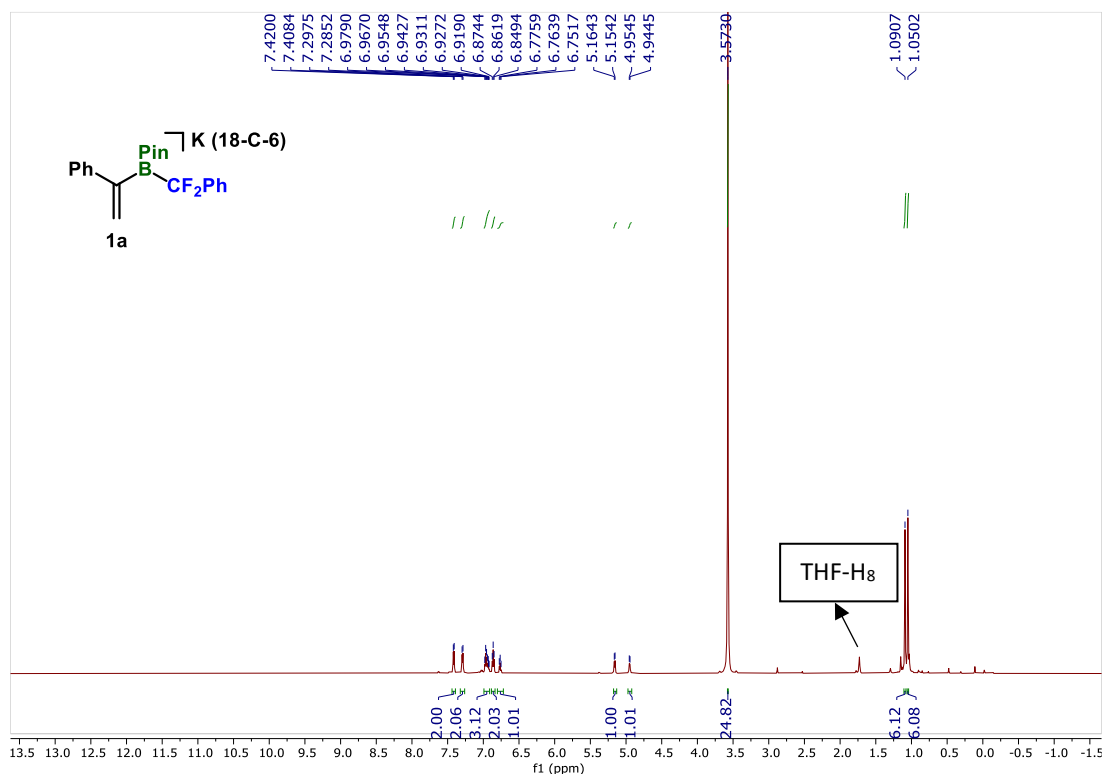


Fig. S1. ¹H NMR spectrum (CDCl₃, 25 °C) of **1a**.

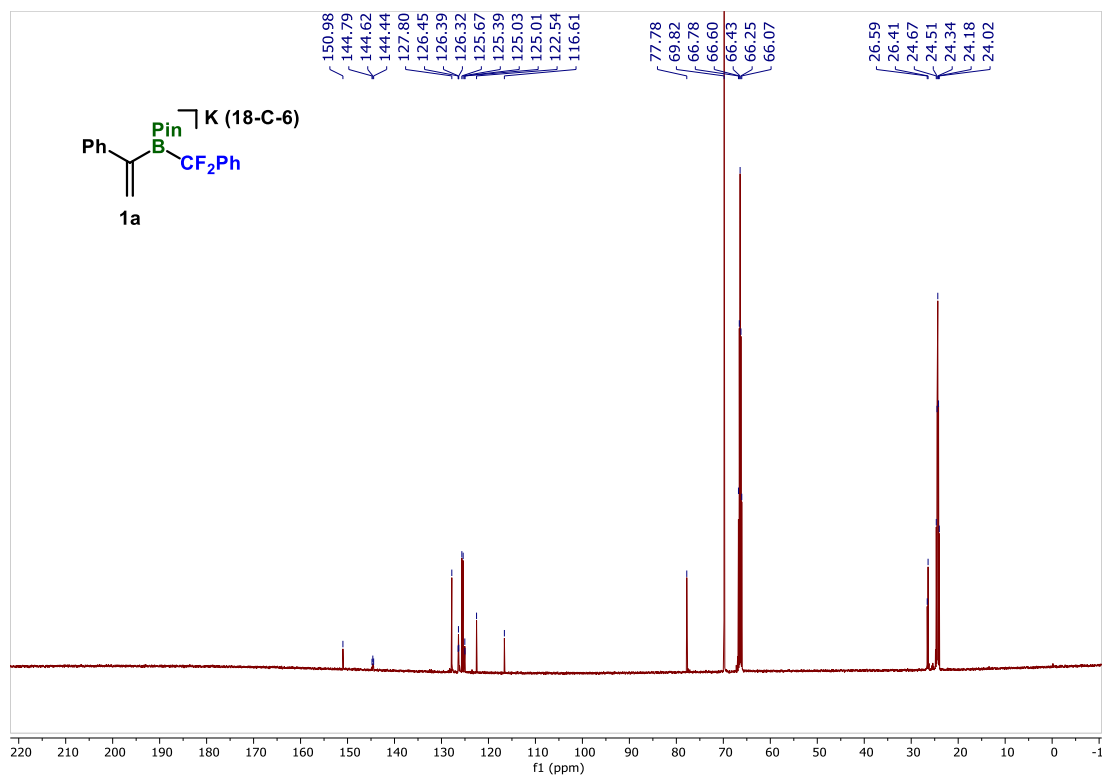


Fig. S2. ¹³C NMR spectrum (CDCl₃, 25 °C) of **1a**.

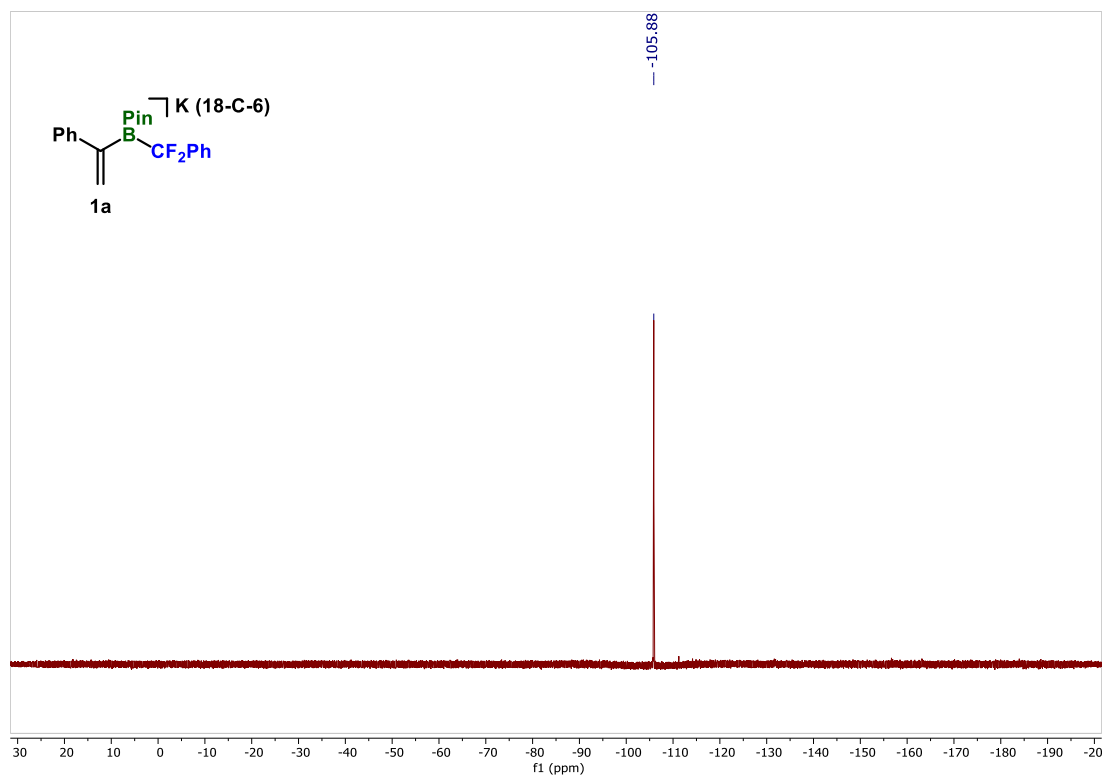


Fig. S3. ¹⁹F NMR spectrum (CDCl₃, 25 °C) of **1a**.

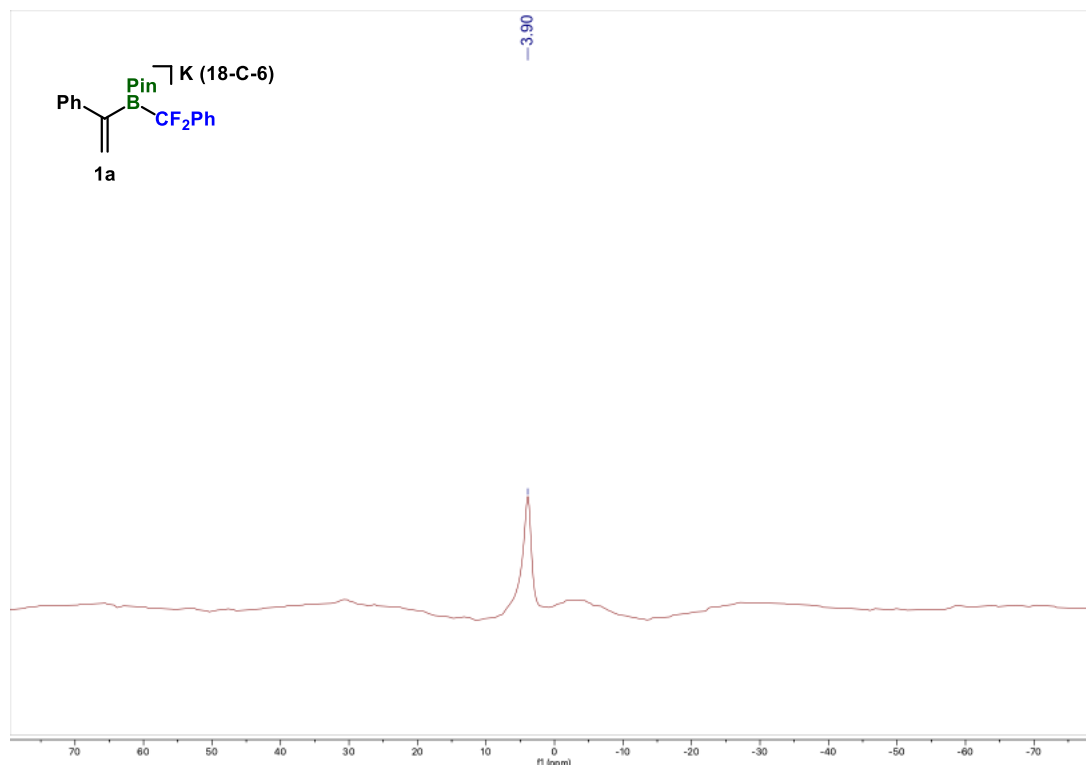
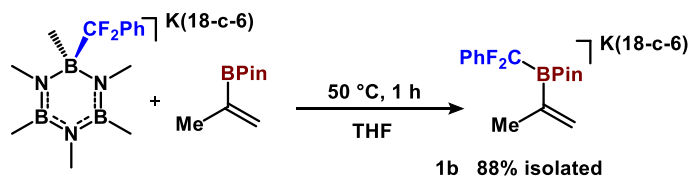


Fig. S4. ^{11}B NMR spectrum (CDCl_3 , 25 °C) of **1a**.

2) Synthesis of **1b**:



In a 20 mL vial, $[\text{K}(18\text{-c-}6)(\text{B}_3\text{N}_3\text{Me}_6\text{-CF}_2\text{Ph})]$ (200 mg, 0.34 mmol) and (1,4-Dioxa-spiro[4,5]dec-7-en-8-boronic acid, pinacol ester) (63.2 μL , 0.34 mmol) were mixed with 5 mL THF and heated for 1.0 h at 50 °C and the conversion was assessed by ^{19}F NMR spectroscopy (PhOCF_3 was added as internal standard). The THF was removed, and the residue was washed with pentane (3 x 6 mL) to afford **1b** as an off-white solid (88%, 203 mg). ^1H NMR (600 MHz, THF-d_8 , ppm) δ 7.47 (d, $J = 7.6$ Hz, 2H), 7.08 (t, $J = 7.6$ Hz, 2H), 7.02 (t, $J = 7.4$ Hz, 1H), 4.67 (d, $J = 6.2$ Hz, 1H), 4.60 (d, $J = 5.3$ Hz, 1H), 3.63 (s, 24H), 1.46 (s, 3H), 1.06 (s, 6H), 0.98 (s, 6H). ^{13}C NMR (125 MHz, THF-d_8 , ppm) δ 144.55 (t, $J_{\text{C-F}} = 21.3$ Hz), 126.34 (t, $J_{\text{C-F}} = 7.5$ Hz), 125.65, 125.31 (t, $J_{\text{C-F}} = 1.3$ Hz), 112.04, 77.55, 69.70, 26.44, 26.36. ^{19}F NMR (564 MHz, THF-d_8 , ppm) δ -106.67 (s, 2F). ^{11}B NMR (192 MHz, THF-d_8 , ppm) δ 3.70 (bs, 1B). ESI-MS: calcd for $\text{C}_{16}\text{H}_{22}\text{BF}_2\text{O}_2$ (M-K(18-c-6)): 295.1681, found: 295.1767.

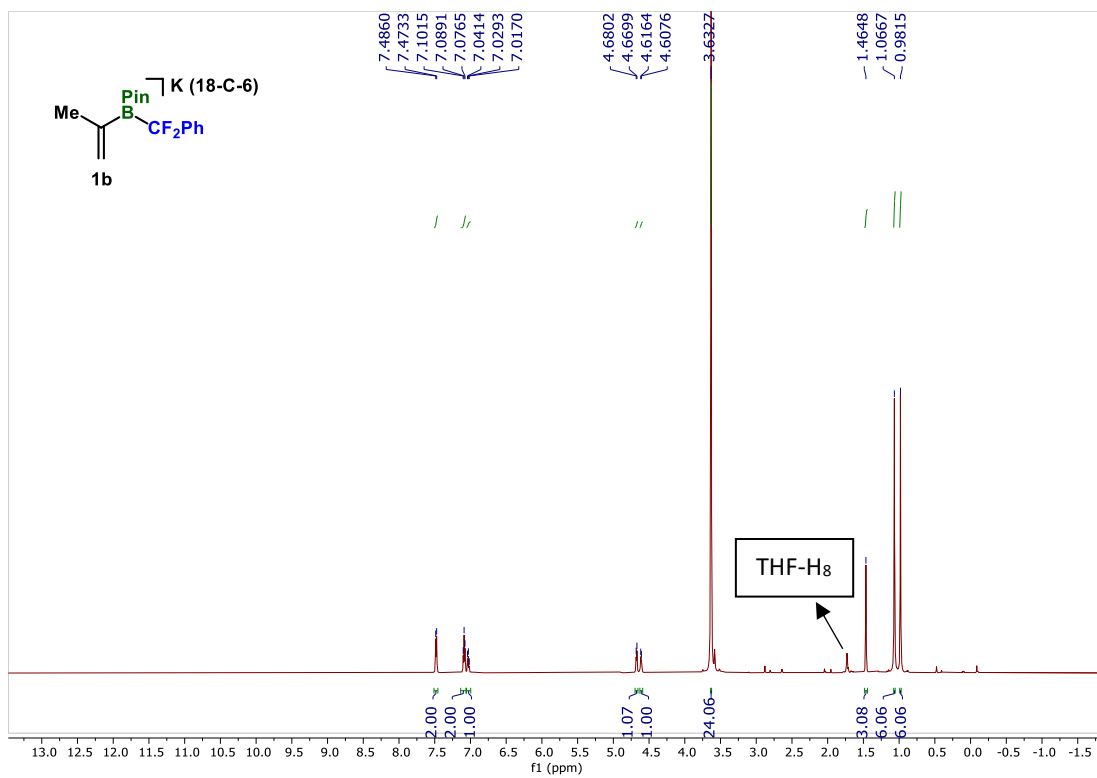


Fig. S5. ¹H NMR spectrum (THF-d₈, 25 °C) of **1b**.

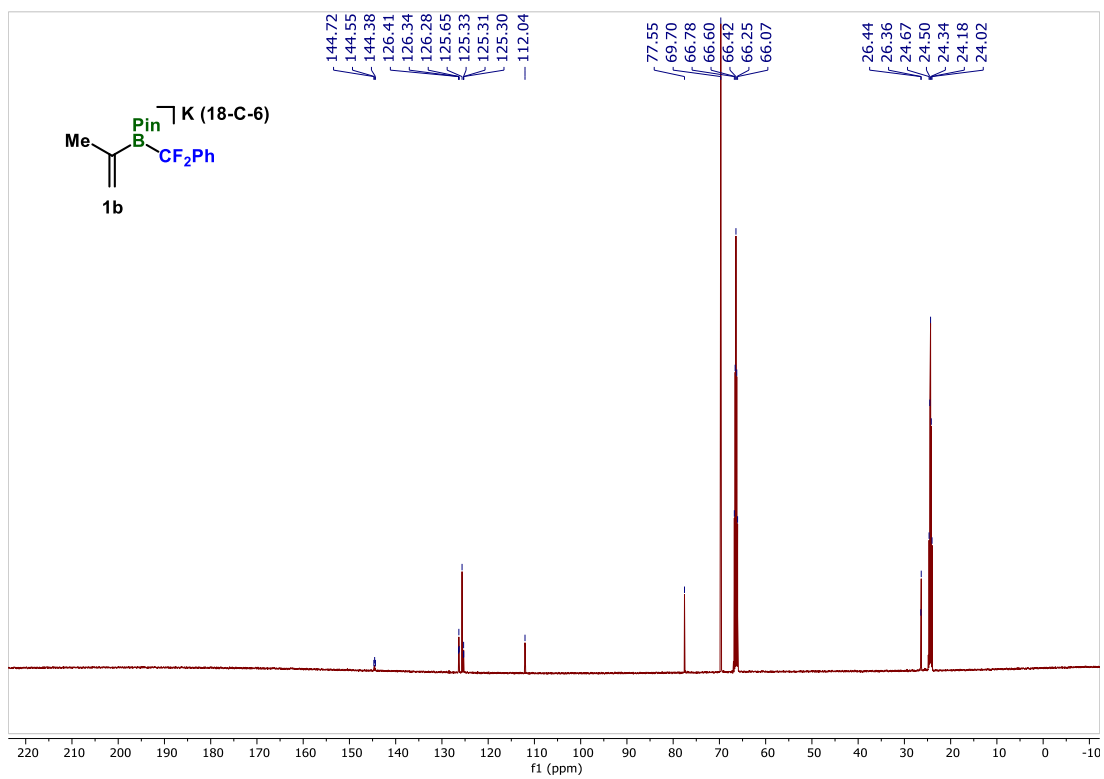


Fig. S6. ¹³C NMR spectrum (THF-d₈, 25 °C) of **1b**.

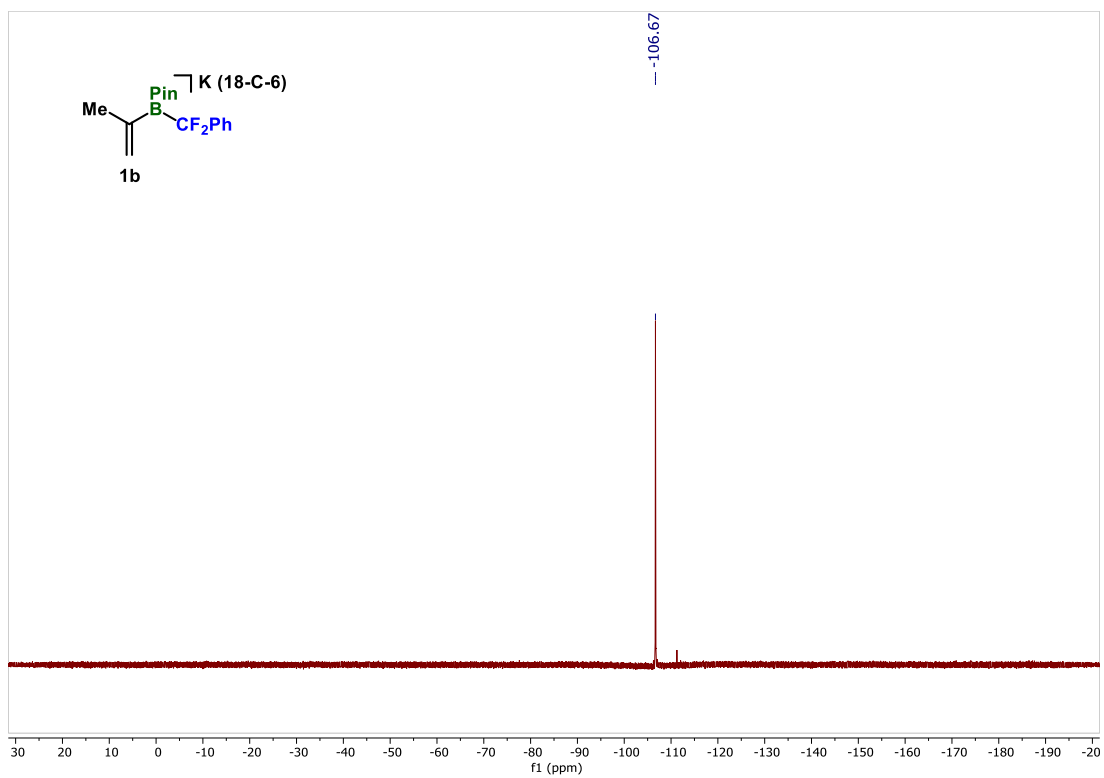


Fig. S7. ¹⁹F NMR spectrum (THF-d₈, 25 °C) of **1b**.

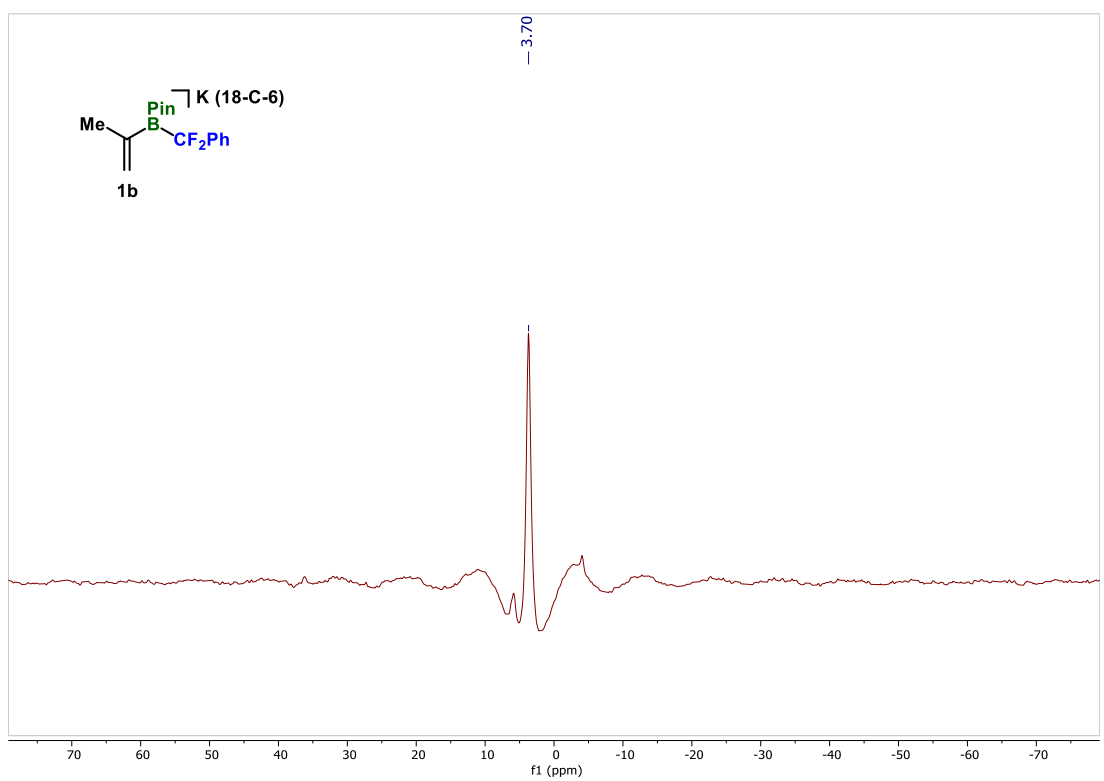
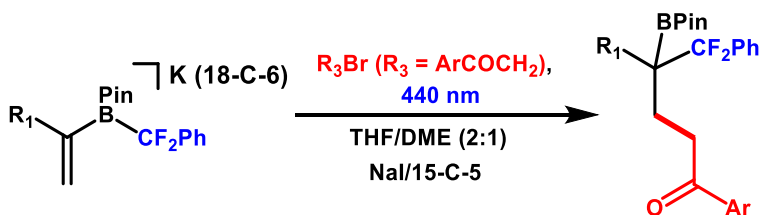


Fig. S8. ¹¹B NMR spectrum (THF-d₈, 25 °C) of **1b**.

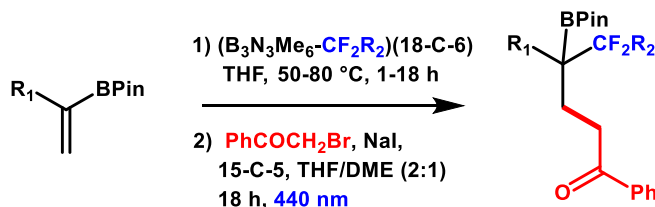
C) Experimental procedures

1) Procedure I: Photochemical reactivity of vinyl pinacol boronate ester derivatives with alkyl bromides.



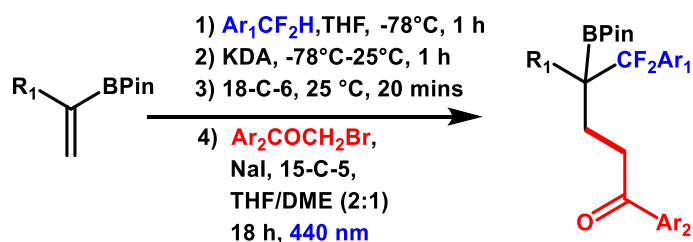
Vinyl pinacol boronate ester ($[\text{R}_1\text{BPin-CF}_2\text{Ph}][\text{K}(18\text{-C-}6)]$ ($\text{R}_1 = \text{Ar}$, alkyl, H)) (0.1 mmol, 1.0 equiv.), NaI (0.05 mmol, 0.5 equiv.) and 15-C-5 (0.05 mmol, 0.5 equiv.) were dissolved in 1.6 mL of THF in a 8 mL vial. To the suspension, a solution of the alkyl halide R_3X (0.15 mmol, 1.5 equiv.) in DME (0.8 mL) was added under irradiation, and the mixture was stirred vigorously overnight under constant irradiation (18 h) before the yield was assessed by ^{19}F NMR spectroscopy (PhOCF_3 used as internal standard). The reaction mixture was diluted with EtOAc (20 mL) and the solution washed with ice-water (2 x 10 mL) and with brine (20 mL). The resulting organic phase was dried over Na_2SO_4 , filtered and concentrated *in vacuo*. The product was purified by column chromatography using hexane-ethyl acetate as eluent.

2) Procedure II: One-pot Photochemical reaction from $[\text{Me}_6\text{B}_3\text{N}_3\text{CF}_2\text{R}_1]\text{K}(18\text{-c-}6)$ and vinyl-BPin derivatives.



$[\text{Me}_6\text{B}_3\text{N}_3\text{CF}_2\text{R}_2]\text{K}(18\text{-c-}6)$ (0.15 mmol, 1.0 equiv.) and vinyl pinacol boronic ester (0.15 mmol, 1.0 equiv.) were dissolved in 2.0 mL of THF in a 20 mL vial/screw cap tube. The reaction mixture was heated for specified time and temperature (depending upon R_2 group, $\text{R}_2 = \text{Ph}$ and CF_3 , 1 h at 50 °C and $\text{R}_2 = \text{H}$, 20 h at 80 °C). Then, NaI (0.075 mmol, 0.5 equiv.) and 15-C-5 (0.075 mmol, 0.5 equiv.) were added. To the suspension, a solution of the alkyl halide R_3X (0.23 mmol, 1.5 equiv.) in DME (1.0 mL) was added under irradiation, and the mixture was stirred vigorously overnight under constant irradiation (18 h) before the yield was assessed by ^{19}F NMR spectroscopy (PhOCF_3 used as internal standard). The reaction mixture was diluted with EtOAc (20 mL) and the solution washed with ice-water (2 x 10 mL) and brine (20 mL). The resulting organic phase was dried over Na_2SO_4 , filtered and concentrated *in vacuo*. The product was purified by column chromatography using hexane-ethyl acetate as eluent.

3) Procedure III: One-pot Photochemical reaction from vinyl-BPin derivatives and difluoromethyl arenes.



Vinyl-BPin derivatives (0.15 mmol, 1.0 equiv.) and difluoromethyl arenes (ArCF_2H) (0.15 mmol, 1.0 equiv.) were dissolved in 2.0 mL THF in a 20 mL vial and cooled to -78°C . $\text{KN}(\text{iPr})_2$ (0.23 mmol, 1.5 equiv.) was added as a solid to the mixture at -78°C . The mixture was rapidly stirred at -78°C for 10 minutes and allowed to warm to 25°C . The mixture was stirred at 25°C for 20 minutes, then 18-crown-6 (0.15 mmol) was added. NaI (0.075 mmol, 0.5 equiv.) and 15-C-5 (0.075 mmol, 0.5 equiv.) were added, affording a suspension. To the suspension, a solution of the alkyl halide $\text{Ar}_2\text{COCH}_2\text{Br}$ (0.23 mmol, 1.5 equiv.) in DME (1.0 mL) was added under irradiation, and the mixture was stirred vigorously overnight under constant irradiation (18 h) before the yield was assessed by ^{19}F NMR spectroscopy (PhOCF_3 used as internal standard). The reaction mixture was diluted with EtOAc (20 mL) and the solution washed with ice-water (2 x 10 mL) and brine (20 mL). The resulting organic phase was dried over Na_2SO_4 , filtered and concentrated *in vacuo*. The product was purified by column chromatography using hexane-ethyl acetate as eluent.

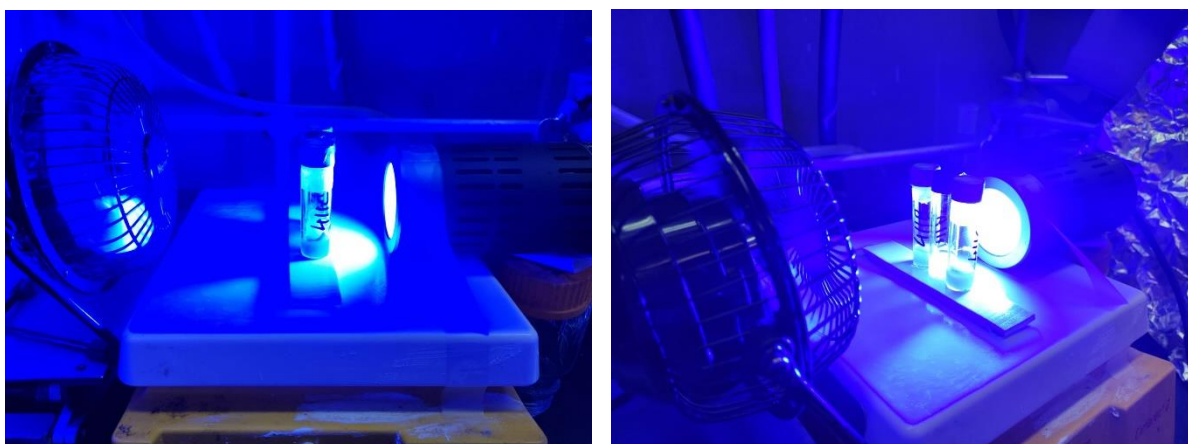
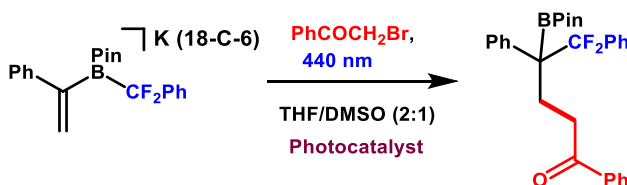


Figure S9: Reaction setup in Kessil LED Lights.

D) Optimization tables

Table S1. Optimization of photocatalyst/activator.

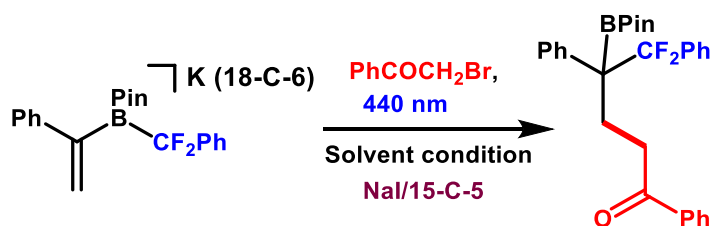


Entry	Photocatalyst	Conversion
-------	---------------	------------

1	Ru(bpy) ₃ Cl ₂ ·6H ₂ O (1 mol%)	38%
2	Ru(bpy) ₃ Cl ₂ ·6H ₂ O (1 mol%)	0% (only THF as solvent)
3	NaI (50 mol%)	53%
4	NaI (150 mol%)	36%
5	NaI (50 mol%)/PPh ₃ (50 mol%)	38%
6	NaI (50 mol%)	56% (4:1:1, THF/DMSO/DMI)
7	NaI (100 mol%)	43% (4:1:1, THF/DMSO/DMI)
8	NaI (20 mol%)	32% (4:1:1, THF/DMSO/DMI)
9	No Catalyst	35%

Vinylboronate ester (0.023 mmol), PhCOCH₂Br (0.035 mmol), THF/DMSO (1.2 mL), 18 h, 28 °C, 440 nm blue light. ¹⁹F NMR yields are reported (PhOCF₃ used as internal standard). DMI = 1,3-Dimethyl-2-imidazolidinone.

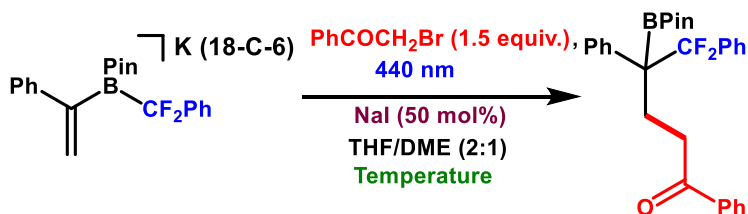
Table S2. Optimization of solvent.



Entry	Solvent	Conversion
1	2:1, THF/DMSO	53%
2	DMSO	30%
3	THF	0%
4	1:1, DMSO/DMI	30%
5	2:1, THF/DME	63%
6	2:1, THF/CH ₃ CN	63%
7	2:1, THF/DMF	58%
8	2:1, THF/DME	70% (50 mol% 15-C-5, as additive)
9	1:1, THF/DME	66% (50 mol% 15-C-5, as additive)
10	DME	64% (50 mol% 15-C-5, as additive)
11	2:1, Dioxane/DME	34% (50 mol% 15-C-5, as additive)
12	2:1, THF/DME (50 °C)	48% (50 mol% 15-C-5, as additive)
13	10:1, THF/DME	40% (50 mol% 15-C-5, as additive)
14	10:1, DME/THF	66% (50 mol% 15-C-5, as additive)
15	2:1, THF/DME (10 h)	55% (50 mol% 15-C-5, as additive)
16 ^a	2:1, THF/DME	0%
17 ^b	2:1, THF/DME	70%
18 ^c	2:1, THF/DME	53%
19 ^d	2:1, THF/DME	0%

Vinylboronate ester (0.023 mmol), PhCOCH₂Br (0.035 mmol), NaI (0.0115 mmol), 15-C-5 (0.0115 mmol), solvent (1.2 mL), 18 h, 28 °C, 440 nm blue light. ¹⁹F NMR yields are reported (PhOCF₃ used as internal standard). ^aStirred in dark condition for 3 days. ^b2 Equivalent PhCOCH₂Br was added. ^c1 Equivalent PhCOCH₂Br was added. ^dHeating at 80 °C in dark.

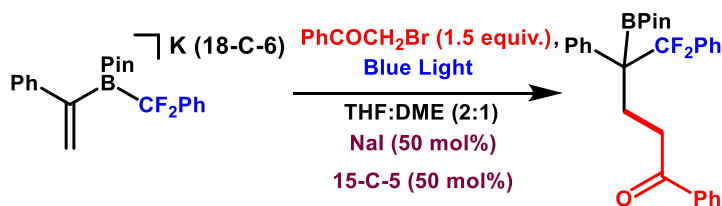
Table S3. Optimization of temperature.



Entry	Temperature	Conversion
1	50 °C	48%
2	28 °C	69%-72%
3	35 °C	70-71%
4	15 °C	68%

Vinylboronate ester (0.023 mmol), PhCOCH₂Br (0.035 mmol), NaI (0.0115 mmol), 15-C-5 (0.0115 mmol), THF+DME (1.2 mL), 18 h, temperature, 440 nm blue light. ¹⁹F NMR yields are reported (PhOCF₃ used as internal standard).

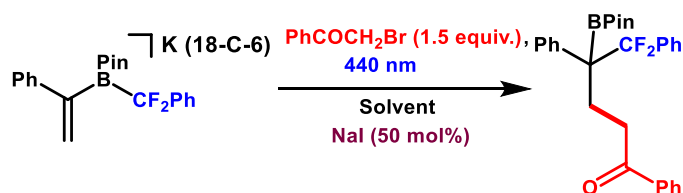
Table S4. Optimization of light source.



Entry	Light (nm)	Conversion	
1	390	THF:DME	53%
		THF:CH ₃ CN	57%
2	427	THF:DME	68%
		THF:CH ₃ CN	60%
3	440	THF:DME	70%
		THF:CH ₃ CN	61%
4	456	THF:DME	56%
		THF:CH ₃ CN	62%

Vinylboronate ester (0.023 mmol), PhCOCH₂Br (0.035 mmol), NaI (0.0115 mmol), 15-C-5 (0.0115 mmol), THF+DME (1.2 mL), 18 h, 28 °C, 440 nm blue light. ¹⁹F NMR yields are reported (PhOCF₃ used as internal standard).

Table S5. Optimization of distance of light source.



a) 4 cm distance:

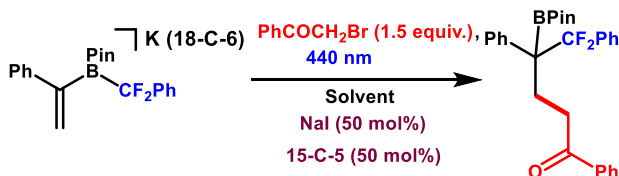
Entry	Solvent	Conversion
1	2:1, THF/DME	63%
2	2:1, THF/DMSO	53%

b) 6 cm distance:

Entry	Solvent	Conversion
1	2:1, THF/DME	50%
2	2:1, THF/DMSO	44%

Vinylboronate ester (0.023 mmol), PhCOCH₂Br (0.035 mmol), THF+DME (1.2 mL), 18 h, 28 °C, 440 nm blue light. ¹⁹F NMR yields are reported (PhOCF₃ used as internal standard).

c) 2 cm distance:



Entry	Solvent	Conversion
1	2:1, THF/DME	68%
2	2:1, THF/CH ₃ CN	53%

Vinylboronate ester (0.023 mmol), PhCOCH₂Br (0.035 mmol), NaI (0.0115 mmol), 15-C-5 (0.0115 mmol), THF+DME (1.2 mL), 18 h, 28 °C, 440 nm blue light. ¹⁹F NMR yields are reported (PhOCF₃ used as internal standard).

E) Representative calculations for the conversion of a reaction and side product analysis

VinylBPIn-CF₂Ph (1a) : 0.0227 mmol

PhOCF₃ : 0.0454 mmol (2 equiv. with respect to 1a).

In ¹⁹F NMR spectrum 2 equiv. of PhOCF₃ peak (-58.47 ppm) was integrated with 300. Thus, 2F atom corresponds to 100 values of integration if the reaction furnished 100% conversion. Compound **3a** peak was integrated with 70.37 which corresponds to 70% conversion.

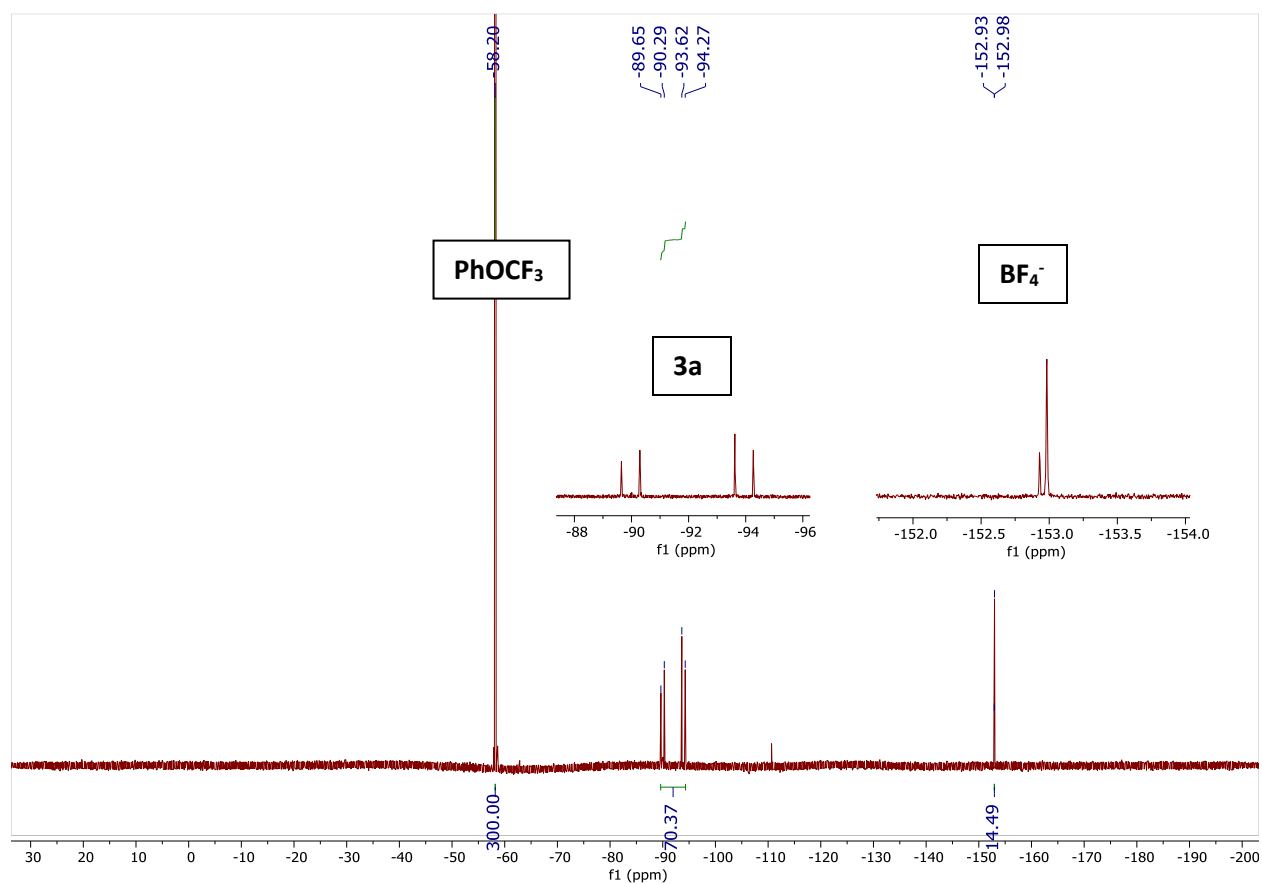


Fig. S10: ^{19}F NMR spectrum (THF- d_8 , 25 °C) of the optimized reaction condition. An impurity is observed at -152.93 to -152.98 ppm (<15%), which we attribute to BF_4^- .

1) Experiment to characterize the side product (BF_4^-)

Following the procedure 1 (ESI, page: S9), the reaction was performed. Upon the completion of the reaction, the reaction vial was charged with the internal standard (PhOCF_3) and the ^{19}F NMR of the crude reaction mixture was obtained. The NMR tube was then loaded with 15 mg of NaBF_4 , shaken well, and the ^{19}F NMR was obtained. The peak at -152.93 to -152.98 ppm grew substantially, which indicates the presence of BF_4^- as the common byproduct in our reaction.

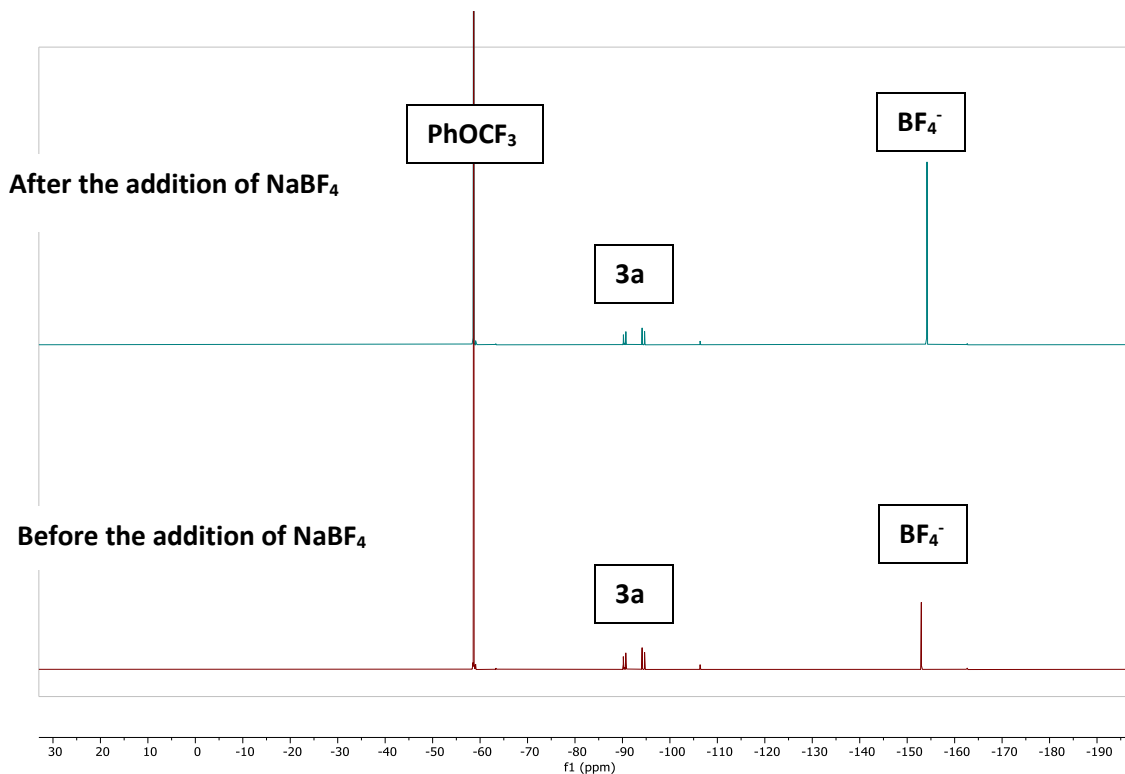
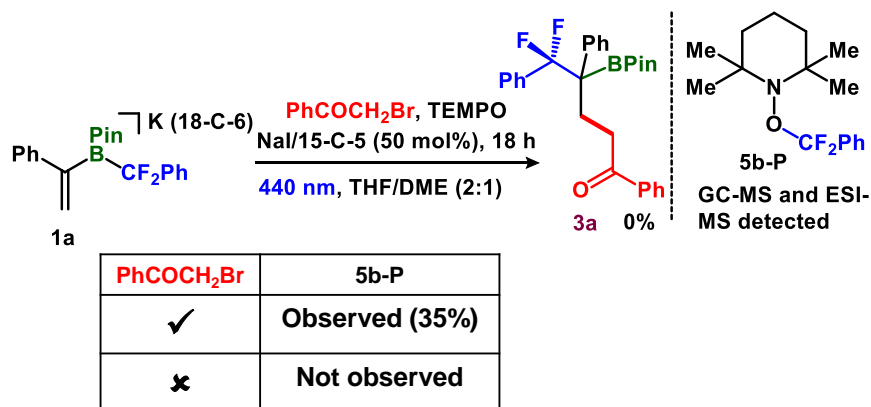


Fig. S11: ^{19}F NMR spectrum (THF) of the reaction mixture before the addition of NaBF_4 to the reaction mixture (below) and after the addition of NaBF_4 to the reaction mixture (above).

F) Procedure for the control experiments

1) Addition of TEMPO:



Vinyl-pinacol boronate ester (**1a**) (0.023 mmol, 1.0 equiv.), NaI (0.00115 mmol, 0.5 equiv.) and 15-C-5 (0.00115 mmol, 0.5 equiv.) were dissolved in 0.8 mL of THF in a 4 mL vial. To the suspension, a solution of PhCOCH_2Br (0.35 mmol, 1.5 equiv.) and TEMPO (0.35 mmol, 1.5 equiv.) in DME (0.4 mL) was added under irradiation, and the mixture was stirred vigorously overnight under constant irradiation (18 h) before the yield was assessed by ^{19}F NMR spectroscopy (PhOCF_3 used as internal standard). The TEMPO

addition product **5b-P** was observed in ^1H , ^{19}F NMR spectroscopy (consistent with prior literature⁴) and was confirmed by GC-MS and ESI-MS.

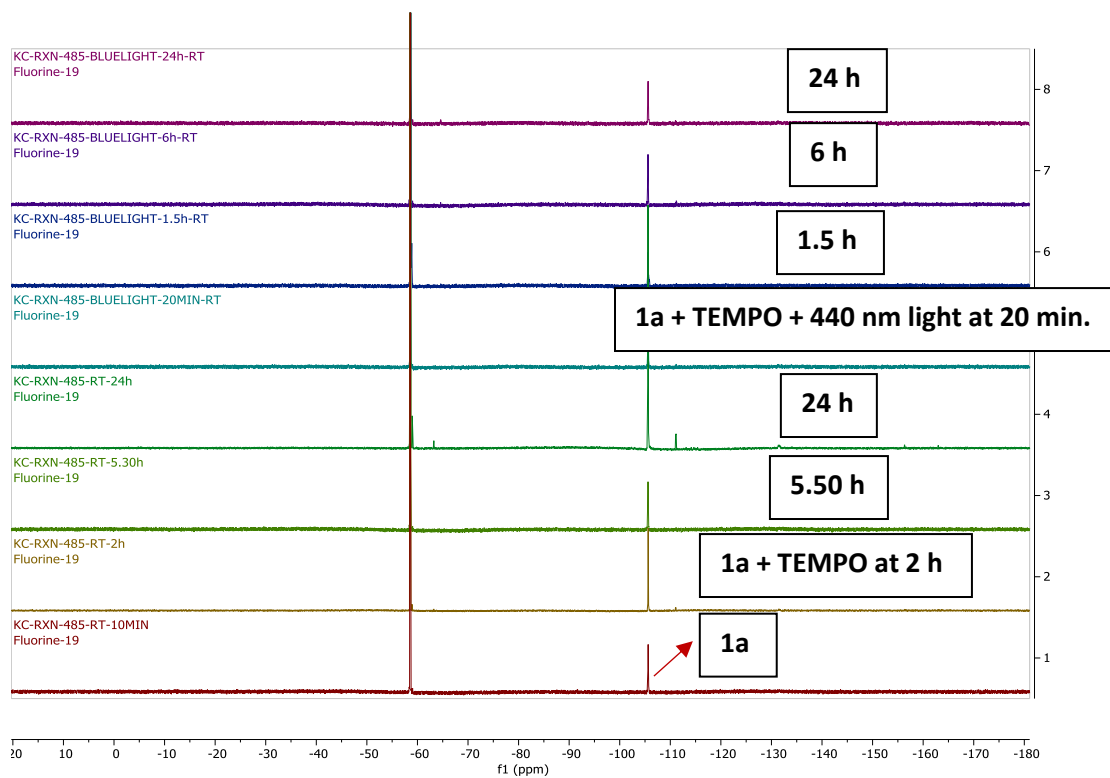


Fig. S12. Stacked ^{19}F NMR spectrum (THF- d_8 , 25 °C) of the reaction mixture without PhCOCH_2Br .

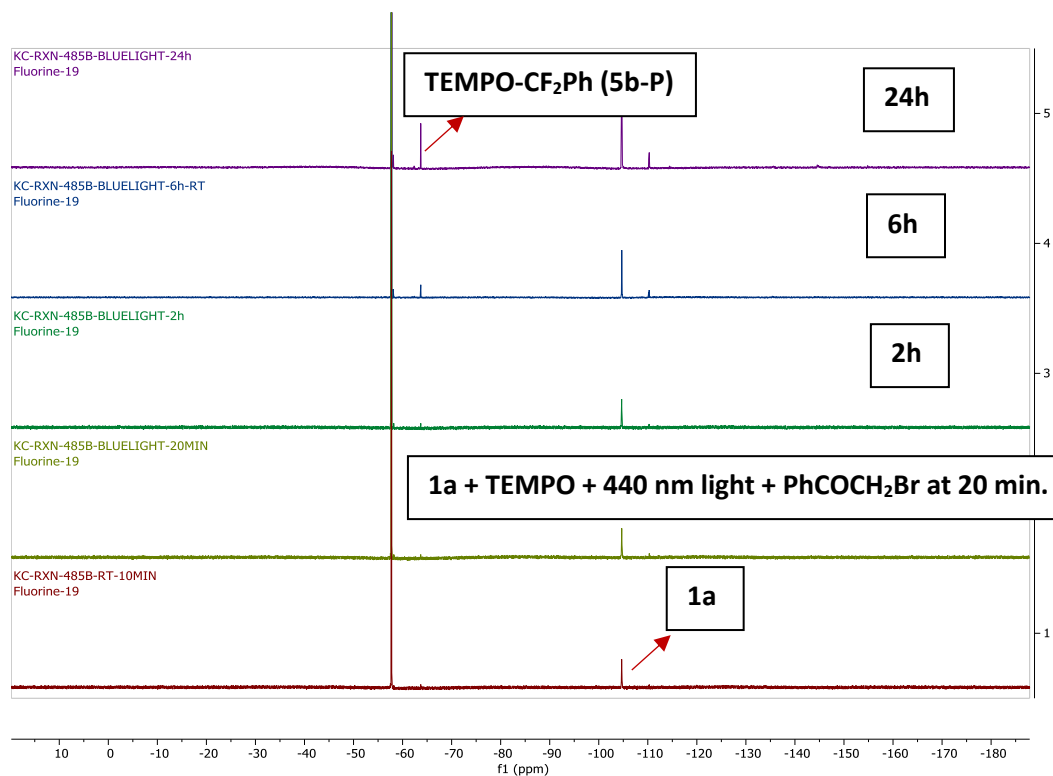
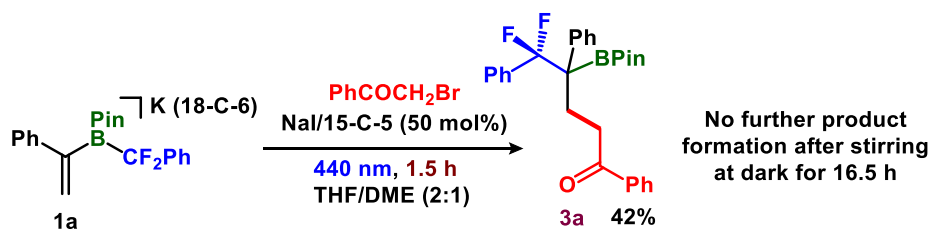


Fig. S13. Stacked ^{19}F NMR spectrum (THF- d_8 , 25 °C) of the reaction mixture with PhCOCH_2Br .

2) Effect of light after reaction initiation:



Two parallel reactions were set up that differ in light exposure:

- a) Vinyl-pinacol boronate ester **1a** (0.023 mmol, 1.0 equiv.), NaI (0.00115 mmol, 0.5 equiv.) and 15-C-5 (0.00115 mmol, 0.5 equiv.) were dissolved in 0.8 mL of THF in a 4 mL vial. To the suspension, a solution of PhCOCH_2Br (0.35 mmol, 1.5 equiv.) in DME (0.4 mL) was added under irradiation, and the mixture was stirred vigorously overnight under constant irradiation (1.5 h) before the yield was assessed by ^{19}F NMR spectroscopy (PhOCF_3 used as internal standard).

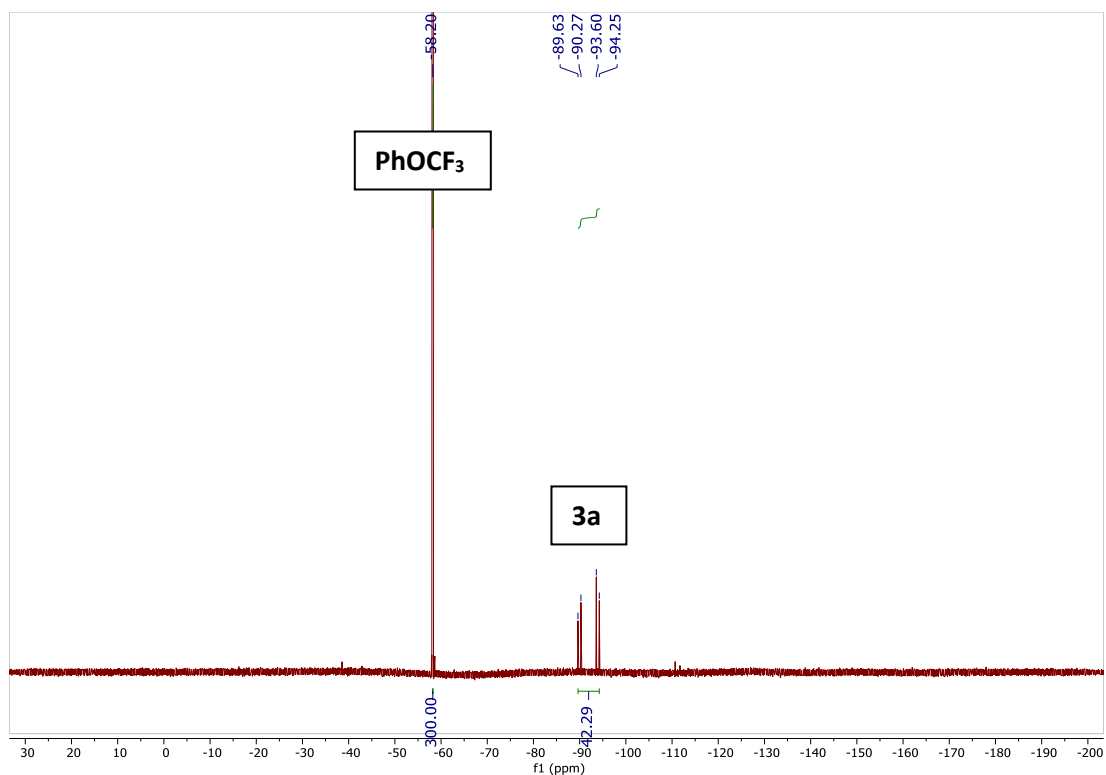


Fig. S14. ^{19}F NMR spectrum (THF- d_8 , 25 °C) of the reaction mixture after 1.5 h irradiation.

- b) An identical reaction was performed, and after constant *irradiation* for 1.5 h, the reaction was stirred in the dark for 16.5 h. The yield, as assessed by ^{19}F NMR spectroscopy, suggests no difference in product formation between these two reactions.

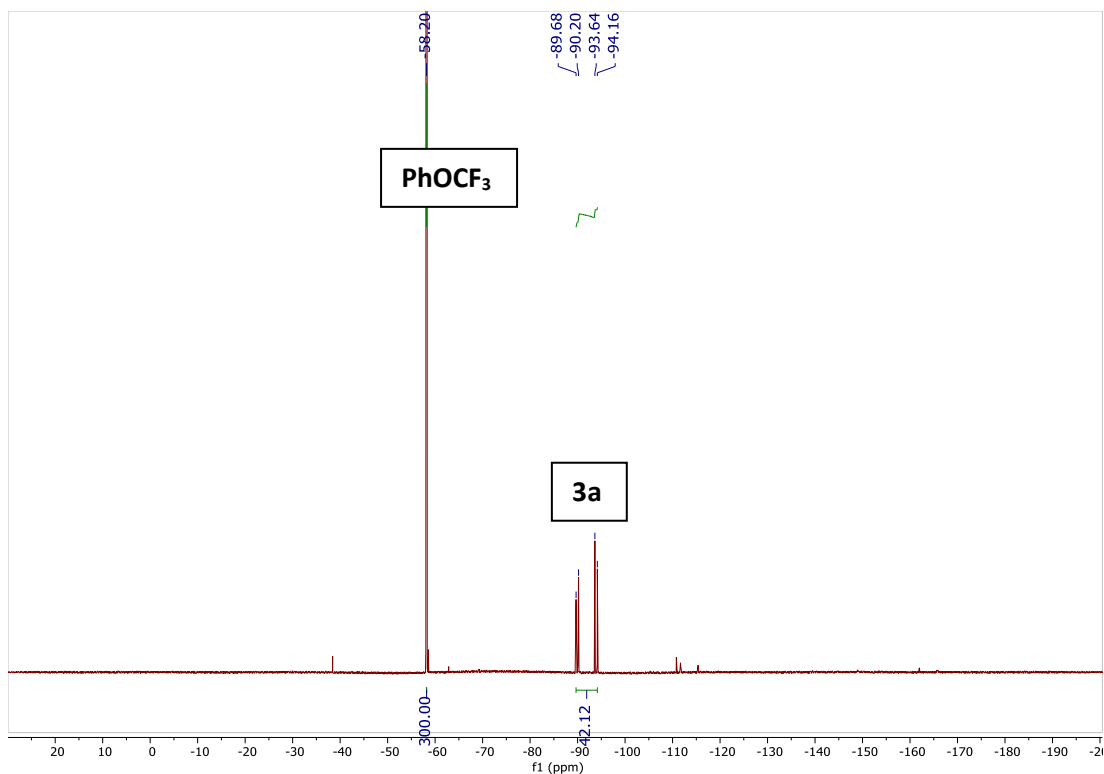
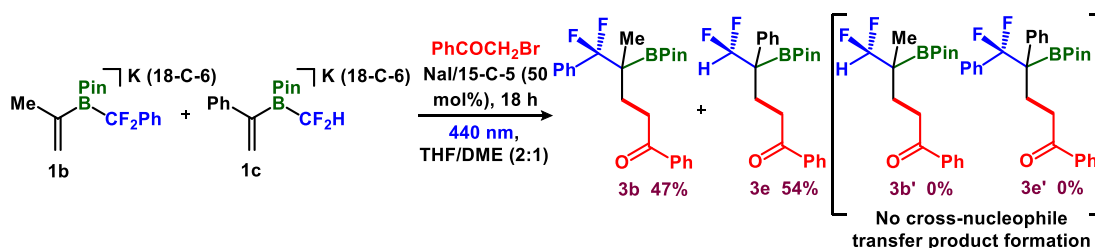


Fig. S15. ^{19}F NMR spectrum (THF- d_8 , 25 $^{\circ}\text{C}$) of the reaction mixture after 1.5 h irradiation and in the dark for 16.5 h.

3) Cross-over experiment:



Vinyl-pinacol boronate ester, **1b** and **1c** (0.023 mmol, 1.0 equiv.), NaI (0.00115 mmol, 0.5 equiv.) and 15-C-5 (0.00115 mmol, 0.5 equiv.) were dissolved in 1.0 mL of THF in a 4 mL vial. To the suspension, a solution of PhCOCH₂Br (0.35 mmol, 1.5 equiv.) in DME (0.50 mL) was added under irradiation, and the mixture was stirred vigorously overnight under constant irradiation (18 h) before the yield was assessed by ^{19}F NMR spectroscopy (PhOCF₃ used as internal standard). The ^{19}F NMR spectra suggests no cross-nucleophile transfer product formation (3b' and 3e').

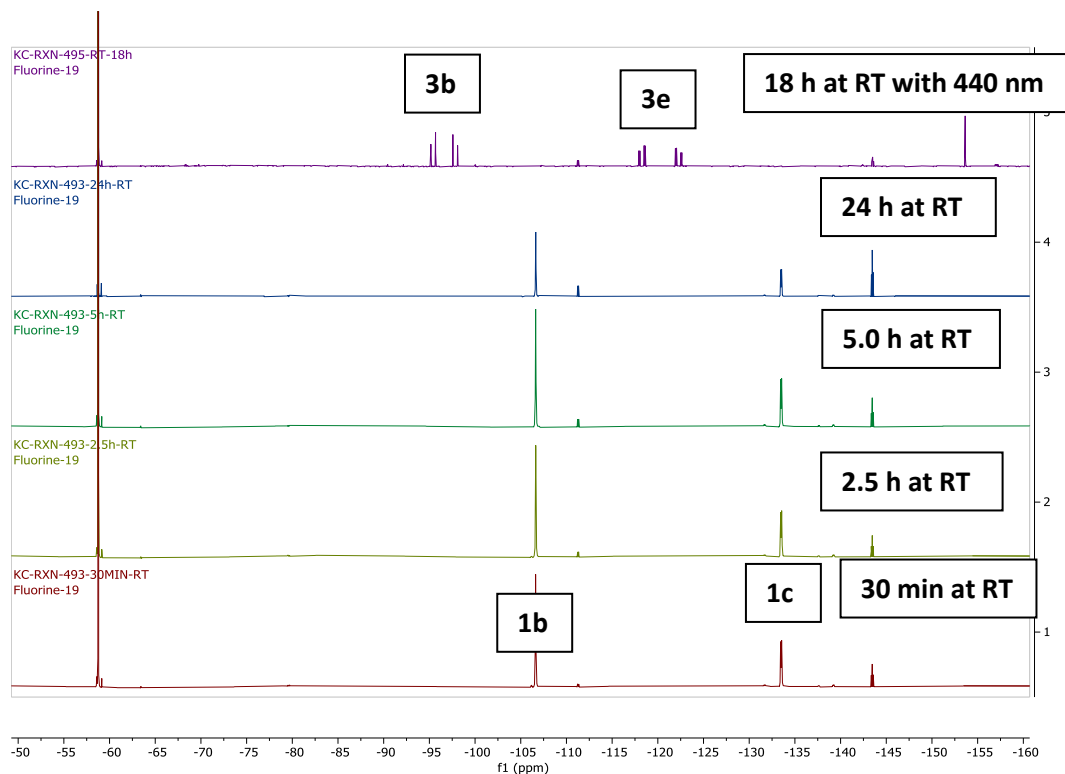


Fig. S16. ^{19}F NMR spectrum (THF- d_8 , 25 °C) of the cross-over experiments.

G) Procedure for estrone derivative synthesis

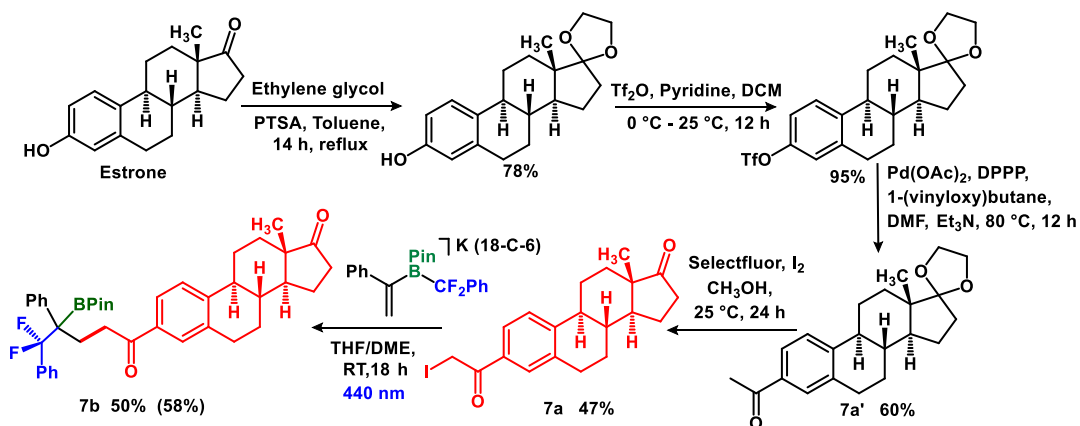


Fig. S17. Scheme for the estrone derivative synthesis.

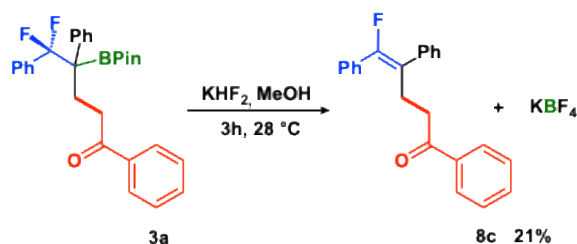
The synthesis of estrone derivative **8a'** was carried out following the literature procedures.⁵

To a solution of **8a'** (1.84 mmol) in MeOH (20 mL), iodine (1.1 mmol) and Selectfluor (0.92 mmol) were added, and the reaction suspension stirred at 25 °C for 24 h. The solvent was removed under reduced pressure and the crude reaction mixture dissolved in CH_2Cl_2 (50 mL). Insoluble material was filtered off, the solution was washed with aq. sodium thiosulfate pentahydrate (10%, 50 mL) and H_2O (50

mL), and dried over Na₂SO₄. The solvent was evaporated, and pure **8a** was purified by flash chromatography (SiO₂; hexanes/CH₂Cl₂).

Vinyl-pinacol boronate ester (**1a**) (0.1 mmol, 1.0 equiv.) was dissolved in 2.0 mL of THF in a 8 mL vial. To the suspension, a solution of **8a** (0.15 mmol, 1.5 equiv.) in DME (1.0 mL) was added under irradiation, and the mixture was stirred vigorously overnight under constant irradiation (18 h) before the yield was assessed by ¹⁹F NMR spectroscopy (PhOCF₃ used as internal standard). The final product **8b** was isolated by column chromatography using hexanes/dichloromethane as eluent.

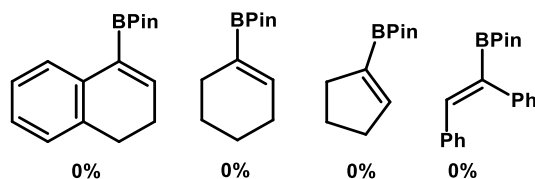
H) Procedure for derivatization reaction using KHF₂



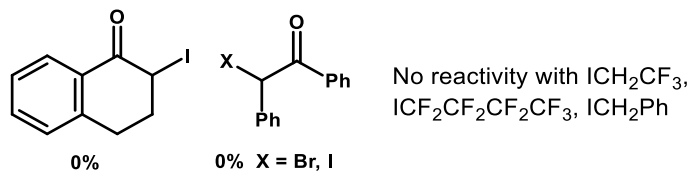
To a solution of **3a** (0.045 mmol, 1 equiv.) in MeOH, KHF₂ (0.225 mmol, 5 equiv.) was added and the mixture was stirred for 3h at room temperature. The solvent was removed in vacuo and excess pentane was added. The insoluble particles were removed by filtration and the resulting pentane solution was concentrated in vacuo. The product **8c** was obtained as a transparent sticky oil.

I) List of unreactive substrates

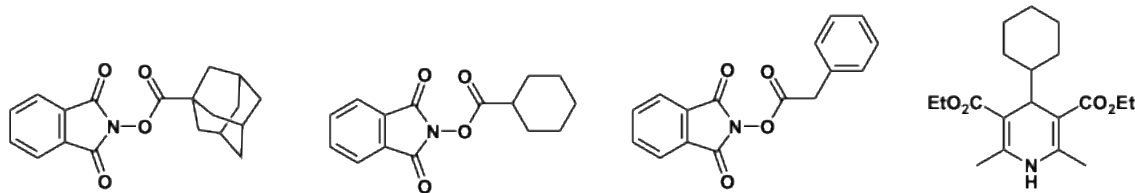
1) Vinyl-pinacol boron derivatives: We examined various other vinyl-pinacol boron derivatives noted below under our optimized conditions, as well as using additional photocatalysts (Ru(bpy)₃Cl₂·6H₂O or 4CzIPN). These substrates did not afford ¹⁹F NMR spectra consistent with products, which we note is also true for literature reports.⁶



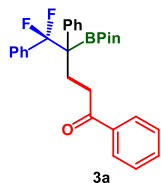
2) Other photoactive coupling partners: In addition to the pro-radical sources noted in the main text, we also examined the radical coupling partners show below, but observed no positive reaction.



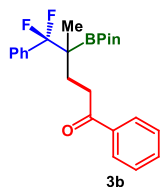
3) Redox-active esters: We tried a couple of redox-active esters, with and without photocatalysts under various solvent conditions but observed no positive reaction.



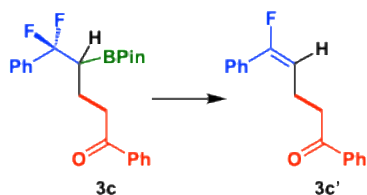
J) Characterization data of compounds



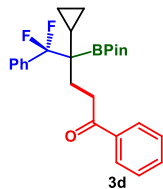
(3a) Pale yellow oil (procedure I: 0.1 mmol scale, 67% isolated, 32 mg), (procedure II: 0.15 mmol scale, 60% isolated, 43 mg), (one-pot synthesis: 0.15 mmol scale, 54% isolated, 38 mg). $^1\text{H NMR}$ (500 MHz, CDCl_3 , ppm) δ 7.90 (d, $J = 8.9$ Hz, 2H), 7.51 (t, $J = 9.1$ Hz, 1H), 7.40 (t, $J = 9.5$ Hz, 2H), 7.29-7.20 (m, 6H), 7.16 (t, $J = 9.6$ Hz, 2H), 6.95 (d, $J = 9.6$ Hz, 2H), 3.27-3.19 (m, 1H), 2.90-2.82 (m, 1H), 2.56-2.42 (m, 2H), 1.30 (s, 12H). $^{13}\text{C NMR}$ (125 MHz, CDCl_3 , ppm) δ 199.95, 137.00, 138.85 (dd, $J_{\text{C-F}} = 6.3, 2.5$ Hz), 135.53 (t, $J_{\text{C-F}} = 18.8$ Hz), 133.91 (t, $J_{\text{C-F}} = 203.8$ Hz), 132.91, 130.62, 129.21 (t, $J_{\text{C-F}} = 1.3$ Hz), 128.52, 128.04, 127.75, 127.07, 127.04, 127.01, 126.96, 124.79, 84.17, 35.45, 24.84, 24.81, 24.66 (t, $J_{\text{C-F}} = 5$ Hz). $^{19}\text{F NMR}$ (376 MHz, CDCl_3 , ppm) δ -89.42 (d, $J_{\text{F-F}} = 240.6$ Hz, 1F), -93.78 (d, $J_{\text{F-F}} = 244.4$ Hz, 1F). $^{11}\text{B NMR}$ (128 MHz, CDCl_3 , ppm) δ 33.09 (s, 1B), **ESI-MS**: calcd for $\text{C}_{29}\text{H}_{31}\text{BF}_2\text{NaO}_3$ ($\text{M}+\text{Na}$) $^+$: 499.2232, found: 499.2227.



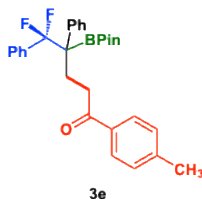
(3b) Transparent oil (Procedure I: 0.1 mmol scale, 42% isolated, 18 mg). $^1\text{H NMR}$ (500 MHz, CDCl_3 , ppm) δ 7.94 (d, $J = 7.5$ Hz, 2H), 7.53 (t, $J = 7.4$ Hz, 1H), 7.46-7.42 (m, 4H), 7.37-7.35 (m, 3H), 3.09-3.02 (m, 1H), 2.95-2.88 (m, 1H), 2.18-2.12 (m, 1H), 1.73-1.67 (m, 1H), 1.27 (s, 6H), 1.25 (s, 6H), 1.06 (s, 3H). $^{13}\text{C NMR}$ (125 MHz, CDCl_3 , ppm) δ 199.04, 134.85 (t, $J_{\text{C-F}} = 28.8$ Hz), 132.14, 131.92, 128.36, 127.55, 127.08, 126.66, 125.58 (t, $J_{\text{C-F}} = 7.5$ Hz), 124.85 (t, $J_{\text{C-F}} = 247.5$ Hz), 82.95, 34.30, 26.94 (t, $J_{\text{C-F}} = 5.0$ Hz), 23.60, 23.77, 16.00 (t, $J_{\text{C-F}} = 6.3$ Hz). $^{19}\text{F NMR}$ (376 MHz, CDCl_3 , ppm) δ -93.85 (d, $J_{\text{F-F}} = 240.6$ Hz, 1F), -93.78 (d, $J_{\text{F-F}} = 240.6$ Hz, 1F). $^{11}\text{B NMR}$ (128 MHz, CDCl_3 , ppm) δ 32.83 (s, 1B), **ESI-MS**: calcd for $\text{C}_{24}\text{H}_{29}\text{BF}_2\text{NaO}_3$ ($\text{M}+\text{Na}$) $^+$: 437.2076, found: 437.2070.



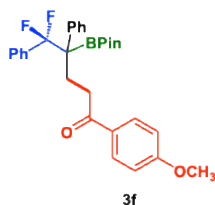
(3c) Dark yellow oil. This compound is not stable to column condition, and degrades to **(3c')**. **¹H NMR** for **(3c')** (500 MHz, CDCl₃, ppm) δ 7.98 (m, 2H), 7.56 (m, 1H), 7.51-7.46 (m, 4H), 7.36-7.30 (m, 3H), 5.55 (dt, *J* = 37.6 Hz, 7.5 Hz, 1H), 3.17 (t, *J* = 7.2 Hz, 2H), 2.72 (qd, *J* = 7.5 Hz, 1.5 Hz, 2H). **¹⁹F NMR** for **(3c')** (376 MHz, CDCl₃, ppm) δ 119.81 (d, *J*_{F-H} = 38.6 Hz)



(3d) Transparent oil (Procedure II: 0.15 mmol scale, 65% isolated, 43 mg). **¹H NMR** (500 MHz, CDCl₃, ppm) δ 7.99-7.96 (m, 2H), 7.55-7.50 (m, 3H), 7.43 (t, *J* = 7.6 Hz, 2H), 7.37-7.32 (m, 3H), 3.27-3.20 (m, 1H), 3.16-3.09 (m, 1H), 2.17-2.11 (m, 1H), 1.76-1.70 (m, 1H), 1.26 (s, 6H), 1.24 (s, 6H), 0.87-0.78 (m, 2H), 0.44-0.40 (m, 2H), 0.38-0.34 (m, 1H). **¹³C NMR** (125 MHz, CDCl₃, ppm) δ 201.05, 143.71, 142.36, 137.14, 136.37 (t, *J*_{C-F} = 28.8 Hz), 132.98, 129.41, 128.65, 128.37, 128.34, 127.61, 127.03 (t, *J*_{C-F} = 6.3 Hz), 126.53 (t, *J*_{C-F} = 255 Hz), 83.70, 36.05, 28.69 (t, *J*_{C-F} = 3.8 Hz), 25.00, 24.19, 14.04 (t, *J*_{C-F} = 3.8 Hz), 3.65, 2.90, 1.16. **¹⁹F NMR** (574 MHz, CDCl₃, ppm) δ -89.71 (d, *J*_{F-F} = 252.6 Hz, 1F), -92.42 (d, *J*_{F-F} = 246.8 Hz, 1F). **¹¹B NMR** (128 MHz, CDCl₃, ppm) δ 29.79 (s, 1B), **ESI-MS**: calcd for C₂₆H₃₁BF₂O₃ (M⁺): 440.2334, found: 440.2315.

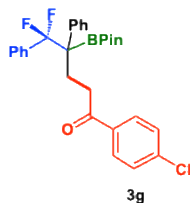


(3e) Transparent oil (Procedure I: 0.1 mmol scale, 53% isolated, 26 mg). **¹H NMR** (500 MHz, CDCl₃, ppm) δ 7.79 (d, *J* = 8.0 Hz, 2H), 7.27-7.18 (m, 8H), 7.14 (t, *J* = 7.7 Hz, 2H), 6.93 (d, *J* = 7.5 Hz, 2H), 3.21-3.15 (m, 1H), 2.85-2.79 (m, 1H), 2.52-2.40 (m, 2H), 2.36 (s, 3H), 1.30 (s, 12H). **¹³C NMR** (125 MHz, CDCl₃, ppm) δ 199.76, 143.76, 136.99 (dd, *J*_{C-F} = 5, 2.5 Hz), 135.65 (t, *J*_{C-F} = 28.8 Hz), 134.64, 130.76, 129.31, 128.30, 127.84, 127.17, 127.15, 126.12, 126.07, 124.93 (t, *J*_{C-F} = 250 Hz), 84.28, 35.43, 24.96, 24.93, 24.85 (t, *J*_{C-F} = 3.8 Hz), 21.74. **¹⁹F NMR** (376 MHz, CDCl₃, ppm) δ -89.33 (d, *J*_{F-F} = 240.7 Hz, 1F), -93.83 (d, *J*_{F-F} = 240.7 Hz, 1F). **¹¹B NMR** (192 MHz, CDCl₃, ppm) δ 32.40 (s, 1B), **ESI-MS**: calcd for C₃₀H₃₃BF₂NaO₃ ((M+Na)⁺): 513.2389, found: 513.2383.

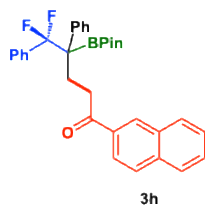


(3f) Transparent oil (Procedure I: 0.1 mmol scale, 62% isolated, 31 mg). **¹H NMR** (500 MHz, CDCl₃, ppm) δ 7.87 (d, *J* = 8.8 Hz, 2H), 7.27-7.19 (m, 6H), 7.14 (t, *J* = 7.6 Hz, 2H), 6.93 (d, *J* = 8.0 Hz, 2H), 6.86 (d, *J* = 8.7 Hz, 2H), 3.82 (s, 3H), 3.19-3.12 (m, 1H), 2.83-2.76 (m, 1H), 2.52-2.39 (m, 2H), 1.30 (s, 12H). **¹³C NMR** (125 MHz, CDCl₃, ppm) δ 198.57, 163.32, 136.90 (dd, *J*_{C-F} = 6.3, 1.3 Hz), 135.53 (t, *J*_{C-F} = 27.5 Hz), 130.64, 130.61,

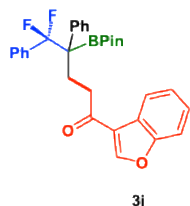
130.29, 130.11, 129.17, 127.71, 127.04, 127.02, 126.99, 126.94, 124.81 (t, $J_{C-F} = 250$ Hz), 113.62, 84.15, 35.06, 26.37 (t, $J_{C-F} = 3.6$ Hz), 24.84, 24.81. **^{19}F NMR** (376 MHz, CDCl_3 , ppm) δ -89.26 (d, $J_{F-F} = 195.5$ Hz, 1F), -93.76 (d, $J_{F-F} = 191.8$ Hz, 1F). **^{11}B NMR** (128 MHz, CDCl_3 , ppm) δ 32.72 (s, 1B), **ESI-MS**: calcd for $\text{C}_{30}\text{H}_{33}\text{BF}_2\text{NaO}_4$ ((M+Na) $^+$): 529.2338, found: 529.2332.



(3g) Transparent oil (Procedure I: 0.1 mmol scale, 60% isolated, 31 mg). **^1H NMR** (500 MHz, CDCl_3 , ppm) δ 7.82 (d, $J = 8.7$ Hz, 2H), 7.36 (d, $J = 8.6$ Hz, 2H), 7.26 (t, $J = 7.4$ Hz, 2H), 7.23-7.21 (m, 4H), 7.15 (t, $J = 7.6$ Hz, 2H), 6.94 (d, $J = 7.7$ Hz, 2H), 3.20-3.14 (m, 1H), 2.83-2.77 (m, 1H), 2.52-2.39 (m, 2H), 1.29 (s, 6H), 1.28 (s, 6H). **^{13}C NMR** (125 MHz, CDCl_3 , ppm) δ 198.78, 139.32, 136.98 (dd, $J_{C-F} = 4.5, 1.5$ Hz), 135.27 (t, $J_{C-F} = 23.8$ Hz), 130.56, 129.49, 129.24, 128.82, 127.79, 127.13, 127.05, 127.00, 126.95, 124.72 (t, $J_{C-F} = 248.5$ Hz), 84.20, 35.48, 24.82, 24.80, 24.67 (t, $J_{C-F} = 3.6$ Hz). **^{19}F NMR** (376 MHz, CDCl_3 , ppm) δ -89.57 (d, $J_{F-F} = 244.4$ Hz, 1F), -93.75 (d, $J_{F-F} = 244.4$ Hz, 1F). **^{11}B NMR** (192 MHz, CDCl_3 , ppm) δ 32.90 (s, 1B), **ESI-MS**: calcd for $\text{C}_{29}\text{H}_{31}\text{BClF}_2\text{O}_3$ ((M+H) $^+$): 511.2023, found: 511.2017.

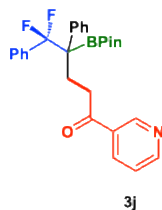


(3h) Transparent oil (Procedure I: 0.1 mmol scale, 65% isolated, 34 mg). **^1H NMR** (500 MHz, CDCl_3 , ppm) δ 8.37 (s, 1H), 7.98 (d, $J = 10.5$ Hz, 1H), 7.88 (d, $J = 8.2$ Hz, 1H), 7.85-7.82 (m, 2H), 7.56 (t, $J = 8.0$ Hz, 1H), 7.50 (t, $J = 8.1$ Hz, 1H), 7.28-7.21 (m, 6H), 7.16 (t, $J = 7.6$ Hz, 2H), 6.96 (d, $J = 8.0$ Hz, 2H), 3.38-3.31 (m, 1H), 3.04-2.97 (m, 1H), 2.62-2.48 (m, 2H), 1.32 (s, 12H). **^{13}C NMR** (125 MHz, CDCl_3 , ppm) δ 199.90, 136.91 (dd, $J_{C-F} = 5.0, 1.3$ Hz), 135.55 (t, $J_{C-F} = 27.5$ Hz), 135.53, 134.33, 132.54, 130.67, 129.58, 129.52, 129.22, 128.35, 127.79, 127.76, 127.12, 127.07, 127.05, 127.02, 126.96, 126.69, 124.81 (t, $J_{C-F} = 248.8$ Hz), 123.95, 103.83, 84.21, 35.44, 24.86, 24.85, 24.78 (t, $J_{C-F} = 3.8$ Hz). **^{19}F NMR** (376 MHz, CDCl_3 , ppm) δ -89.45 (d, $J_{F-F} = 240.6$ Hz, 1F), -93.89 (d, $J_{F-F} = 240.6$ Hz, 1F). **^{11}B NMR** (192 MHz, CDCl_3 , ppm) δ 32.67 (s, 1B), **ESI-MS**: calcd for $\text{C}_{33}\text{H}_{34}\text{BF}_2\text{O}_3$ ((M+H) $^+$): 527.2569, found: 527.2564.

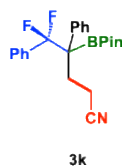


(3i) Transparent oil (Procedure I: 0.1 mmol scale, 59% isolated, 30 mg). **^1H NMR** (500 MHz, CDCl_3 , ppm) δ 7.65 (d, $J = 7.85$ Hz, 1H), 7.52 (d, $J = 8.4$ Hz, 1H), 7.44-7.41 (m, 2H), 7.28-7.22 (m, 7H), 7.16 (t, $J = 7.65$ Hz, 2H), 6.95 (d, $J = 7.8$ Hz, 2H), 3.23-3.16 (m, 1H), 2.90-2.84 (m, 1H), 2.60-2.63 (m, 2H), 1.31 (s, 12H). **^{13}C NMR** (125 MHz, CDCl_3 , ppm) δ 191.06, 155.56, 152.52, 136.70 (dd, $J_{C-F} = 5.0, 1.3$ Hz), 135.48 (t, $J_{C-F} = 27.5$ Hz),

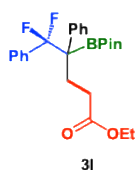
130.63, 129.25, 128.08, 127.79, 127.14, 127.06, 127.01, 126.96, 124.72 (t, J_{C-F} = 250.0 Hz), 123.82, 123.20, 112.63, 112.47, 84.25, 35.82, 24.84, 24.80, 24.52 (t, J_{C-F} = 5.0 Hz). **¹⁹F NMR** (376 MHz, CDCl₃, ppm) δ -89.59 (d, J_{F-F} = 240.7 Hz, 1F), -93.83 (d, J_{F-F} = 244.4 Hz, 1F). **¹¹B NMR** (192 MHz, CDCl₃, ppm) δ 32.65 (s, 1B), **ESI-MS**: calcd for C₃₁H₃₁BF₂NaO₄ ((M+Na)⁺): 539.2181, found: 539.2176.



(3j) Transparent oil (Procedure I: 0.1 mmol scale, 55% isolated, 26 mg). **¹H NMR** (500 MHz, CDCl₃, ppm) δ 9.07 (d, J = 2.2 Hz, 1H), 8.72 (dd, J = 4.8, 1.8 Hz, 1H), 8.15 (dt, J = 8.0, 2.0 Hz, 1H), 7.34 (ddd, J = 8.0, 4.8, 0.90 Hz, 1H), 7.28-7.21 (m, 6H), 7.16 (t, J = 7.7 Hz, 2H), 6.96 (d, J = 7.9 Hz, 2H), 3.27-3.20 (m, 1H), 2.86-2.79 (m, 1H), 2.55-2.42 (m, 2H), 1.29 (s, 6H), 1.28 (s, 6H). **¹³C NMR** (125 MHz, CDCl₃, ppm) δ 198.88, 153.37, 149.66, 136.60 (dd, J_{C-F} = 6.3, 2.5 Hz), 135.45 (t, J_{C-F} = 27.5 Hz), 134.34, 132.17, 130.50, 129.29, 127.86, 127.19, 127.07, 127.03, 126.98, 124.68 (t, J_{C-F} = 248.8 Hz), 123.57, 84.25, 35.85, 24.82, 24.80, 24.45 (t, J_{C-F} = 3.8 Hz). **¹⁹F NMR** (376 MHz, CDCl₃, ppm) δ -89.80 (d, J_{F-F} = 244.4 Hz, 1F), -93.56 (d, J_{F-F} = 244.4 Hz, 1F). **¹¹B NMR** (128 MHz, CDCl₃, ppm) δ 34.51 (s, 1B), **ESI-MS**: calcd for C₂₈H₃₁BF₂NO₃ ((M+H)⁺): 478.2365, found: 478.2060.

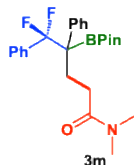


(3k) Transparent oil (from ICH₂CN: 0.1 mmol scale, 50% isolated, 21 mg), (from CH₃CN: 0.1 mmol scale, 42% isolated, 18 mg, CH₃CN was used as solvent for these conditions in presence of 2 equivalent redox-active ester (1,3-dioxoisindolin-2-yl (3r,5r,7r)-adamantane-1-carboxylate) as a radical initiator). **¹H NMR** (500 MHz, CDCl₃, ppm) δ 7.30 (t, J = 7.6 Hz, 1H), 7.25-7.23 (m, 3H), 7.21-7.17 (m, 4H), 6.95 (d, J = 7.5 Hz, 2H), 2.60-2.54 (m, 1H), 2.49-2.43 (m, 1H), 2.39-2.33 (m, 1H), 2.24-2.17 (m, 1H), 1.29 (s, 12H). **¹³C NMR** (125 MHz, CDCl₃, ppm) δ 135.22 (dd, J_{C-F} = 2.5, 1.5 Hz), 134.93 (t, J_{C-F} = 27.5 Hz), 130.13, 129.60, 129.10, 128.18, 127.59, 127.23, 126.96 (t, J_{C-F} = 6.3 Hz), 124.18 (t, J_{C-F} = 250.0 Hz), 120.33, 84.55, 27.36 (t, J_{C-F} = 5.0 Hz), 24.78, 24.73, 14.11. **¹⁹F NMR** (376 MHz, CDCl₃, ppm) δ -90.50 (d, J_{F-F} = 244.4 Hz, 1F), -93.20 (d, J_{F-F} = 244.4 Hz, 1F). **¹¹B NMR** (192 MHz, CDCl₃, ppm) δ 33.46 (s, 1B), **ESI-MS**: calcd for C₂₃H₂₆BF₂NNaO₂ ((M+Na)⁺): 420.1922, found: 420.1913.



(3l) Transparent oil (Procedure I: 0.1 mmol scale, 39% isolated, 18 mg). **¹H NMR** (500 MHz, CDCl₃, ppm) δ 7.26 (t, J = 7.5 Hz, 2H), 7.21-7.18 (m, 4H), 7.15 (t, J = 7.7 Hz, 2H), 6.9 (d, J = 8.1 Hz, 2H), 4.08 (q, J = 14.4, 2.1 Hz, 2H), 2.51-2.42 (m, 1H), 2.41-2.31 (m, 2H), 2.27-2.21 (m, 1H), 1.29 (s, 12H), 1.21 (t, J = 7.2 Hz, 3H). **¹³C NMR** (125 MHz, CDCl₃, ppm) δ 172.70, 135.61 (dd, J_{C-F} = 2.5, 1.5 Hz), 134.52 (t, J_{C-F} = 27.5 Hz), 129.52,

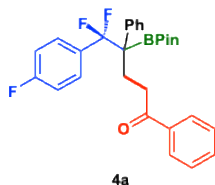
128.16, 126.64, 125.99, 125.97, 125.93, 125.87, 123.61 (t, $J_{C-F} = 248.8$ Hz), 83.13, 59.26, 30.05, 24.46 (t, $J_{C-F} = 5.0$ Hz), 23.76, 23.72, 13.19. ^{19}F NMR (376 MHz, CDCl_3 , ppm) δ -89.72 (d, $J_{F-F} = 244.4$ Hz, 1F), -93.97 (d, $J_{F-F} = 244.4$ Hz, 1F). ^{11}B NMR (128 MHz, CDCl_3 , ppm) δ 32.20 (s, 1B), **ESI-MS**: calcd for $\text{C}_{25}\text{H}_{31}\text{BF}_2\text{NaO}_4$ ((M+Na) $^+$): 467.2181, found: 467.2176.



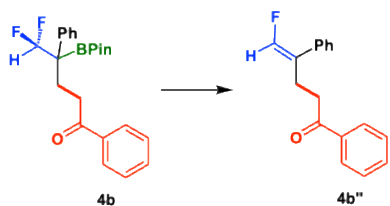
(3m) yellow oil (from $\text{ICH}_2\text{CONMe}_2$, 0.1 mmol scale, 59 % isolated, 28 mg). ^1H NMR (500 MHz, CDCl_3 , ppm) δ 7.40-7.19 (m, 3H), 7.19-7.16 (m, 3H), 7.13 (t, $J = 7.7$ Hz, 2H), 6.91 (d, $J = 8.2$ Hz, 2H), 2.91 (s, 3H), 2.89 (s, 3H), 2.56-2.49 (m, 1H), 2.42-2.37 (m, 2H), 2.21-2.17 (m, 1H), 1.31 (s, 12H). ^{13}C NMR (125 MHz, CDCl_3 , ppm) δ 172.94, 136.85 (d, $J_{C-F} = 5.6$ Hz), 135.49 (t, $J_{C-F} = 28.6$ Hz), 130.66, 129.13, 127.65, 127.01, 126.97, 124.61 (t, $J_{C-F} = 252.1$ Hz), 84.07, 60.40, 37.03, 35.38, 29.86, 25.85 (t, $J_{C-F} = 4.5$ Hz), 24.82, 20.33, 14.22. ^{19}F NMR (376 MHz, CDCl_3 , ppm) δ -89.15 (d, $J_{F-F} = 248.78$ Hz, 1F), -93.70 (d, $J_{F-F} = 242.6$ Hz, 1F). ^{11}B NMR (128 MHz, CDCl_3 , ppm) δ 32.77 (s, 1B). **ESI-MS**: calcd for $\text{C}_{25}\text{H}_{33}\text{BF}_2\text{NO}_3$ ((M+H) $^+$): 444.2522, found: 444.2507.



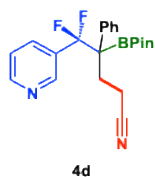
(3n) (Procedure I: 0.1 mmol scale, 13 % isolated, 5.8 mg). ^1H NMR (700 MHz, CDCl_3 , ppm) δ 7.28-7.27 (m, 2H), 7.22-7.20 (m, 4H), 7.16 (t, $J = 7.7$ Hz, 2H), 6.93 (d, $J = 8.3$ Hz, 2H), 2.75 (ddd, $J = 16.8, 11.0, 5.4$ Hz, 1H), 2.49 (ddd, $J = 16.0, 10.7, 5.0$ Hz, 1H), 2.39-2.31 (m, 2H), 1.82 (tt, $J = 8.5, 4.6$ Hz, 1H), 1.32 (s, 12H), 0.99-0.97 (m, 2H), 0.81-0.80 (m, 2H). ^{13}C NMR (126 MHz, CDCl_3 , ppm) δ 210.48, 136.98 (dd, $J_{C-F} = 5.7, 1.7$ Hz), 135.70 (t, $J_{C-F} = 27.9$ Hz), 130.77, 129.29, 127.79, 127.13, 127.10, 127.05, 124.85, 84.25, 40.19, 24.94, 24.91, 24.09, 20.59, 14.28, 10.61, 10.57. ^{19}F NMR (474 MHz, CDCl_3 , ppm) δ -89.69 (d, $J_{F-F} = 243.1$ Hz, 1F), -94.04 (d, $J_{F-F} = 243.0$ Hz, 1F). ^{11}B NMR (160 MHz, CDCl_3 , ppm) δ 32.67 (s, 1B). **ESI-MS**: calcd for $\text{C}_{26}\text{H}_{31}\text{BFO}_3$ ((M-F) $^+$): 421.2345, found: 421.2335.



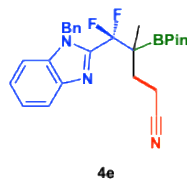
(4a) Transparent oil (purified by pep-TLC). ^1H NMR (600 MHz, CDCl_3 , ppm) δ 7.88 (dd, $J = 8.5, 1.6$ Hz, 2H), 7.60-7.57 (m, 1H), 7.50 (t, $J = 7.5$ Hz, 1H), 7.39 (t, $J = 7.9$ Hz, 2H), 7.12-7.07 (m, 2H), 6.98 (d, $J = 7.9$ Hz, 1H), 6.93 (t, $J = 8.8$ Hz, 1H), 6.91-6.89 (m, 2H), 6.82 (t, $J = 8.6$ Hz, 2H), 3.25-3.19 (m, 1H), 2.86-2.83 (m, 1H), 2.54-2.42 (m, 2H), 1.29 (s, 12H). ^{13}C NMR (125 MHz, CDCl_3 , ppm) δ 198.82, 161.27 (d, $J_{C-F} = 32.5$ Hz), 135.91, 135.66 (dd, $J_{C-F} = 5.0, 1.3$ Hz), 131.90, 129.54, 128.12, 128.05, 127.92, 127.65, 127.59, 127.49, 126.99, 126.80, 126.25, 126.17, 125.79, 125.48 (t, $J_{C-F} = 242.5$ Hz), 115.20, 113.48 (d, $J_{C-F} = 20$ Hz), 112.94 (d, $J_{C-F} = 22.5$ Hz), 83.18, 34.31, 23.79, 23.75, 23.40 (t, $J_{C-F} = 3.8$ Hz). ^{19}F NMR (564 MHz, CDCl_3 , ppm) δ -88.88 (d, $J_{F-F} = 242.5$ Hz, 1F), -93.39 (d, $J_{F-F} = 242.5$ Hz, 1F), -112.29 (s, 1F). ^{11}B NMR (192 MHz, CDCl_3 , ppm) δ 32.59 (s, 1B), **ESI-MS**: calcd for $\text{C}_{29}\text{H}_{31}\text{BF}_3\text{O}_3$ (M+H) $^+$: 495.2318, found: 495.2319.



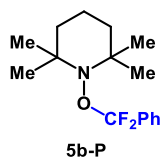
(4b) Yellow oil. This compound is not stable to column condition, and degrades to **(4b'')**. $^1\text{H NMR}$ for **(4b'')** (500 MHz, CDCl_3 , ppm) δ 7.90-7.88 (m, 2H), 7.55-7.52 (m, 1H), 7.44-7.41 (m, 2H), 7.36-7.30 (m, 5H), 6.83 (d, $J = 77.1$ Hz, 1H), 3.08-3.05 (m, 2H), 3.04-2.98 (m, 2H). $^{19}\text{F NMR}$ for **(4b'')** (376 MHz, CDCl_3 , ppm) δ 129.04 (d, $J_{\text{F-H}} = 82.6$ Hz).



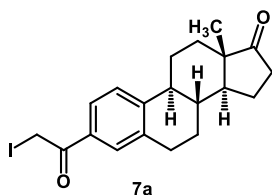
(4d) Light yellow oil (Procedure III, from ICH_2CN (NaI and 15-C-5 are not used) 0.1 mmol scale, 43 % isolated, 17.2 mg). $^1\text{H NMR}$ (600 MHz, CDCl_3 , ppm) δ 8.46 (d, $J = 4.5$, 1H), 8.15 (s, 1H), 7.28-7.20 (m, 4H), 7.14-7.06 (m, 3H), 7.05-7 (m, 1H), 6.98 (d, $J = 7.9$ Hz, 1H), 6.93 (t, $J = 8.8$ Hz, 1H), 6.91-6.89 (m, 2H), 6.82 (t, $J = 8.6$ Hz, 2H), 3.25-3.19 (m, 1H), 2.64-2.33 (m, 3H), 2.21-2.14 (m, 1H), 1.25 (s, 12H). $^{13}\text{C NMR}$ (125 MHz, CDCl_3 , ppm) δ 150.64, 149.62, 148.45 (t, $J_{\text{C-F}} = 7.0$ Hz), 134.94 (t, $J_{\text{C-F}} = 6.7$ Hz), 131.21 (t, $J_{\text{C-F}} = 28.1$ Hz), 130.16, 129.55, 128.68, 128.24, 123.59 (t, $J_{\text{C-F}} = 251.1$ Hz), 122.88, 121.90, 120.24, 84.90, 26.99 (t, $J_{\text{C-F}} = 4.1$ Hz), 24.88, 14.30 $^{19}\text{F NMR}$ (564 MHz, CDCl_3 , ppm) δ -92.65 (d, $J_{\text{F-F}} = 251.2$ Hz, 1F), -94.45 (d, $J_{\text{F-F}} = 248.8$ Hz, 1F), $^{11}\text{B NMR}$ (192 MHz, CDCl_3 , ppm) δ 31.96 (s, 1B), **ESI-MS**: calcd for $\text{C}_{22}\text{H}_{25}\text{BF}_2\text{N}_2\text{NaO}_2$ ($\text{M}+\text{Na}$) $^+$: 421.1875, found: 421.1863.



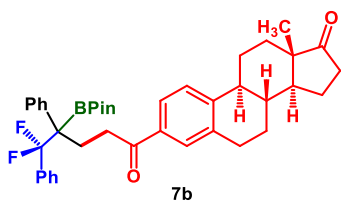
(4e) Transparent oil (Procedure III, from ICH_2CN (NaI and 15-C-5 are not used, 0.1 mmol scale, 39 % isolated, 18 mg). $^1\text{H NMR}$ (600 MHz, CDCl_3 , ppm) δ 7.74-7.69 (m, 1H), 7.31-7.27 (m, 2H), 7.27-7.25 (m, 1H), 7.25 (d, $J = 2.1$ Hz, 1H), 7.23-7.21 (m, 1H), 7.20-7.18 (m, 1H), 7.16-7.07 (m, 2H), 5.57 (m, 2H), 2.62-2.45 (m, 2H), 2.30-2.20 (m, 1H), 2.19-2.10 (m, 1H), 1.31 (s, 3H), 1.28 (s, 6H), 1.26 (s, 6H). $^{13}\text{C NMR}$ (125 MHz, CDCl_3 , ppm) δ 146.62 (t, $J_{\text{C-F}} = 32.2$ Hz), 140.66, 136.08, 135.99, 128.96, 127.97, 126.56, 124.70, 123.18, 122.70 (t, $J_{\text{C-F}} = 245.1$ Hz), 120.65, 120.61, 111.33, 83.79, 48.66, 29.84, 28.80 (t, $J_{\text{C-F}} = 4.9$ Hz), 24.95, 24.88, 15.64 (t, $J_{\text{C-F}} = 5.4$ Hz), 13.76, $^{19}\text{F NMR}$ (564 MHz, CDCl_3 , ppm) δ -95.57 (d, $J_{\text{F-F}} = 274.1$ Hz, 1F), -97.40 (d, $J_{\text{F-F}} = 271.2$ Hz, 1F), $^{11}\text{B NMR}$ (192 MHz, CDCl_3 , ppm) δ 29.51 (s, 1B), **ESI-MS**: calcd for $\text{C}_{26}\text{H}_{31}\text{BF}_2\text{N}_2\text{O}_2$ ($\text{M}+\text{H}$) $^+$: 466.2477, found: 466.2491.



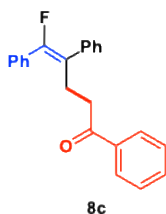
(5b-P). $^1\text{H NMR}$ (500 MHz, CDCl_3 , ppm) 7.68-7.59 (m, 2H), 7.47-7.41 (m, 3H), 1.69-1.54 (m, 5H), 1.41-1.36 (m, 1H), 1.26 (t, $J = 3.2$ Hz, 6H), 1.19 (s, 6H). $^{19}\text{F NMR}$ (471 MHz, THF- d_8 , ppm) δ -63.70 (s). **GC-MS:** 127 (CF_2Ph^+), 156 (TEMPO^+), 268 ($(\text{M}-\text{CH}_3)^+$), 283 (M^+). **ESI-MS:** calcd for $\text{C}_{16}\text{H}_{24}\text{F}_2\text{NO}$ ($(\text{M}+\text{H})^+$): 284.1820, found: 284.1830.



(7a) White solid (1.84 mmol scale, 47% isolated, 365 mg). $^1\text{H NMR}$ (500 MHz, CDCl_3 , ppm) δ 7.73-7.67 (m, 2H), 7.36 (d, $J = 8.2$ Hz, 1H), 4.30 (s, 2H), 3.00-2.90 (m, 2H), 2.56-2.40 (m, 2H), 2.35-2.30 (m, 1H), 2.17-2.01 (m, 3H), 1.98-1.94 (m, 1H), 1.66-1.41 (m, 6H), 0.89 (s, 3H). $^{13}\text{C NMR}$ (125 MHz, CDCl_3 , ppm) δ 220.55, 192.84, 146.56, 137.15, 131.19, 129.76, 126.59, 125.95, 50.62, 47.97, 44.89, 37.84, 35.91, 31.63, 29.41, 26.34, 25.62, 21.70, 13.92, 1.88. **ESI-MS:** calcd for $\text{C}_{20}\text{H}_{23}\text{IO}_2$ ($(\text{M}+\text{H})^+$): 423.0821, found: 423.0818.



(7b) Transparent oil (0.1 mmol scale, 50% isolated, 33 mg). $^1\text{H NMR}$ (500 MHz, CDCl_3 , ppm) δ 7.66 (dd, $J = 8.3, 1.9$ Hz, 1H), 7.62 (s, 1H), 7.31 (d, $J = 8.2$ Hz, 1H), 7.25 (t, $J = 7.4$ Hz, 2H), 7.22-7.18 (m, 4H), 7.14 (t, $J = 7.6$ Hz, 2H), 6.93 (d, $J = 7.4$ Hz, 2H), 3.21-3.14 (m, 1H), 2.96-2.89 (m, 2H), 2.87-2.80 (m, 1H), 2.50-2.39 (m, 3H), 2.32-2.27 (m, 1H), 2.13-1.99 (m, 3H), 1.97-1.94 (m, 1H), 1.63-1.40 (m, 7H), 1.31 (s, 12H), 0.88 (s, 3H). $^{13}\text{C NMR}$ (125 MHz, CDCl_3 , ppm) δ 220.56, 199.80 (d, $J_{\text{C-F}} = 3.8$ Hz), 145.23, 136.85 (dd, $J_{\text{C-F}} = 2.5, 1.3$ Hz), 135.53 (t, $J_{\text{C-F}} = 27.5$ Hz), 134.66, 130.65, 129.19, 128.69, 127.72, 127.06, 127.02, 126.98, 126.93, 125.53, 124.80 (t, $J_{\text{C-F}} = 250.0$ Hz), 84.17, 50.52, 47.90, 44.71, 37.84, 35.82, 35.29, 31.55, 29.34 (t, $J_{\text{C-F}} = 2.5$ Hz), 26.31, 25.59, 24.85, 24.84, 21.60, 13.82. $^{19}\text{F NMR}$ (376 MHz, CDCl_3 , ppm) δ -89.35 (d, $J_{\text{F-F}} = 240.6$ Hz, 1F), -93.93 (dd, $J_{\text{F-F}} = 240.7, 11.3$ Hz, 1F). $^{11}\text{B NMR}$ (192 MHz, CDCl_3 , ppm) δ 31.67 (s, 1B). **ESI-MS:** calcd for $\text{C}_{41}\text{H}_{47}\text{BF}_2\text{NaO}_4$ ($(\text{M}+\text{Na})^+$): 675.3433, found: 675.3425.



(7c) Transparent sticky oil (Procedure H: 21% isolated). $^1\text{H NMR}$ (500 MHz, CD_3OD , ppm) δ 7.88 (dd, 7.1 Hz, 2H), 7.58 (m, 1H), 7.46 (t, 7.08 Hz, 2H), 7.27 (m, 3H), 7.18-7.12 (m, 7H), 3.09-3.04 (m, 4H) $^{13}\text{C NMR}$ (125 MHz, CD_3OD , ppm) δ 202.27, 156.96, 155.01, 139.84 (d, $J_{\text{C-F}} = 7.7$ Hz), 138.59, 134.81, 134.46, 134.23, 131.28, 131.25, 130.32, 130.23, 130.04, 130.03, 128.81, 129.76, 129.63, 129.35 (d, $J_{\text{C-F}} = 3.1$ Hz), 129.06, 122.17, 122.00, 38.05 (d, $J_{\text{C-F}} = 1.9$ Hz), 28.05 (d, $J_{\text{C-F}} = 7.1$ Hz). $^{19}\text{F NMR}$ (376 MHz, CD_3OD , ppm) δ 105.39.

K) Computational Details

Electronic structure calculations were performed using Gaussian 16 revision C.01.⁷ The M06-2X functional⁸ was used with D3 empirical dispersion⁹ and an ultrafine integration grid for all atoms. The SMD solvent model¹⁰ was used with the previously reported parameters for 1,2-dimethoxyethane.¹¹ All calculations were performed with the LANL2DZ basis set and LANL effective-core potential¹² applied to I, and the 6-311++G(d,p) basis set¹³ applied to all other atoms. After geometry optimization, the geometries were confirmed to have the correct number of imaginary vibrational frequencies (zero for local minima, one for transition states). IRC calculations¹⁴ confirmed that the transition states were connected to the correct local minima. The free energy (G) of each structure was calculated at T = 298.15 K using vibrational frequency analysis.

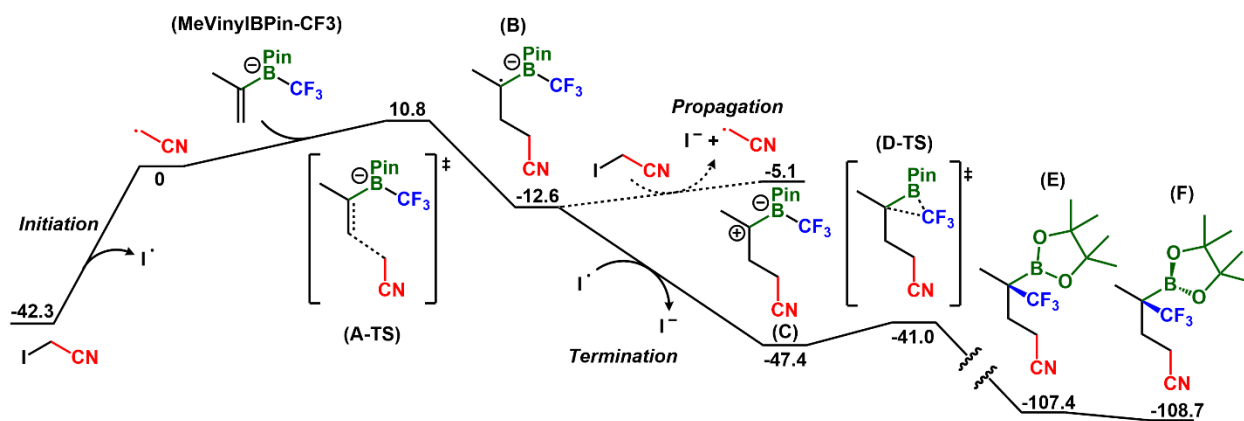
In the proposed mechanism (pathway A), the initial step is photolytic cleavage of iodoacetonitrile, followed by radical addition of $\cdot\text{CH}_2\text{CN}$ to the propenyl boronate (MeVinylBPIn-CF₃). Single-electron transfer from the resulting intermediate B to I \cdot affords intermediate C, which undergoes 1,2-boronate rearrangement to the final product F.

Several alternate pathways were considered. Pathway B undergoes the same initial radical addition to form B, but the 1,2-boronate rearrangement precedes single-electron transfer. Unlike pathway A, the 1,2-boronate rearrangement (B to G) is thermodynamically unfavored ($\Delta G = 6.0$ kcal/mol). Additionally, the formation of intermediate G requires an intramolecular electron transfer from the α -carbon to the nitrile group. Accordingly, pathway B is unlikely.

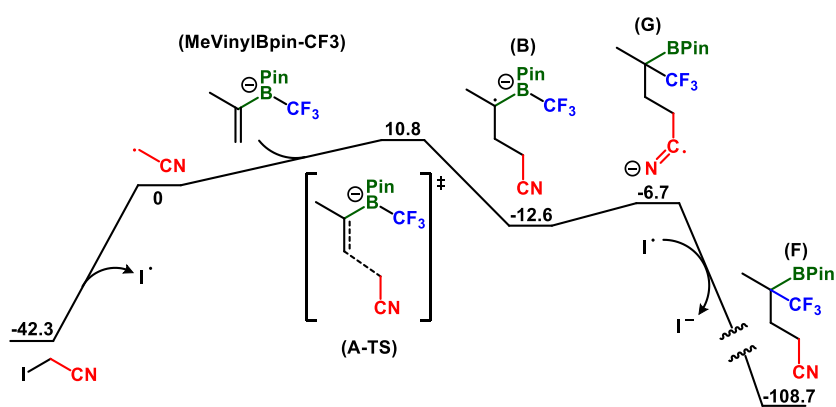
Pathway C begins with radical addition of I \cdot instead of $\cdot\text{CH}_2\text{CN}$. Intermediate H undergoes single-electron transfer to $\cdot\text{CH}_2\text{CN}$ to afford cyclic intermediate J. Intermediate K is formed by a 1,2-boronate rearrangement. Nucleophilic attack of K by $\cdot\text{CH}_2\text{CN}$ affords the final product F. Pathway C is unlikely because the single-electron transfer step ($\Delta G = 10.3$ kcal/mol) is uphill, unlike pathway A.

Pathway D begins with single electron transfer of the starting propenyl boronate to the I \cdot radical. (This is favored by 2.8 kcal/mol over the I \cdot radical addition in pathway C.) The resulting intermediate L has a significantly lengthened B-C bond (2.93 Å) and could dissociate into the 2-propenyl radical and trifluoromethyl-BPin (M). However, fragmentation into $\cdot\text{CF}_3$ and propenyl-BPin (MeVinylBPIn) is also thermodynamically accessible. This can undergo radical rebound of $\cdot\text{CF}_3$ followed by radical addition of $\cdot\text{CH}_2\text{CN}$ to afford the final product. However, this pathway is not supported by the radical crossover experiment, which indicated that dissociation of a fluoroalkyl radical does not occur.

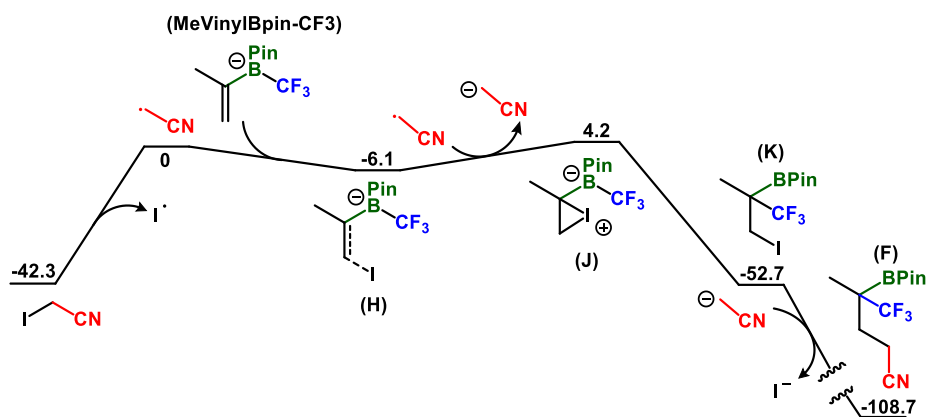
Pathway E is a non-radical mechanism that begins with a 1,2-boronate rearrangement to afford the carbanion intermediate O. Nucleophilic attack of iodoacetonitrile affords the final product F. Pathway E is unlikely because the barrier to carbanion formation ($\Delta G^\ddagger > 23.5$ kcal/mol) is significantly higher than the barrier to radical addition in Pathway A ($\Delta G^\ddagger = 10.8$ kcal/mol).



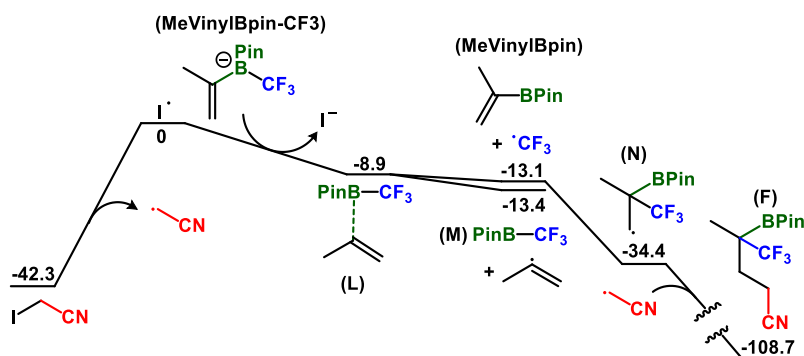
Pathway A: Proposed Mechanism (free energies are in units of kcal/mol)



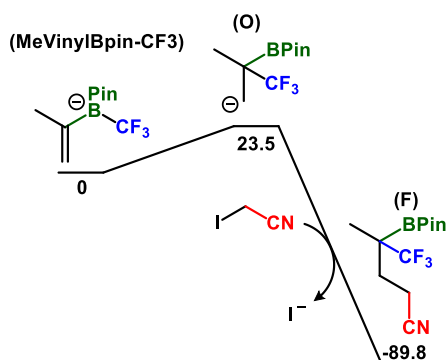
Pathway B: Radical Addition then 1,2-Boronate Rearrangement



Pathway C: Radical Addition of I·



Pathway D: Initial single-electron transfer to I⁻



Pathway E: Non-radical mechanism

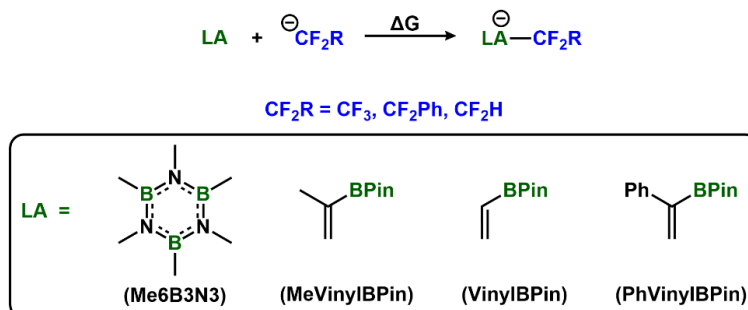
Table S6. Calculated DFT energies of the 1,2-boronate rearrangement mechanism

Entry	Structure	Single-Point Energy (Hartrees)	G (Hartrees)	# Imaginary Frequencies
1	ICH ₂ CN	-143.468848	-143.461655	0
2	·CH ₂ CN (radical)	-132.076443	-132.068670	0
3	⁻ CH ₂ CN (anion)	-132.215698	-132.209161	0
4	I· (radical)	-11.308028	-11.325530	0
5	I ⁻ (anion)	-11.507599	-11.524447	0
6	2-Propenyl radical	-117.196929	-117.156678	0
7	·CF ₃ (radical)	-337.554728	-337.568157	0
8	MeVinylBPin	-528.520445	-528.305722	0
9	MeVinylBPin-CF ₃ ⁻	-866.273298	-866.051951	0
10	A-TS	-998.351830	-998.103339	1
11	B	-998.393838	-998.140769	0
12	C	-998.251941	-997.997296	0
13	D-TS	-998.244273	-997.987112	1
14	E	-998.354239	-998.092791	0
15	F	-998.356514	-998.094875	0
16	G	-998.388069	-998.131248	0
17	H	-877.605075	-877.387275	0
18	J	-877.451860	-877.230345	0
19	K	-877.544907	-877.320975	0

20	L	-866.082441	-865.867230	0
21	M	-748.874275	-748.717654	0
22	N	-866.138219	-865.915886	0
23	O	-866.238079	-866.014430	0

To find the fluoroalkyl binding affinity for each Lewis acid (LA), ΔG values were calculated for the scheme below.

Table S7. Calculated fluoroalkyl binding energies



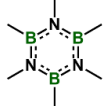
Entry	Lewis Acid	CF_2R^-	ΔG (kcal/mol)
1		CF_3^-	-7.9
2		CF_2Ph^-	-11.3
3		CF_2H^-	-17.9
4		CF_3^-	-12.8
5		CF_2Ph^-	-16.7
6		CF_2H^-	-19.1
7		CF_3^-	-12.9
8		CF_2Ph^-	-17.0
9		CF_2H^-	-23.3
10		CF_3^-	-14.1
11		CF_2Ph^-	-18.1
12		CF_2H^-	-24.6

Table S8. Calculated DFT energies for fluoroalkyl binding

Entry	Structure	Single-Point Energy (Hartrees)	G (Hartrees)	# Imaginary Frequencies
1	CF_3^-	-337.709387	-337.725873	0
2	CF_2Ph^-	-469.458696	-469.392724	0
3	CF_2H^-	-238.424414	-238.431548	0
4	Me6B3N3	-478.470108	-478.248354	0
5	Me6B3N3- CF_3^-	-816.215314	-815.986814	0
6	Me6B3N3- CF_2Ph^-	-947.971890	-947.659129	0
7	Me6B3N3- CF_2H^-	-716.946003	-716.708436	0
8	MeVinylBPin	-528.520445	-528.305722	0
9	MeVinylBPin- CF_3^-	-866.273298	-866.051951	0

10	MeVinylBPin-CF2Ph ⁻	-998.031281	-997.725002	0
11	MeVinylBPin-CF2H ⁻	-767.000565	-766.767654	0
12	VinylBPin	-489.211964	-489.023361	0
13	VinylBPin-CF3 ⁻	-826.965209	-826.769789	0
14	VinylBPin-CF2Ph ⁻	-958.724007	-958.443196	0
15	VinylBPin-CF2H ⁻	-727.696933	-727.492003	0
16	PhVinylBPin	-720.236467	-719.972989	0
17	PhVinylBPin-CF3 ⁻	-1057.992550	-1057.721396	0
18	PhVinylBPin-CF2Ph ⁻	-1189.750945	-1189.394497	0
19	PhVinylBPin-CF2H ⁻	-958.724306	-958.443786	0

L) Quantum Yield Measurement

Photon Flux Measurement

The ferrioxalate actinometry procedure to measure photon flux is adapted from prior literature.^{15, 16, 17} This experiment was performed in ambient atmosphere in the dark under red LED lights. A 25mL phenanthroline solution was prepared by dissolving 1,10-phenanthroline (25 mg) and anhydrous sodium acetate (3.39 g) in 0.5M aqueous H₂SO₄. A 25mL ferrioxalate (0.15 M) solution was prepared by dissolving potassium trisoxalatoferrate (III) trihydrate (1.84 g, 3.75 mmol) in 0.05M aqueous H₂SO₄.

A Kessil lamp (440 nm, PR160 series) was set to 25% intensity and allowed to warm up for at least an hour. For each timepoint (t = 0, 5, 10, 15 s), a 2 mL aliquot of the ferrioxalate solution was irradiated in a cuvette (path length = 1 cm) at a distance of 10cm from the Kessil lamp. Phenanthroline solution (1 mL) was added, and then the mixture was allowed to sit for ca. 30 minutes. The mixture was diluted 10-fold using deionized water. The absorbance of the diluted solution was measured at 510 nm.

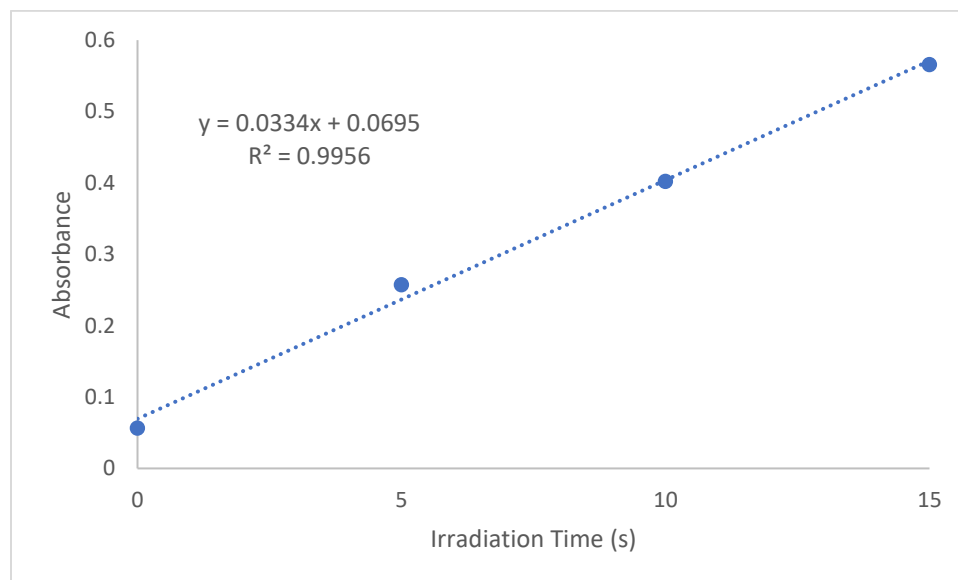


Figure S18. Absorbance of ferrioxalate solution at 440 nm after irradiation at 510 nm.

The slope of the absorbance-time plot was found to be $\Delta A/t = 0.0334/s$.

The equation for photon flux (in mol photon/s) is,¹⁷

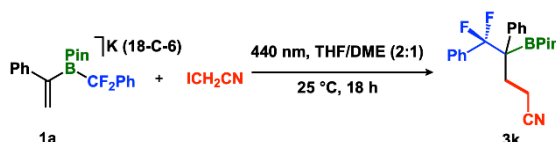
$$\text{photon flux} = \frac{V}{l \cdot \epsilon \cdot \Phi \cdot f} \cdot \frac{\Delta A}{t}$$

V is the final volume of the diluted sample (0.030L), and l is the path length (1 cm). ϵ is the molar absorptivity of the Fe^{2+} product at 510 nm ($11050 \text{ L mol}^{-1} \text{ cm}^{-1}$).¹⁶ Φ is the quantum yield of the reaction (1.01 at 436 nm for a 0.15 M ferrioxalate solution).¹⁶ f is the fraction of light absorbed by the 0.15 M ferrioxalate solution at 440 nm. The absorbance of the 0.15 M ferrioxalate solution was found to be $A = 2.3089$ at 440 nm, giving $f = 1 - 10^{-A} = 0.9951$.

The calculated photon flux is $9.02 \cdot 10^{-8} \text{ mol photon/s}$. For a 2 mL sample with a path length of 1 cm, the cross-sectional area is 2 cm^2 , giving the photon flux per area,

$$\text{photon flux per area} = \frac{9.02 \cdot 10^{-8} \text{ mol photon/s}}{2 \text{ cm}^2} = 4.51 \cdot 10^{-8} \frac{\text{mol photon}}{\text{s} \cdot \text{cm}^2}$$

Quantum Yield Measurement



1a (30. mg, 0.045 mmol, 1.0 equiv.), THF (1 mL), DME (0.5 mL), and iodoacetonitrile (5 μL , 0.069 mmol, 1.5 equiv.) were combined in a UV-vis cuvette (1 cm path length) equipped with a stir bar. The sealed cuvette was removed from the glovebox. While stirring, the cuvette was illuminated for 1 h at a distance of 10 cm from the Kessil lamp (440 nm, PR160 series, 25% intensity). (The lamp was allowed to warm up for at least an hour before the reaction was performed.) The yield of (0.0034 mmol, 7.5%) was assessed by ^{19}F NMR (PhOCF_3 used as internal standard).

The quantum yield Φ is calculated from the equation,

$$\Phi = \frac{\text{mol product}}{\text{mol photon absorbed}}$$

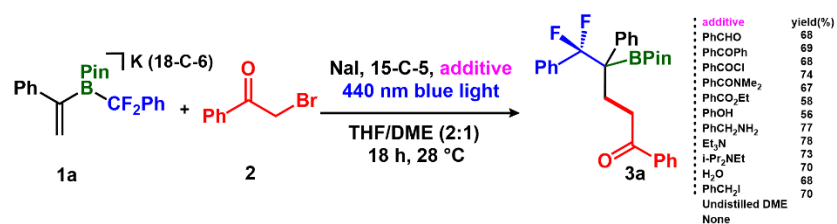
The proposed reaction mechanism begins with photolysis of iodoacetonitrile. The absorbance of iodoacetonitrile (0.046 M, 10 μL in 3 mL 2:1 THF/DME, 1 cm path length) under reaction conditions was found to be $A = 0.030$. The fraction of light (f) absorbed by the iodoacetonitrile is $f = 1 - 10^{-A} = 0.0667$. The cross-sectional area of a 1.5 mL reaction volume in a 1 cm cuvette is 1.5 cm^2 . The mol photons absorbed by the iodoacetonitrile during the $t = 1 \text{ h}$ reaction is,

$$\begin{aligned} \text{mol photon absorbed} &= (\text{photon flux per area}) \cdot (\text{cross-sectional area}) \cdot t \cdot f \\ &= 4.51 \cdot 10^{-8} \frac{\text{mol photon}}{\text{s} \cdot \text{cm}^2} \cdot 1.5 \text{ cm}^2 \cdot 3600 \text{ s} \cdot 0.0667 = 1.626 \cdot 10^{-5} \text{ mol photon} \end{aligned}$$

Calculating the quantum yield,

$$\Phi = \frac{3.4 \cdot 10^{-6} \text{ mol product}}{1.626 \cdot 10^{-5} \text{ mol photon}} = 0.21$$

M) Tolerance test to common functional groups



Vinyl pinacol boronate ester ([R1BPin-CF₂Ph][K(18-C-6)] (R1 = Ar, alkyl, H)) (0.015 mmol, 1.0 equiv.), NaI (0.0075mmol, 0.5 equiv.) and 15-C-5 (0.0075 mmol, 0.5 equiv.) were dissolved in 0.8 mL of THF in a 8 mL vial. To the suspension, a solution of the 2-bromo acetophenone (0.023 mmol, 1.5 equiv.), **additive** (0.023 mmol, 1.5 equiv.) in DME (0.4 mL) was added under irradiation, and the mixture was stirred vigorously overnight under constant irradiation (18 h) before the yield was assessed by ¹⁹F NMR spectroscopy (PhOCF₃ used as internal standard)

N) Spectroscopic data of the products

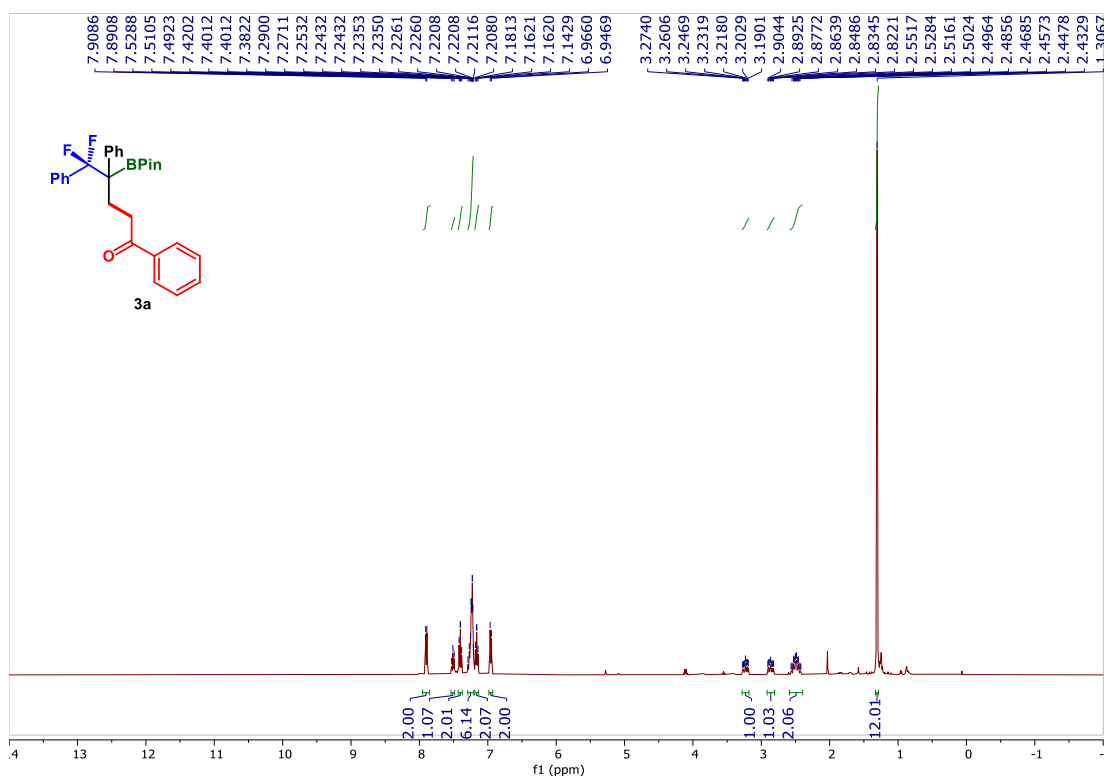


Fig. S19. ¹H NMR spectrum (CDCl₃, 25 °C) of **3a**.

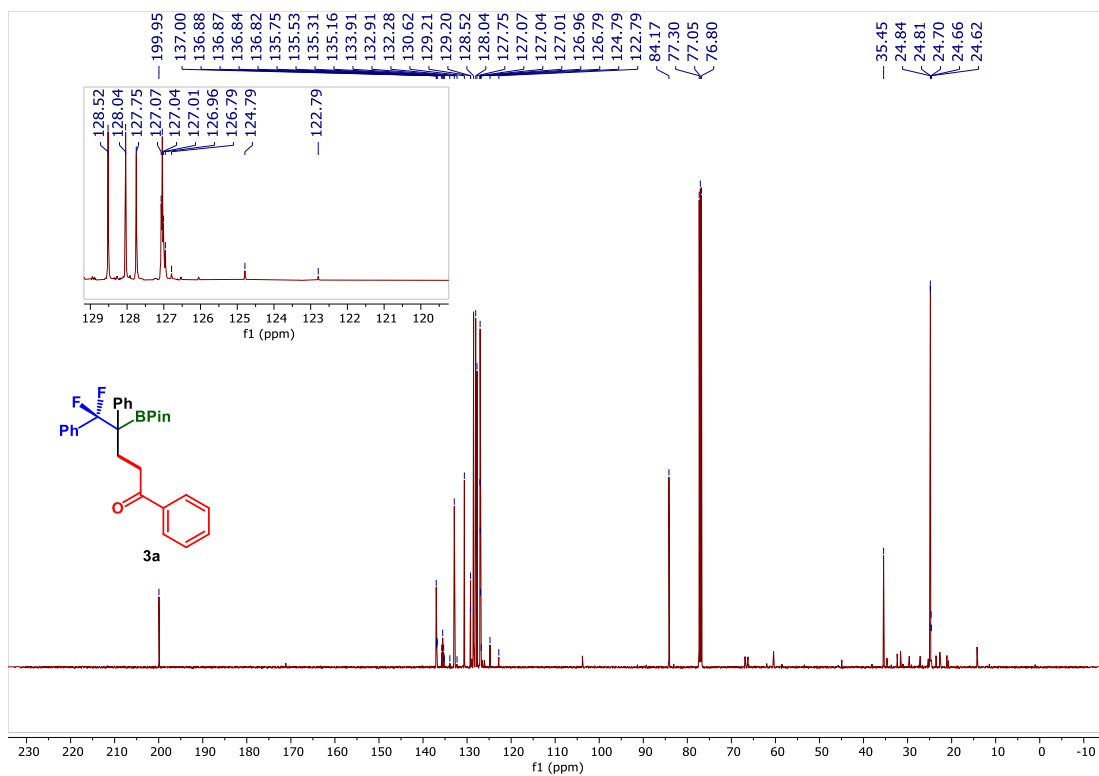


Fig. S20. ¹³C NMR spectrum (CDCl₃, 25 °C) of **3a**.

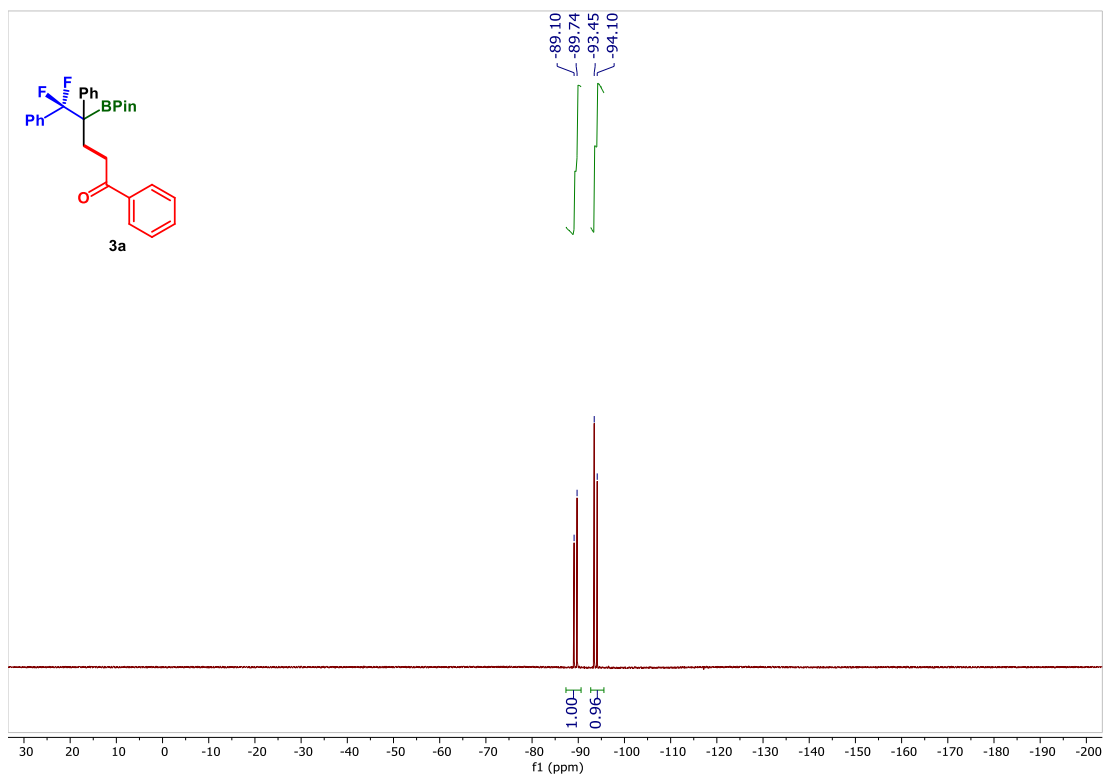


Fig. S21. ¹⁹F NMR spectrum (CDCl₃, 25 °C) of **3a**.

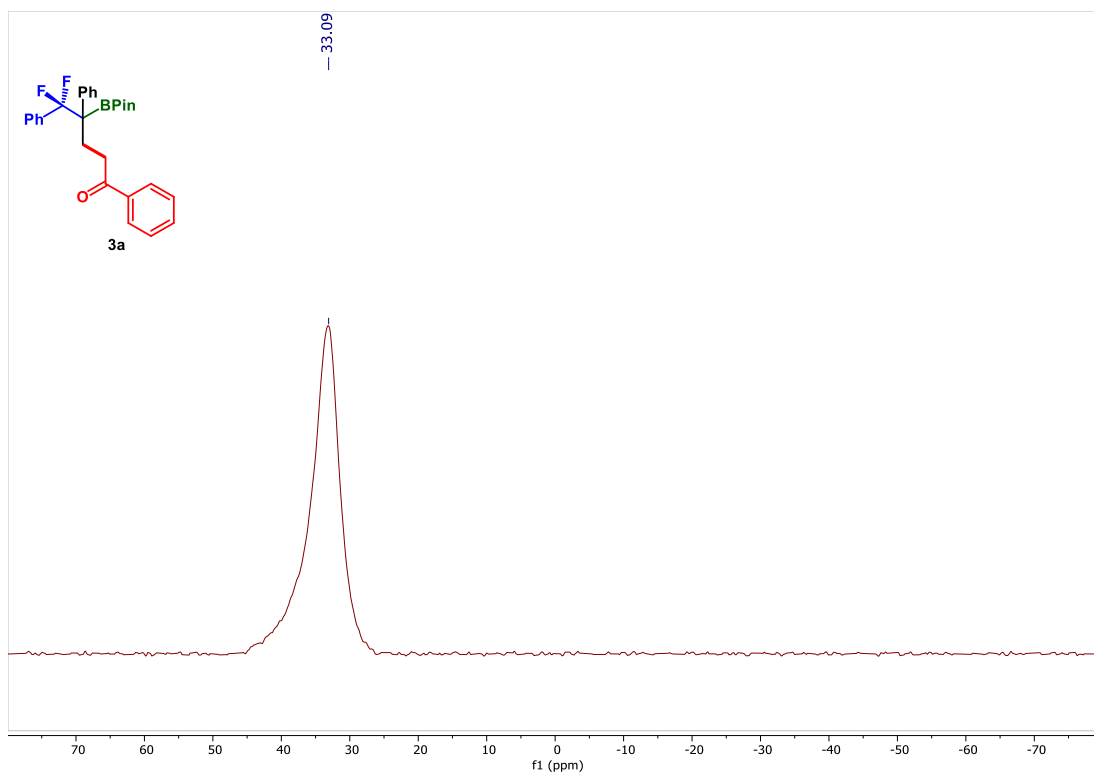


Fig. S22. ¹¹B NMR spectrum (CDCl₃, 25 °C) of **3a**.

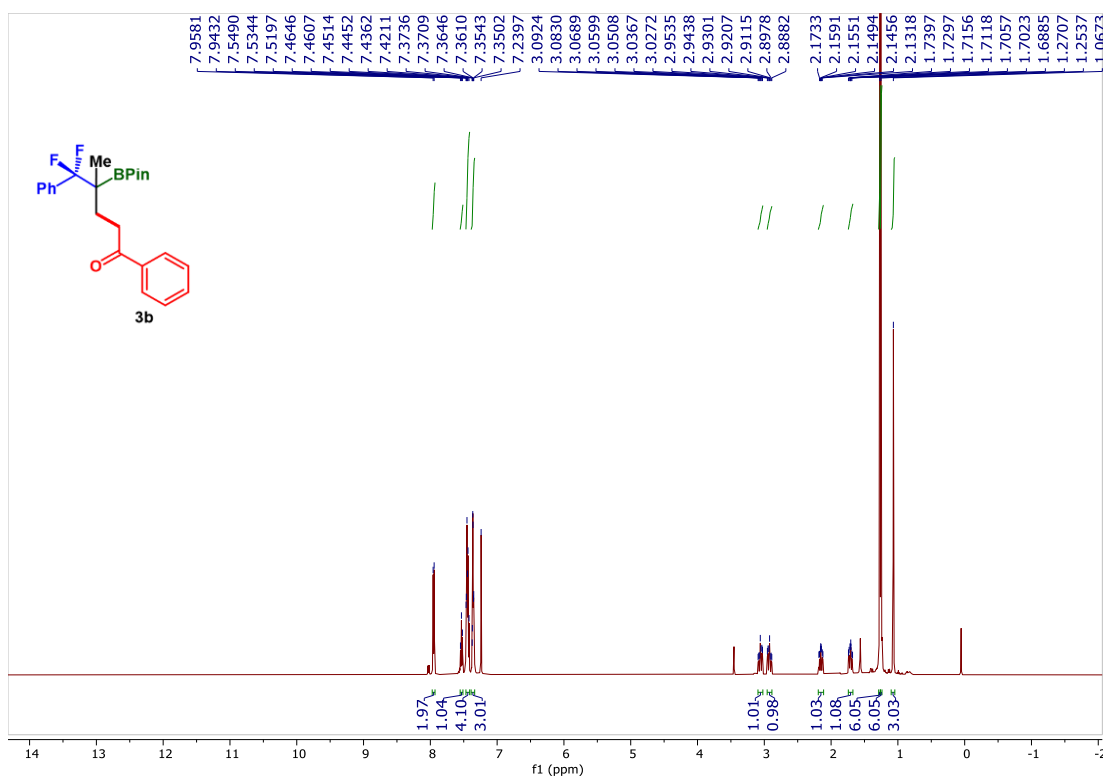


Fig. S23. ¹H NMR spectrum (CDCl₃, 25 °C) of **3b**.

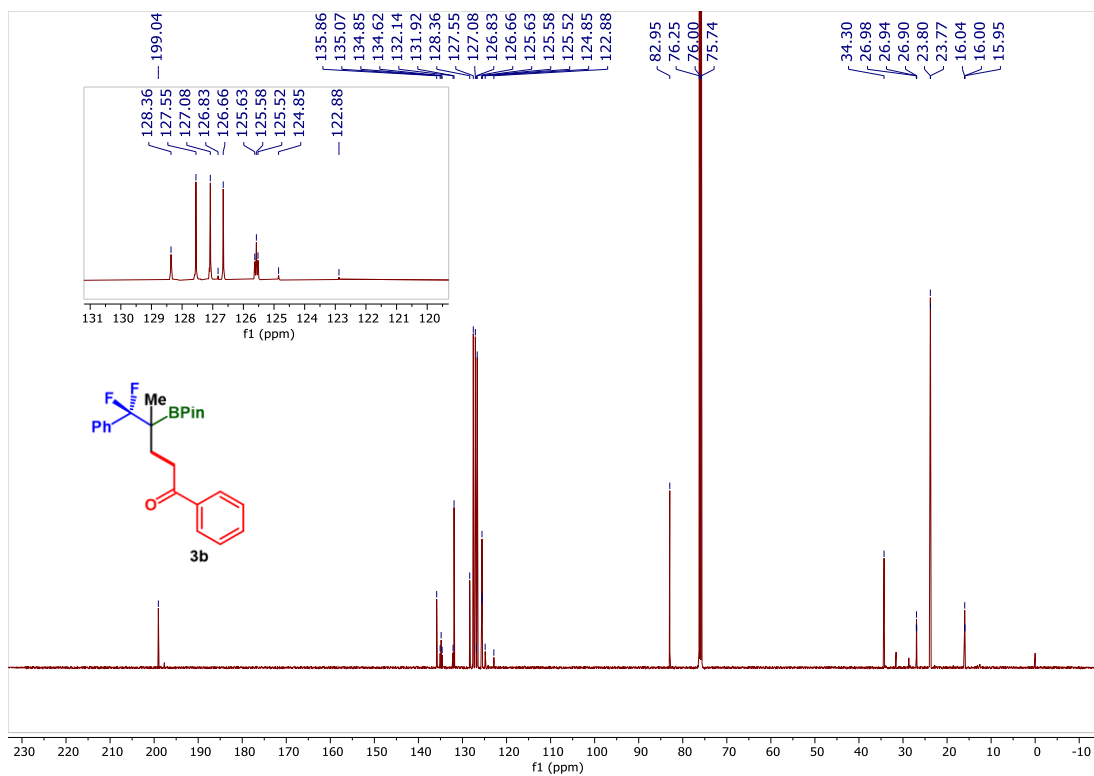


Fig. S24. ^{13}C NMR spectrum (CDCl_3 , 25 °C) of **3b**.

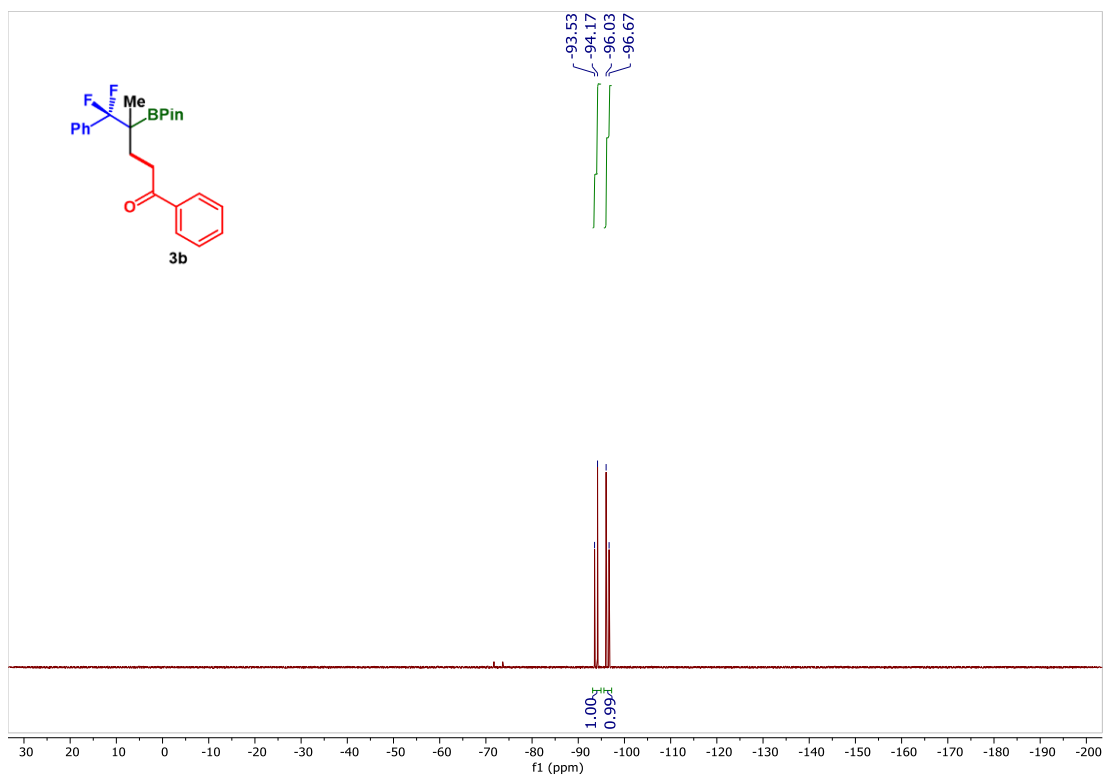


Fig. S25. ^{19}F NMR spectrum (CDCl_3 , 25 °C) of **3b**.

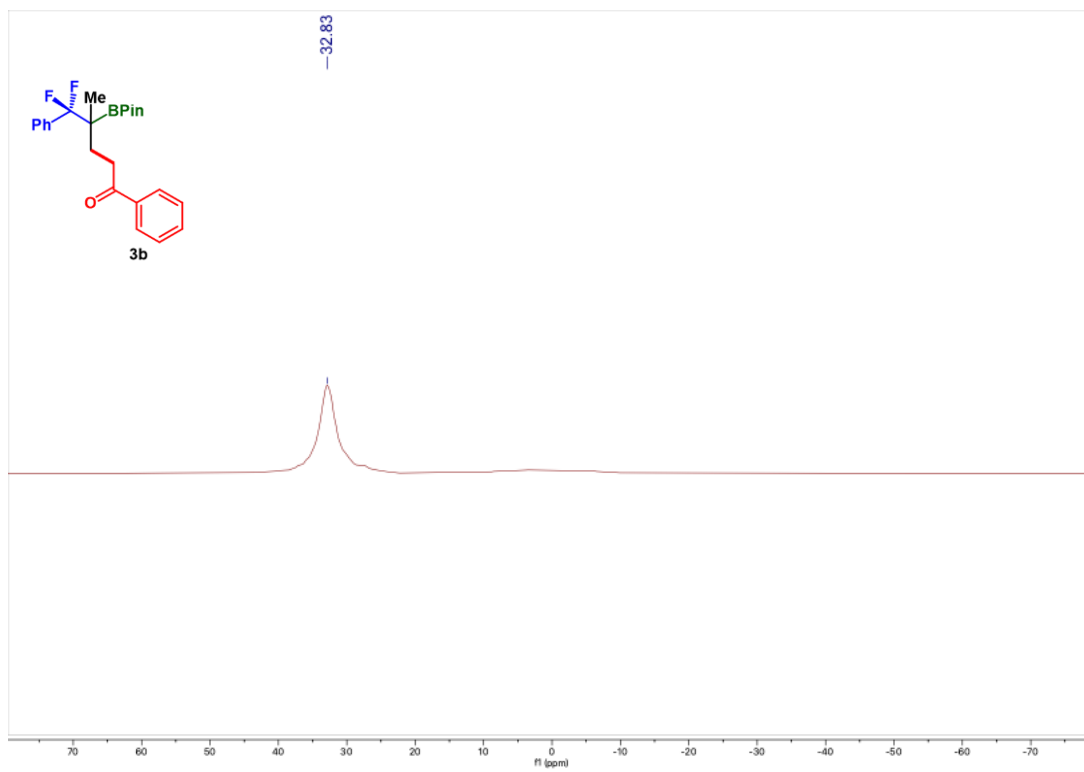


Fig. S26. ^{11}B NMR spectrum (CDCl_3 , 25 °C) of **3b**.

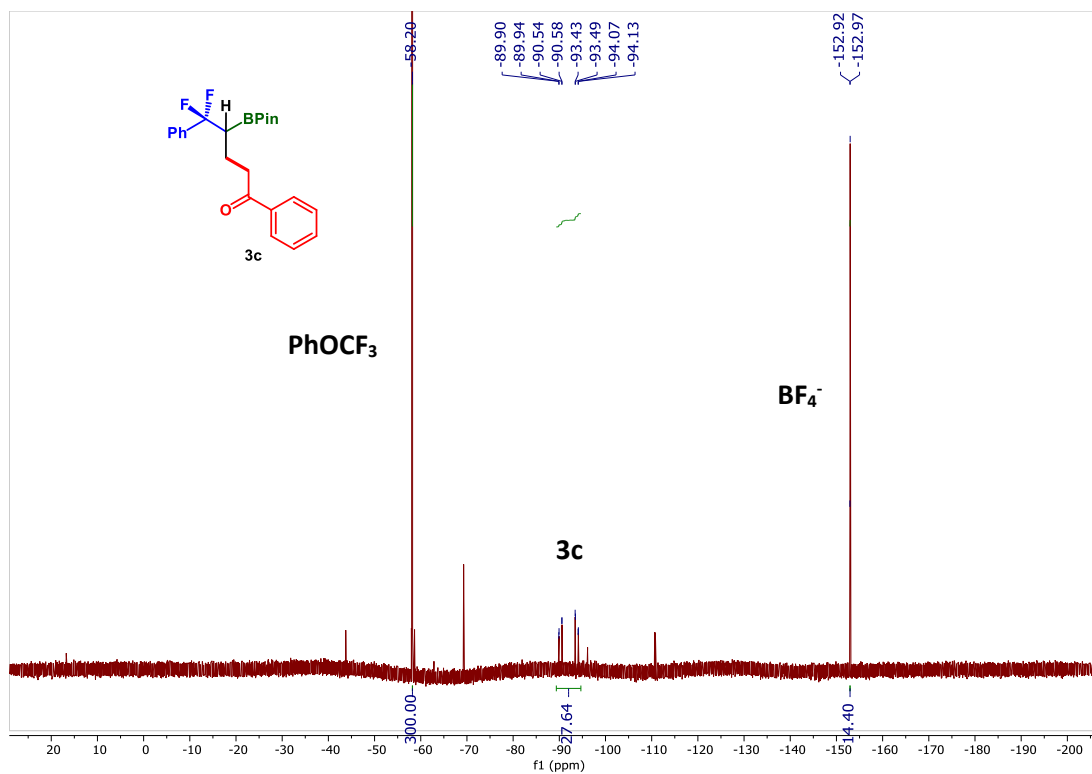


Fig. S27. ¹⁹F NMR spectrum (THF-H₈, 25 °C) of **3c**

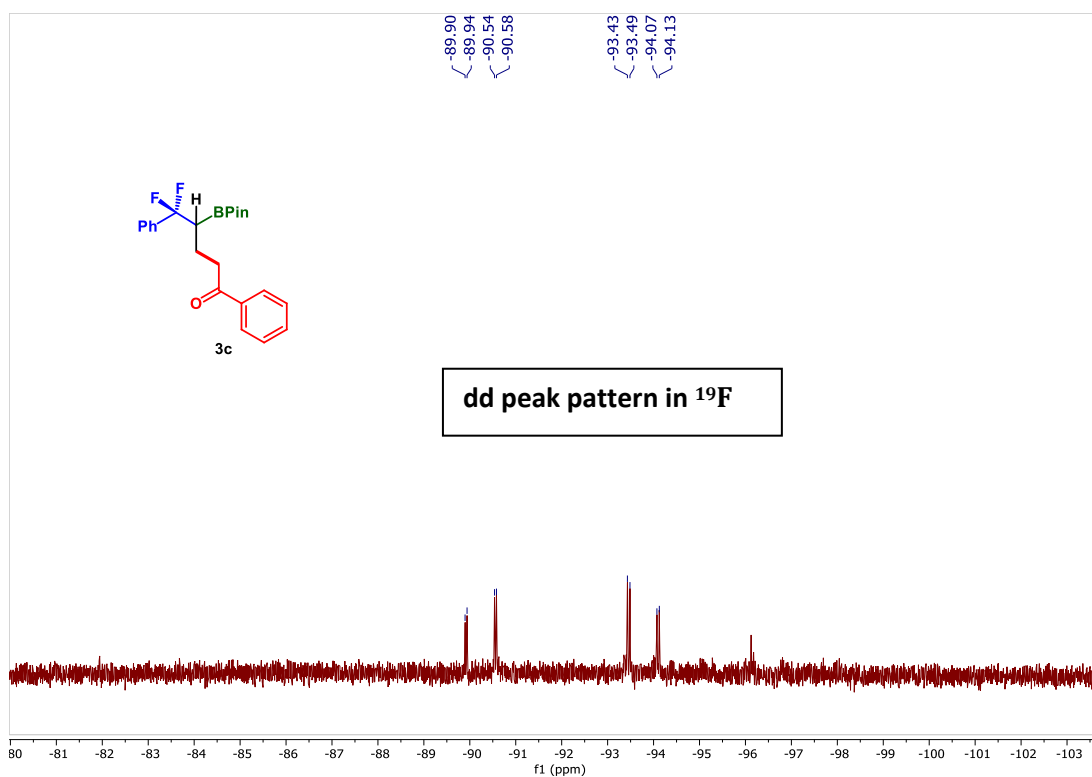


Fig. S28. ¹⁹F NMR spectrum (THF-H₈, 25 °C) of **3c** highlighting product peak.

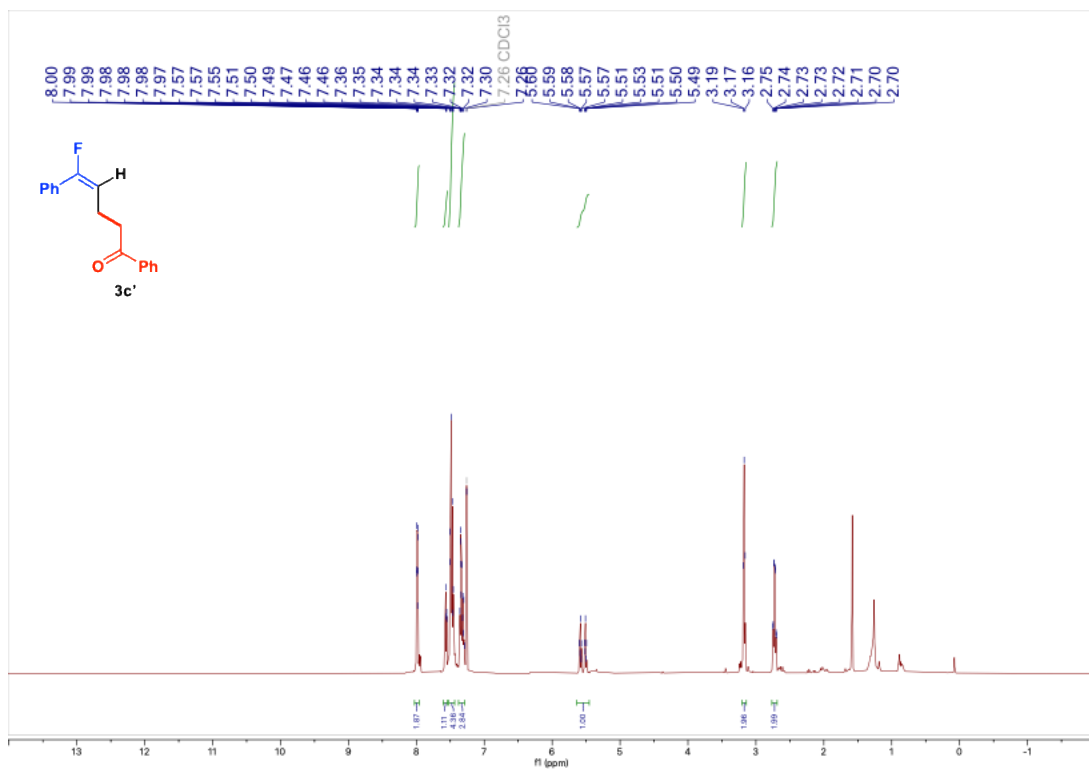


Fig. S29. ¹H NMR spectrum (CDCl₃, 25 °C) of **3c'**

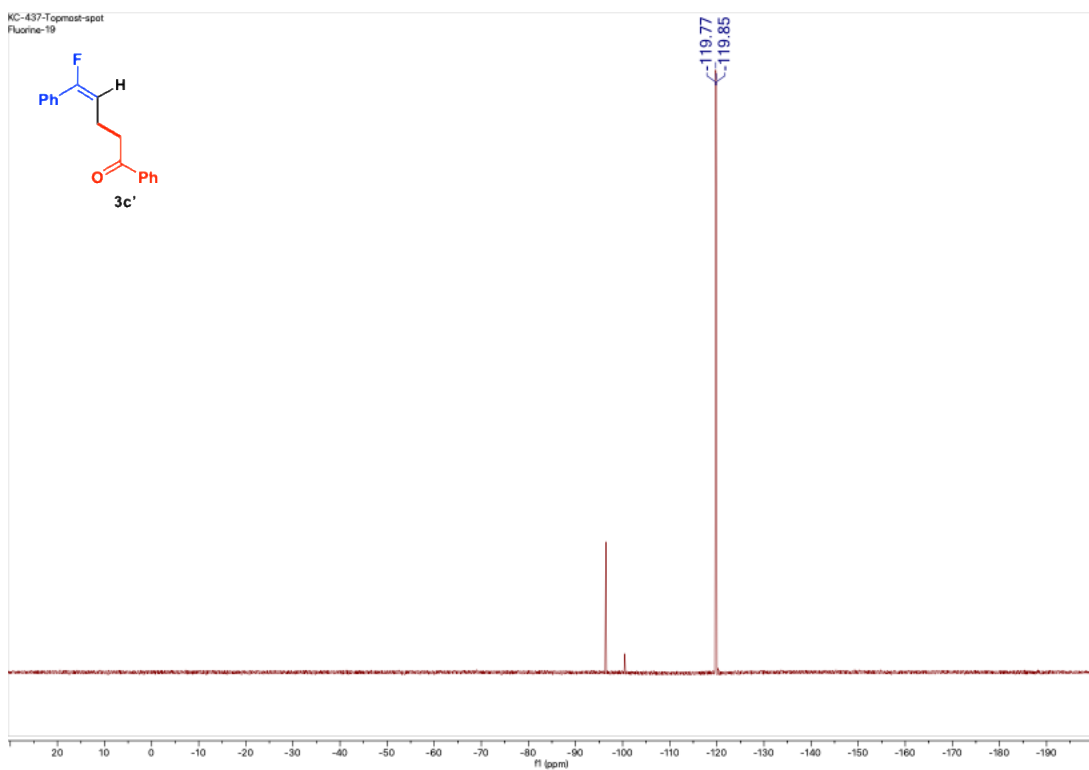


Fig. S30. ¹⁹F NMR spectrum (CDCl₃, 25 °C) of **3c'**

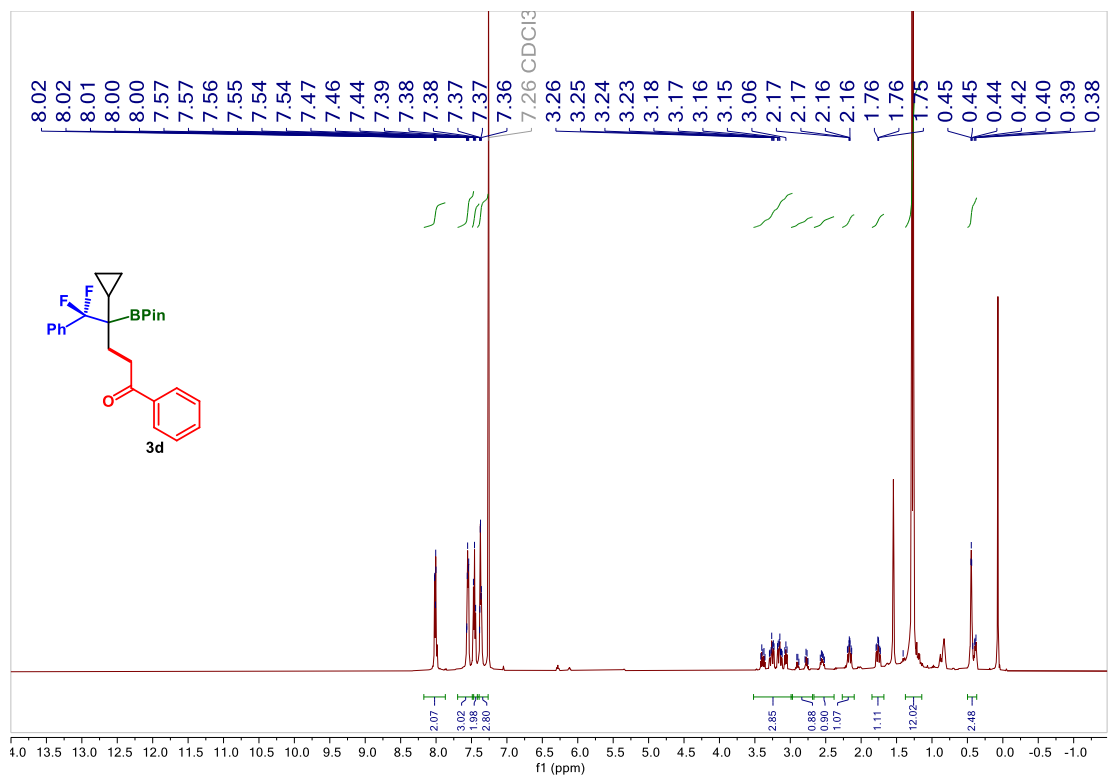


Fig. S31. ¹H NMR spectrum (CDCl₃, 25 °C) of 3d.

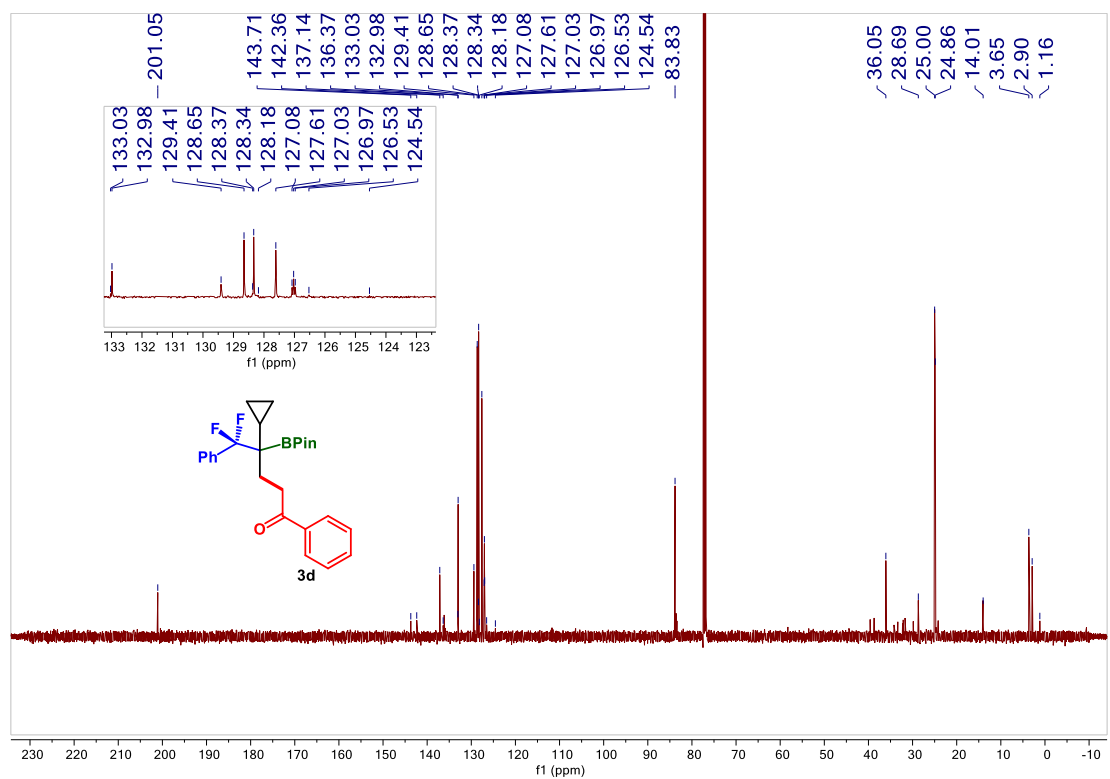


Fig. S32. ¹³C NMR spectrum (CDCl₃, 25 °C) of 3d.

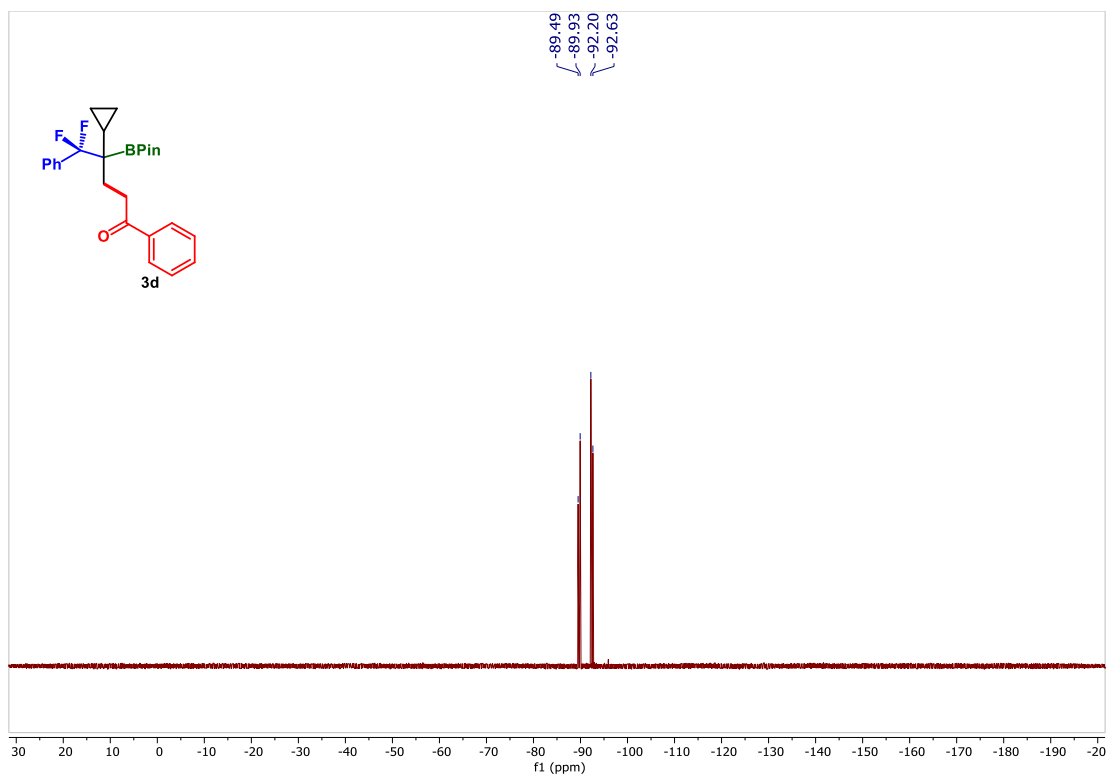


Fig. S33. ^{19}F NMR spectrum (CDCl_3 , 25 $^\circ\text{C}$) of **3d**.

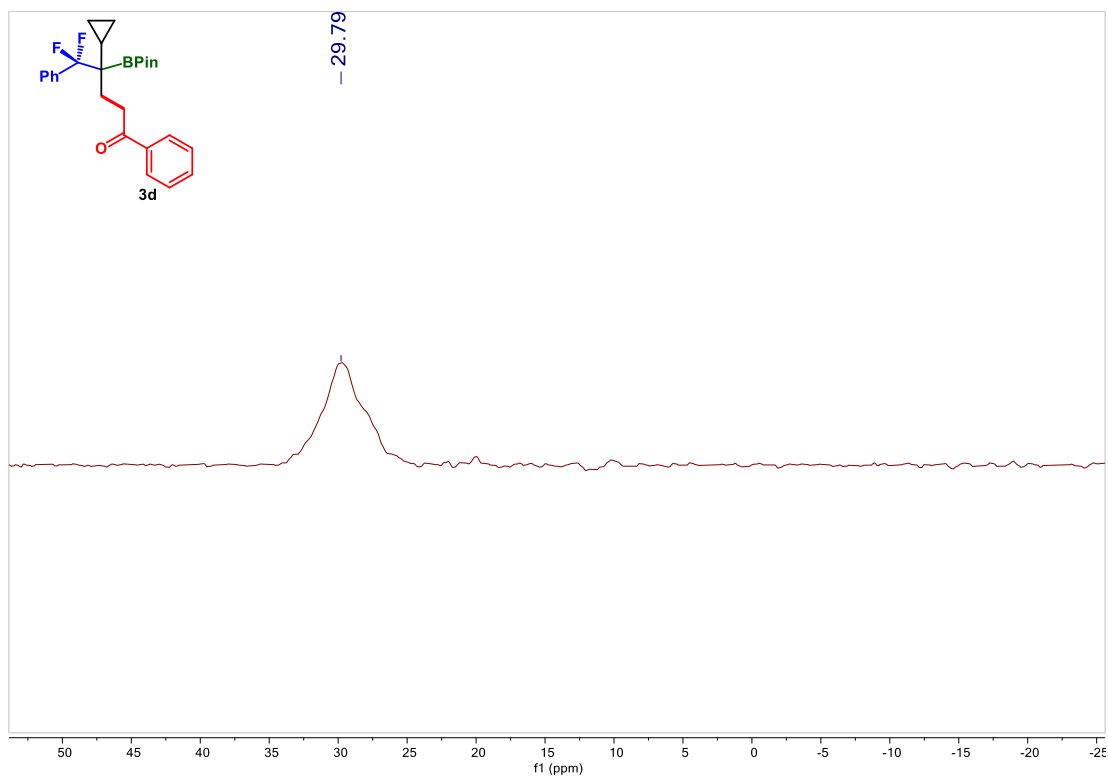


Fig. S34. ^{11}B NMR spectrum (CDCl_3 , 25 $^\circ\text{C}$) of **3d**.

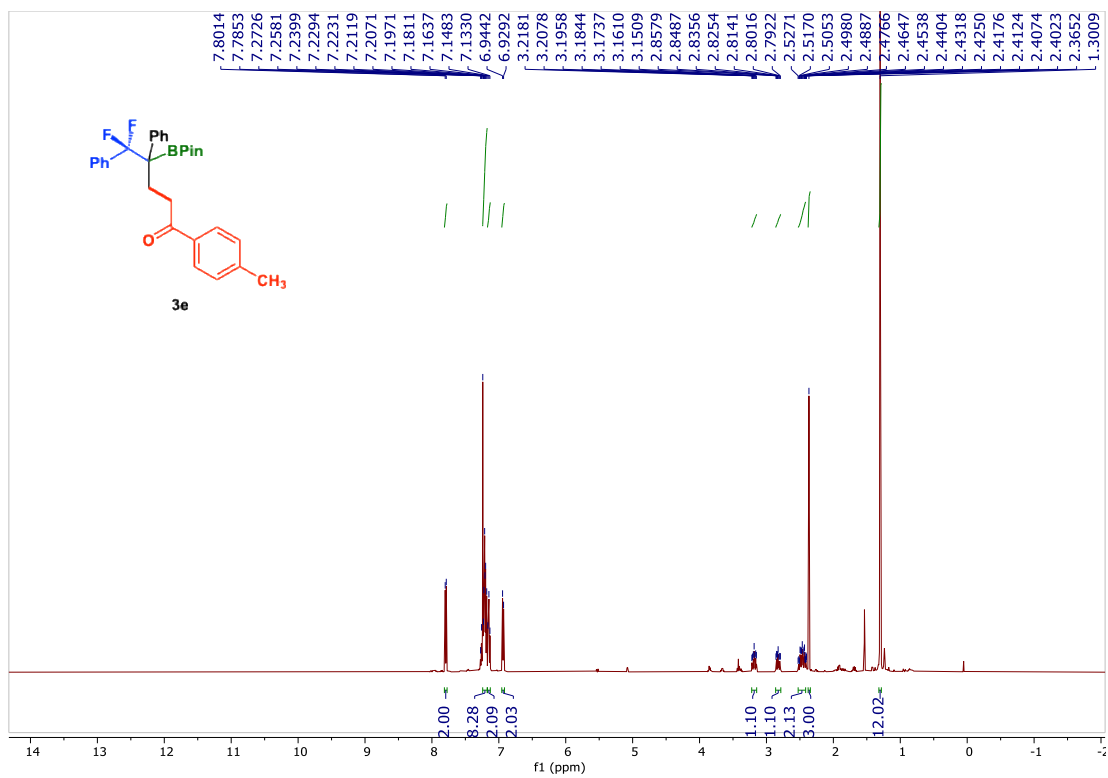


Fig. S35. ¹H NMR spectrum (CDCl₃, 25 °C) of **3e**.

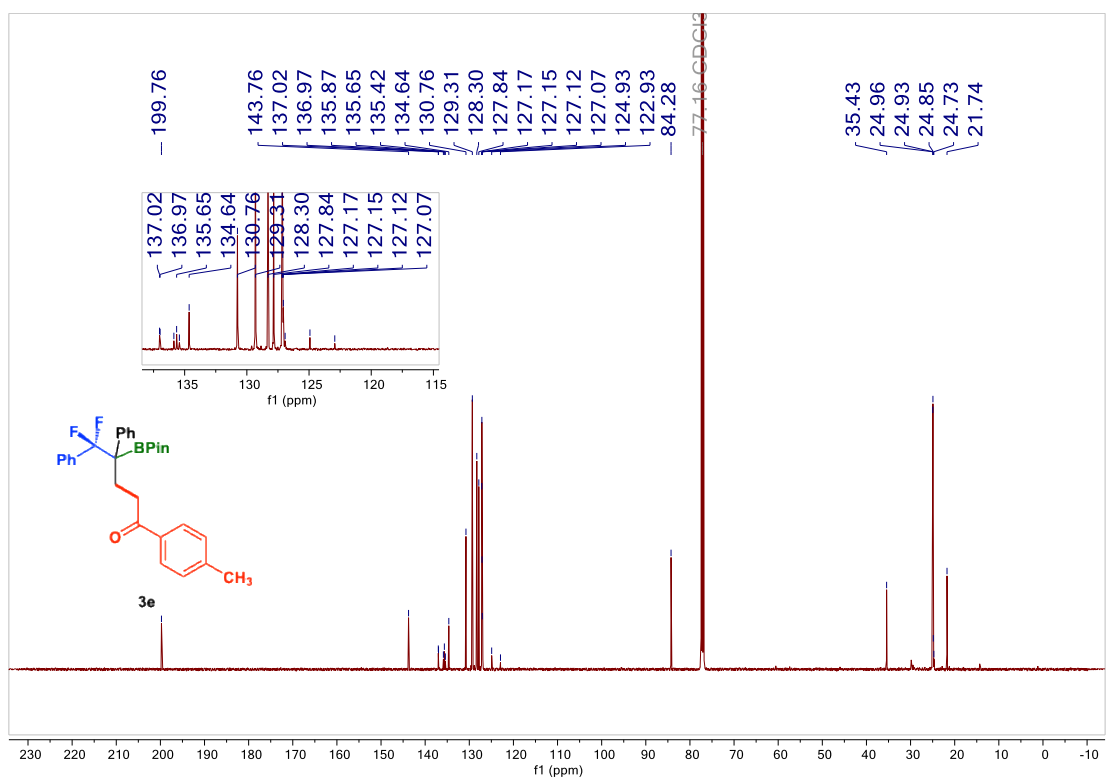


Fig. S36. ¹³C NMR spectrum (CDCl₃, 25 °C) of **3e**.

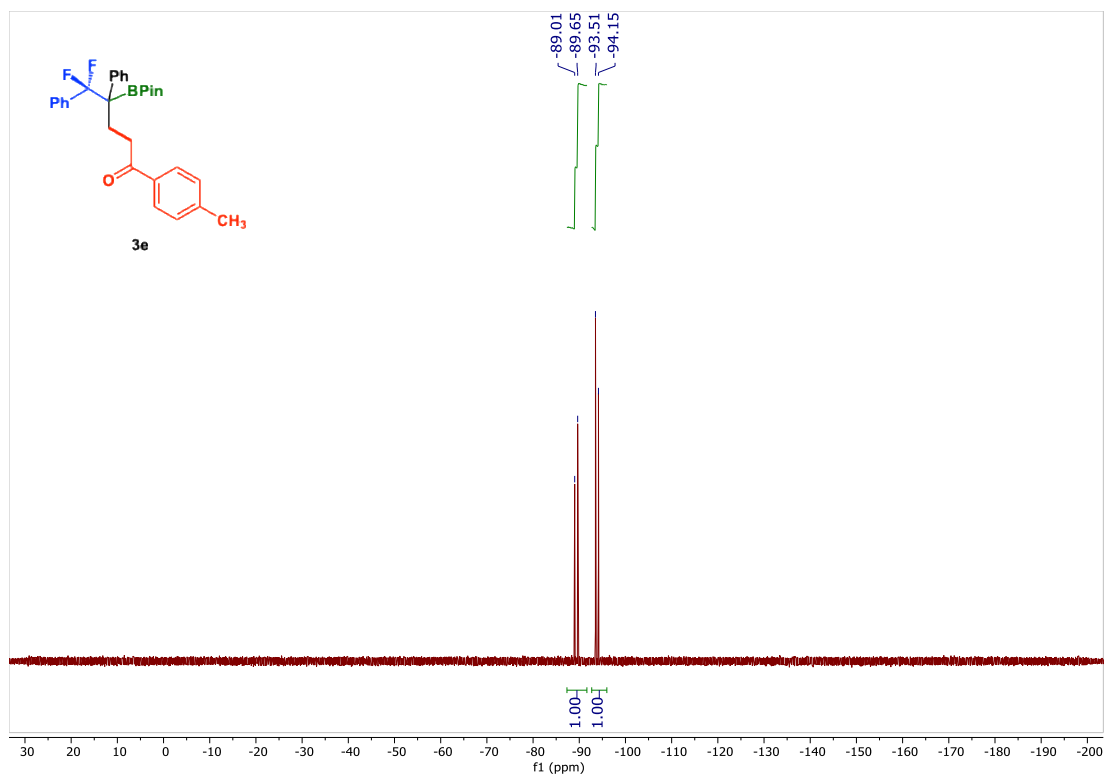


Fig. S37. ¹⁹F NMR spectrum (CDCl₃, 25 °C) of **3e**.

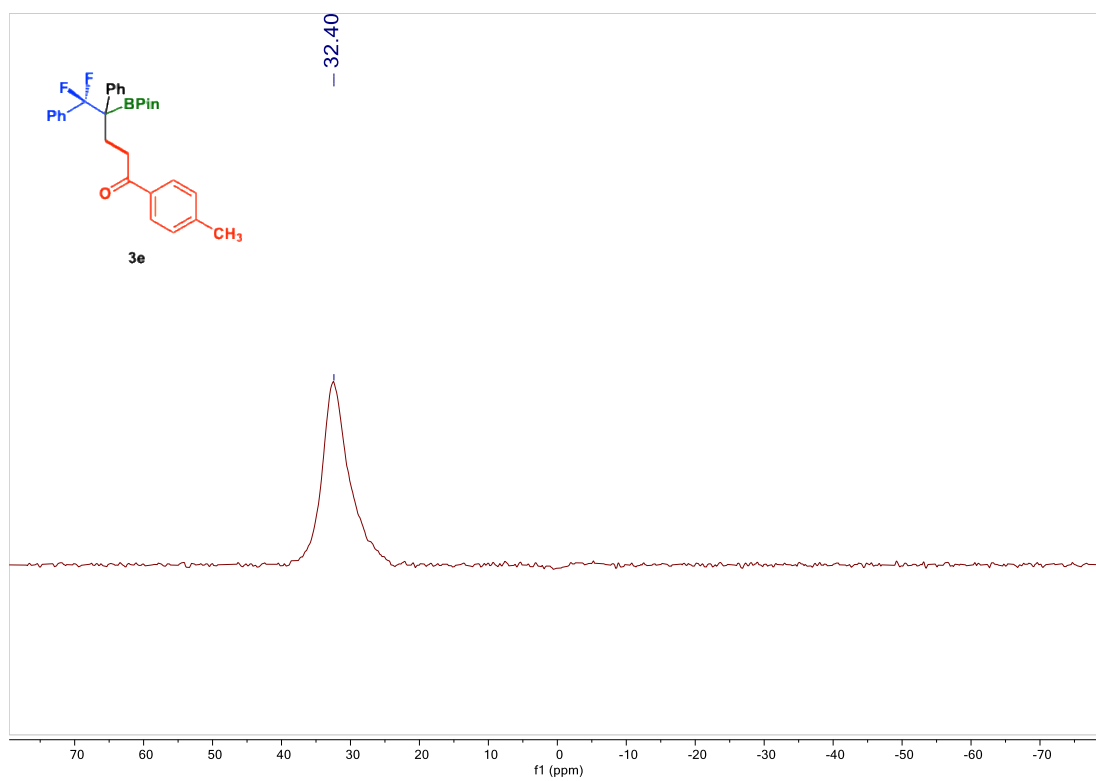


Fig. S38. ¹¹B NMR spectrum (CDCl₃, 25 °C) of **3e**.

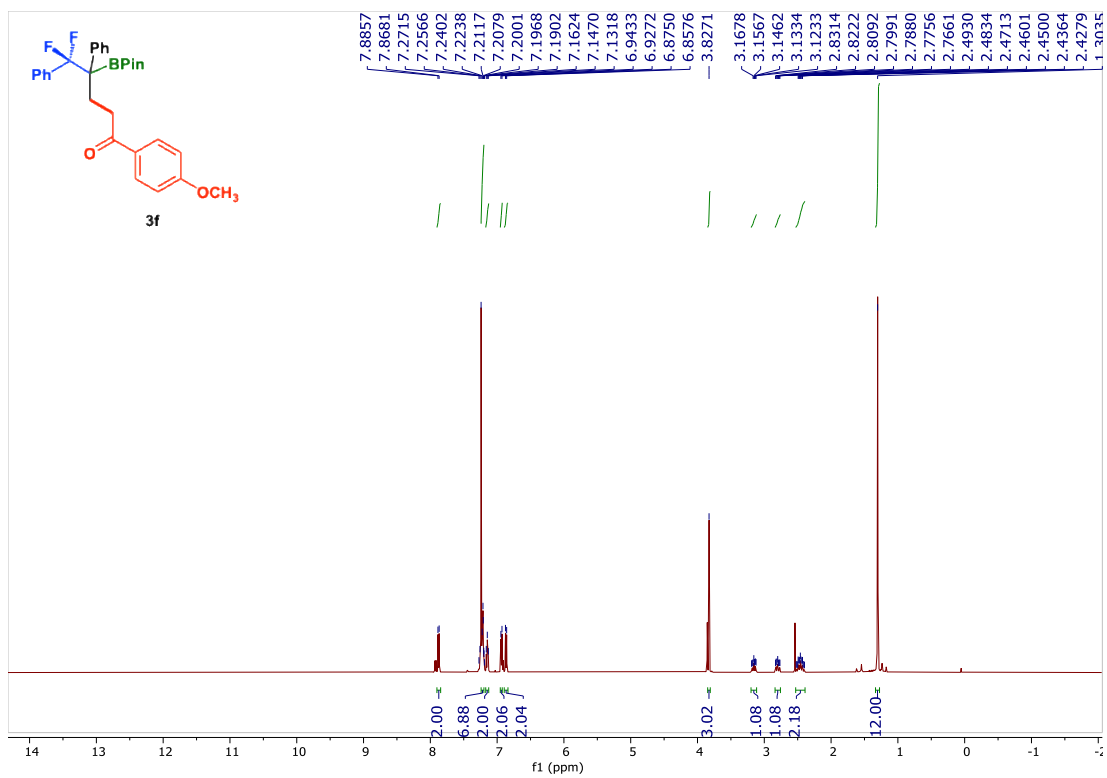


Fig. S39. ¹H NMR spectrum (CDCl₃, 25 °C) of **3f**.

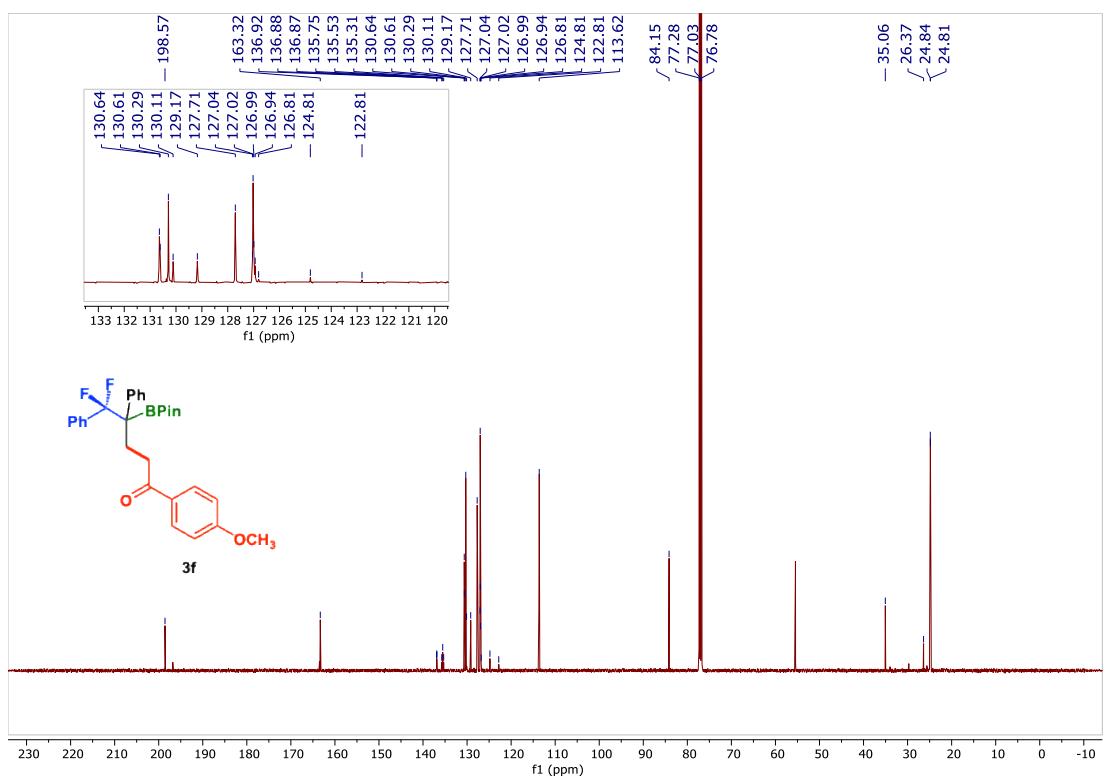


Fig. S40. ¹³C NMR spectrum (CDCl₃, 25 °C) of **3f**.

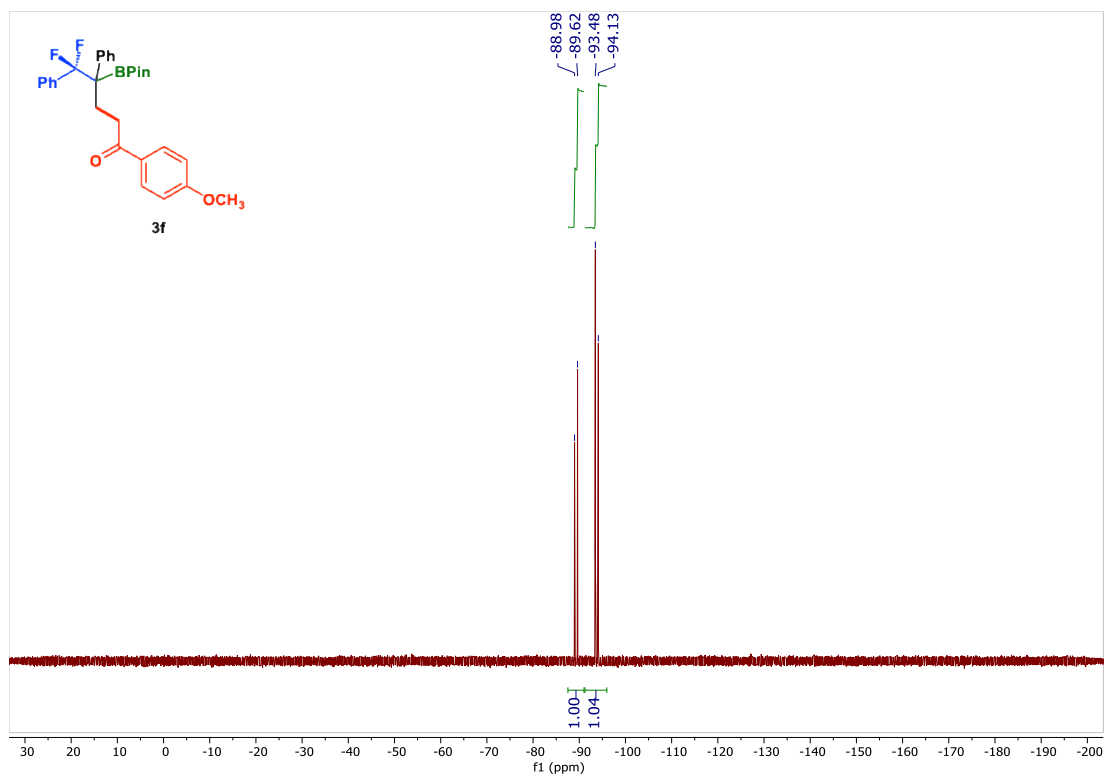


Fig. S41. ^{19}F NMR spectrum (CDCl_3 , 25°C) of **3f**.

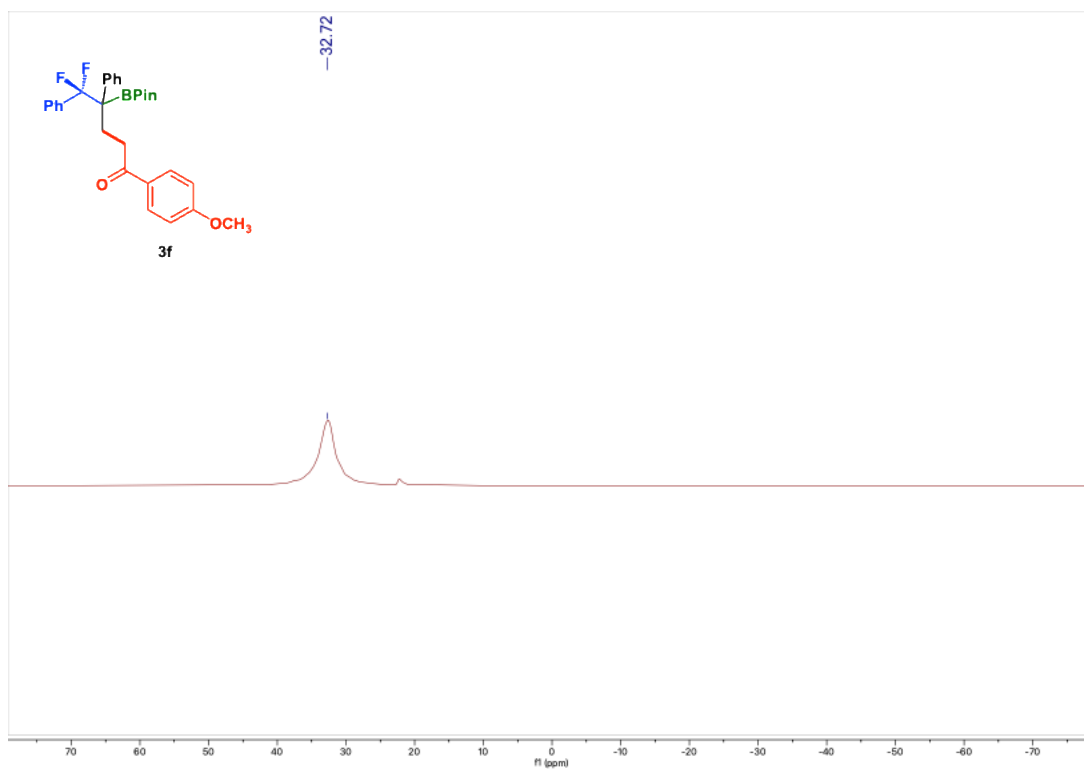


Fig. S42. ^{11}B NMR spectrum (CDCl_3 , 25°C) of **3f**.

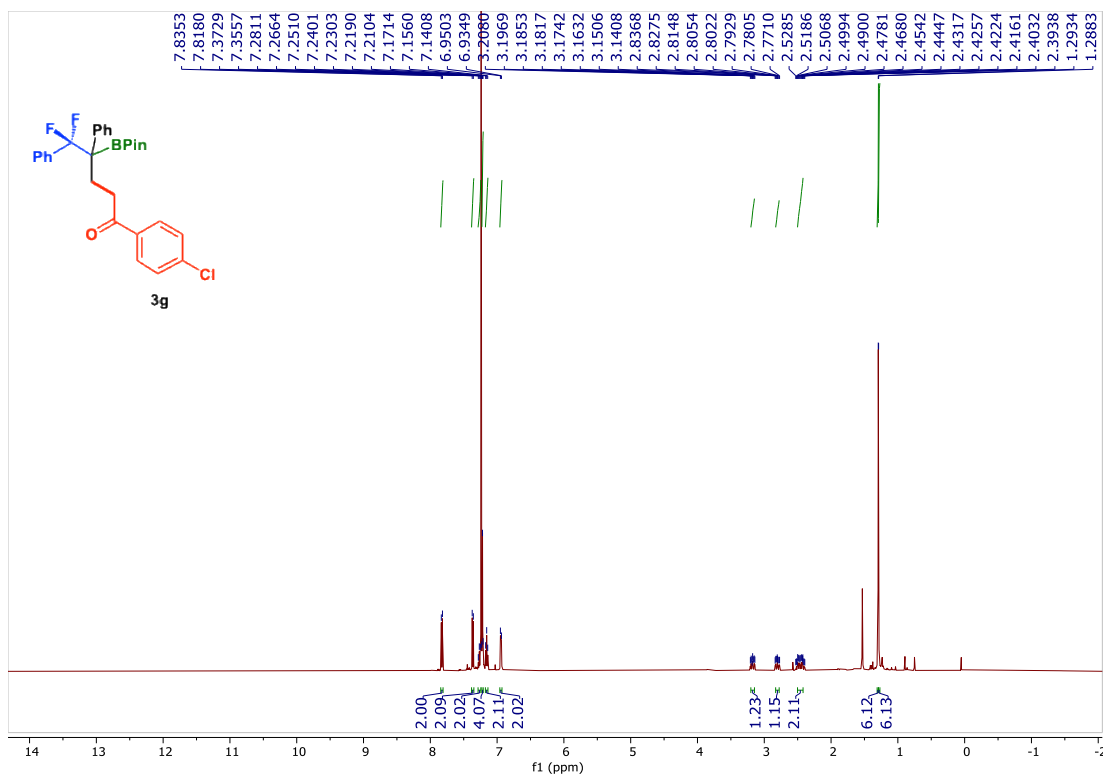


Fig. S43. ¹H NMR spectrum (CDCl₃, 25 °C) of **3g**.

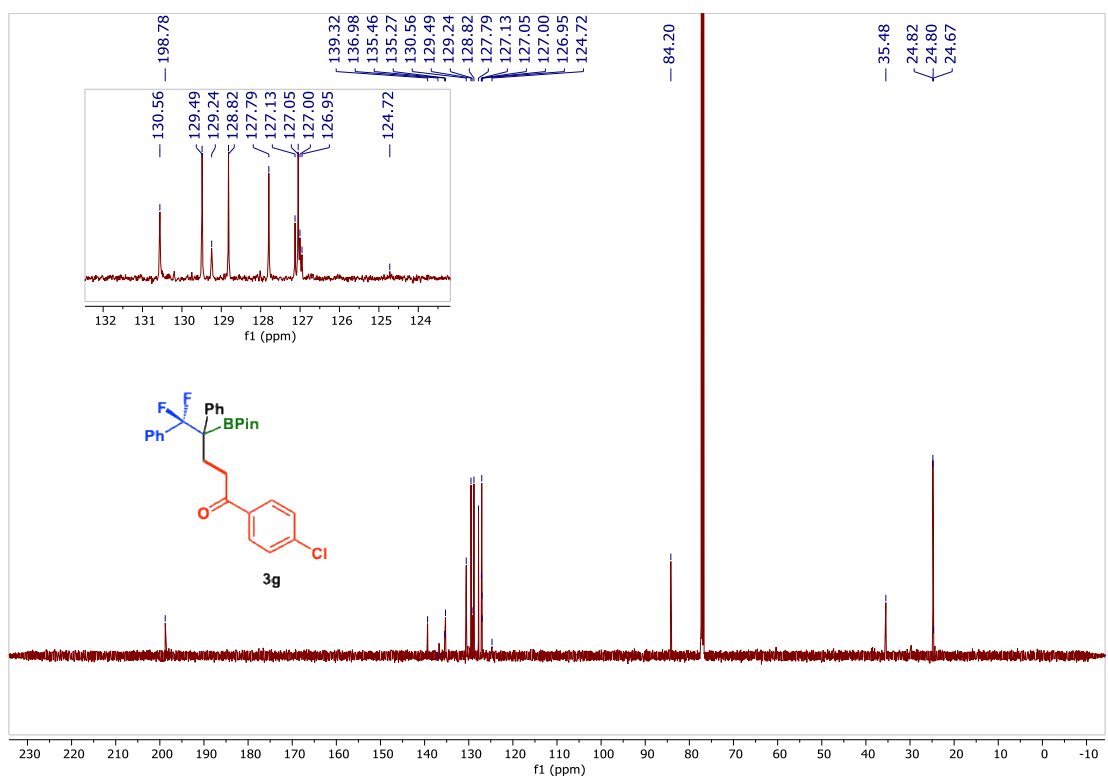


Fig. S44. ¹³C NMR spectrum (CDCl₃, 25 °C) of **3g**.

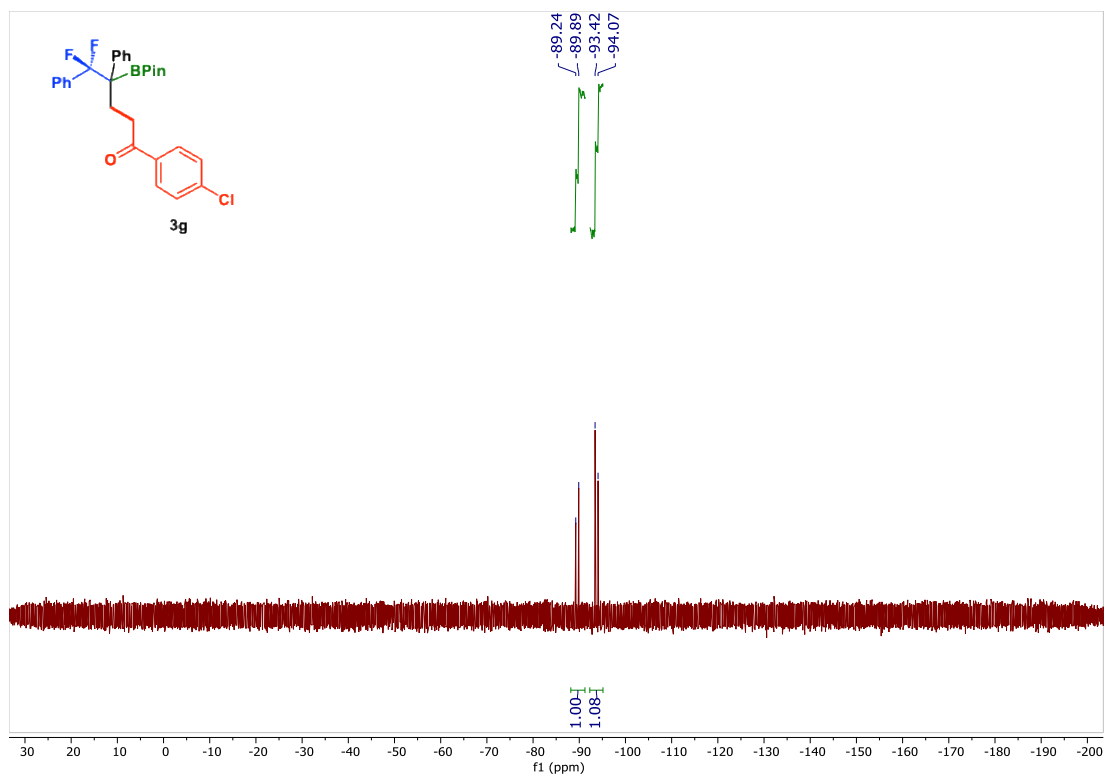


Fig. S45. ^{19}F NMR spectrum (CDCl_3 , 25 °C) of **3g**.

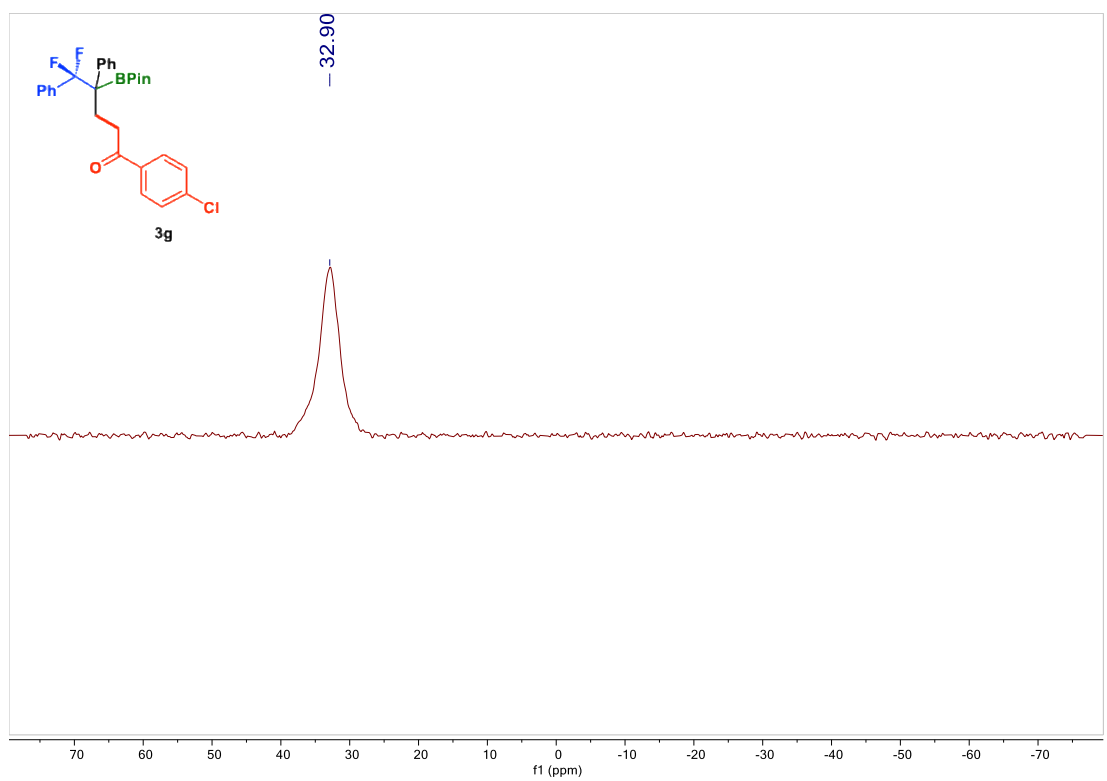


Fig. S46. ^{11}B NMR spectrum (CDCl_3 , 25 °C) of **3g**.

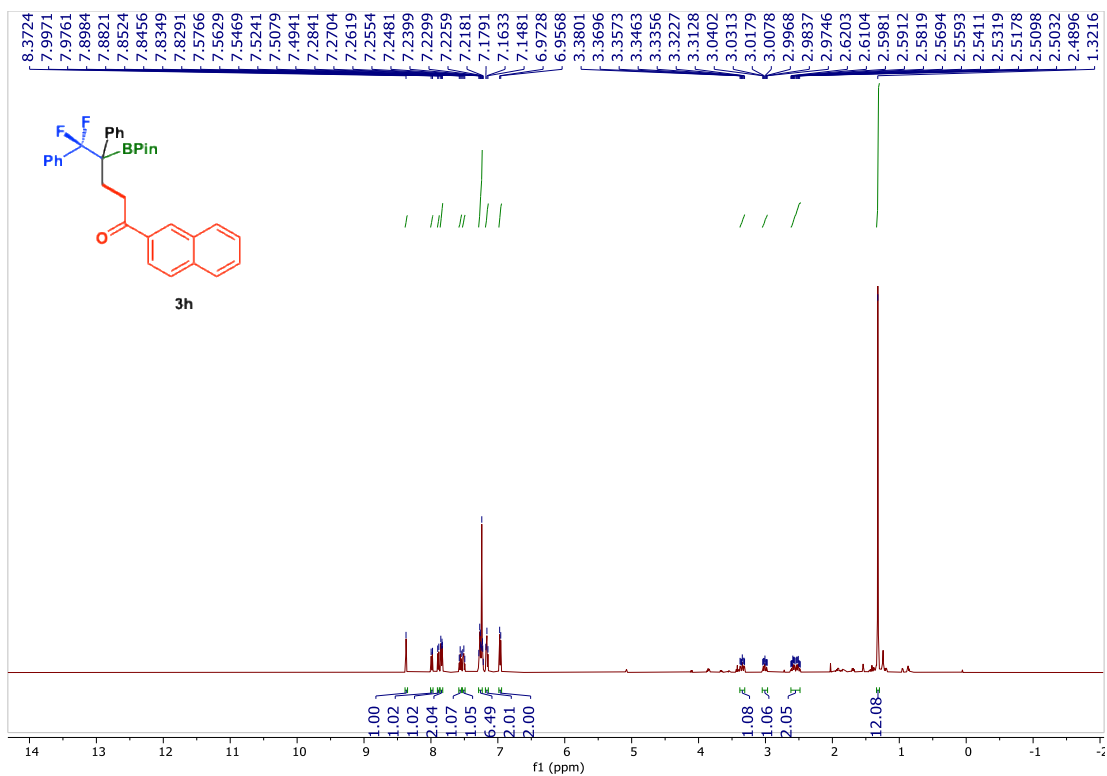


Fig. S47. ¹H NMR spectrum (CDCl₃, 25 °C) of **3h**.

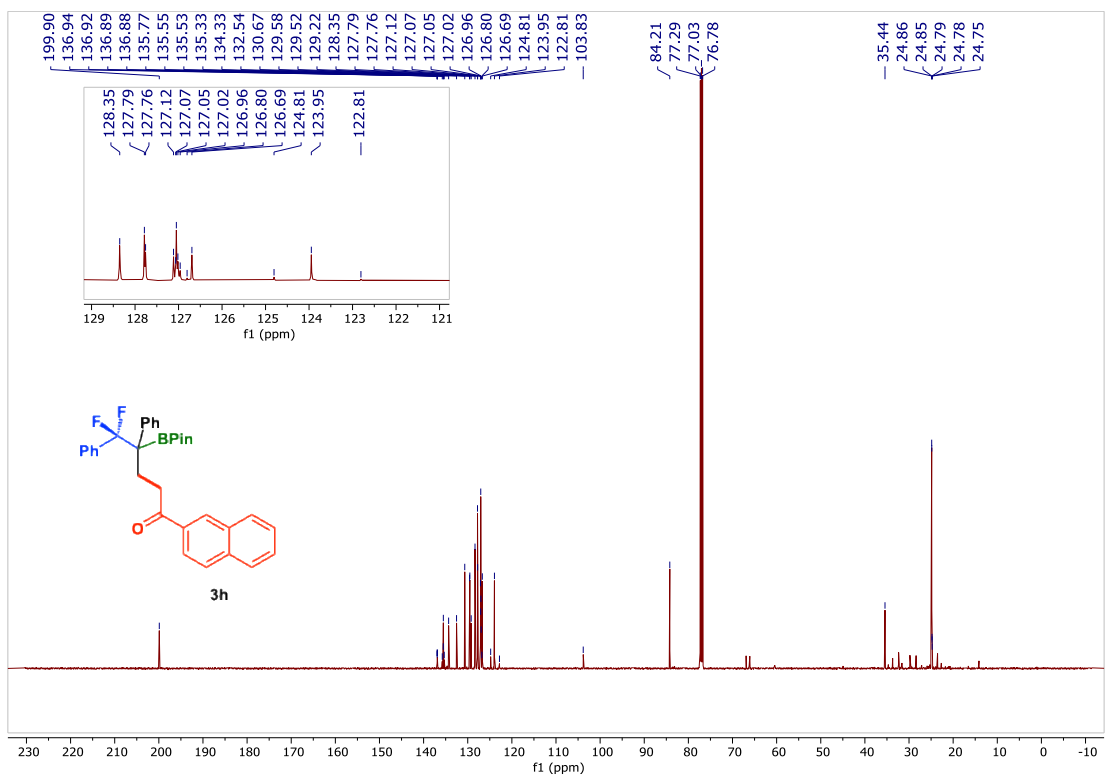


Fig. S48. ¹³C NMR spectrum (CDCl₃, 25 °C) of **3h**.

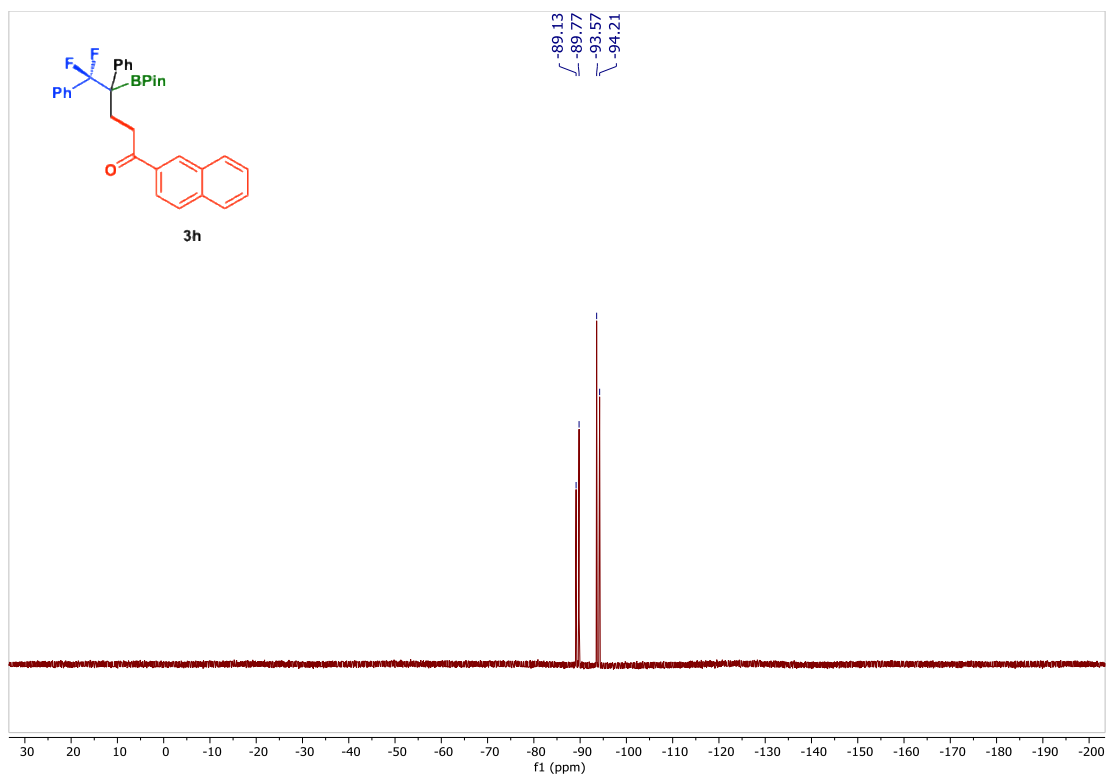


Fig. S49. ^{19}F NMR spectrum (CDCl_3 , 25 °C) of **3h**.

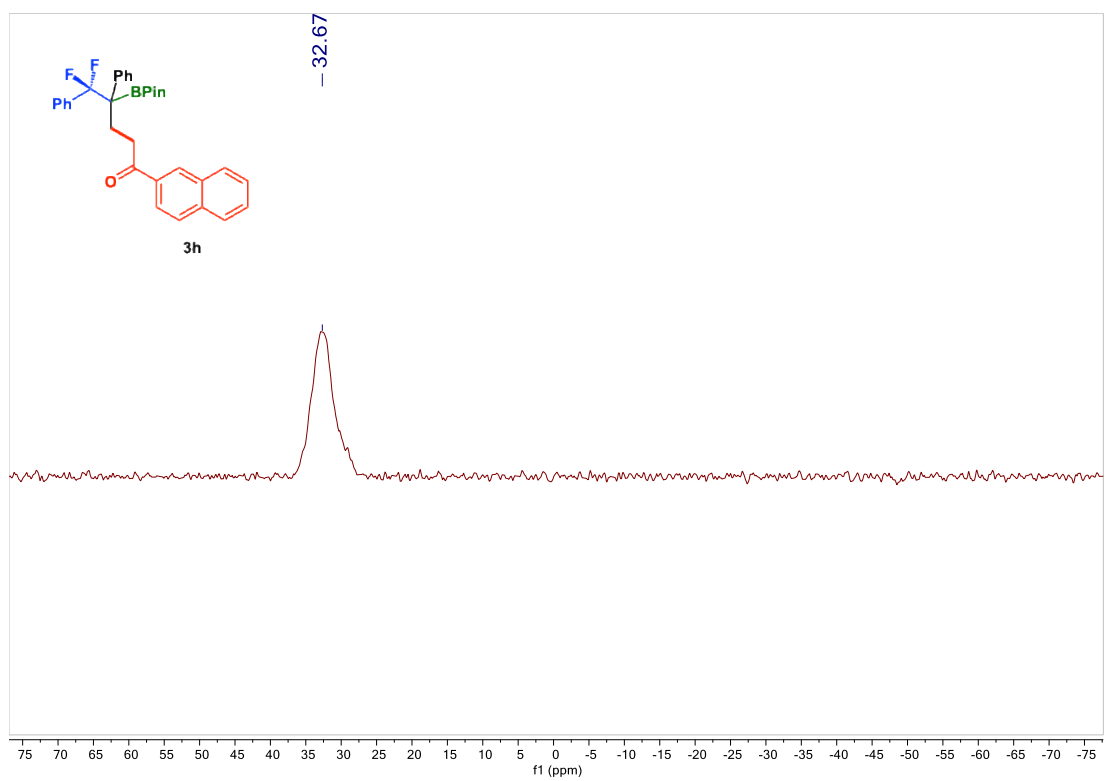


Fig. S50. ^{11}B NMR spectrum (CDCl_3 , 25 °C) of **3h**.

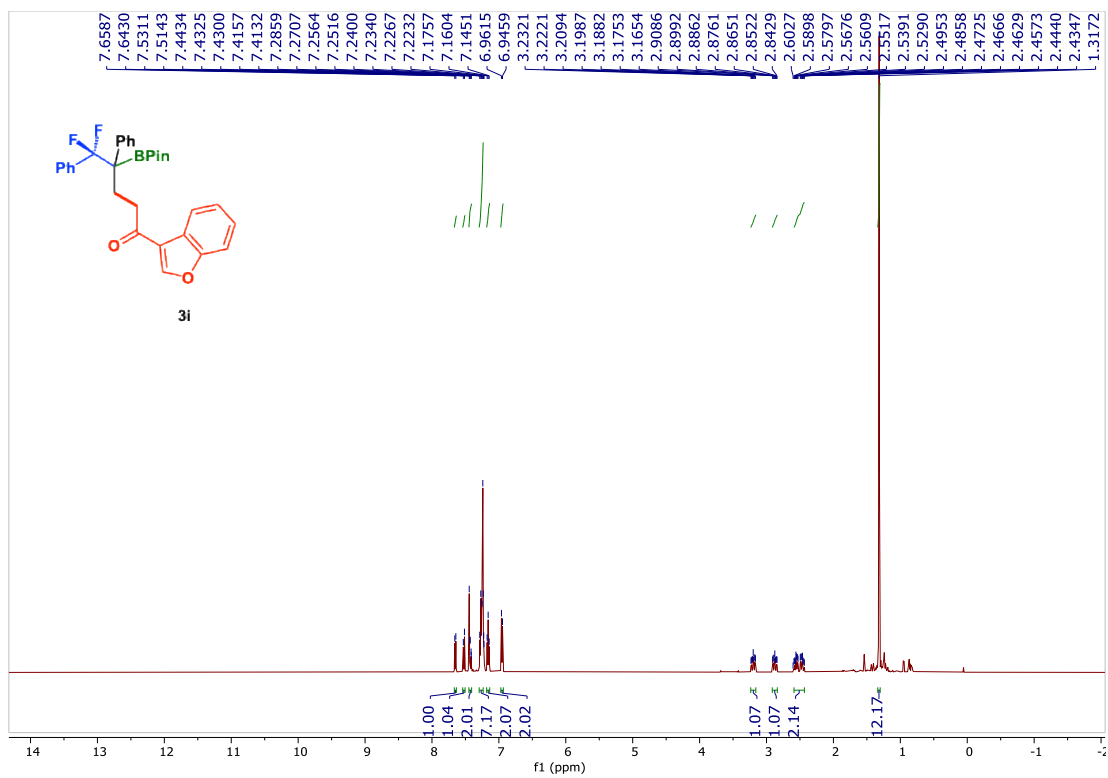


Fig. S51. ¹H NMR spectrum (CDCl₃, 25 °C) of **3i**.

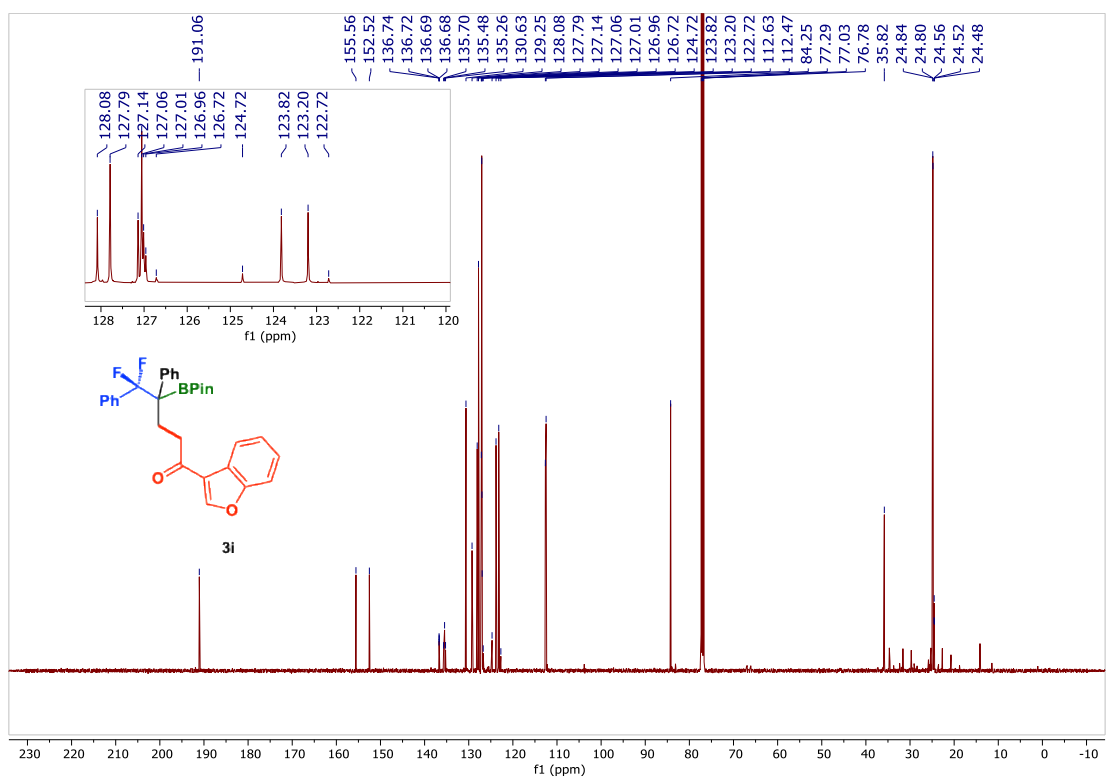


Fig. S52. ¹³C NMR spectrum (CDCl₃, 25 °C) of **3i**.

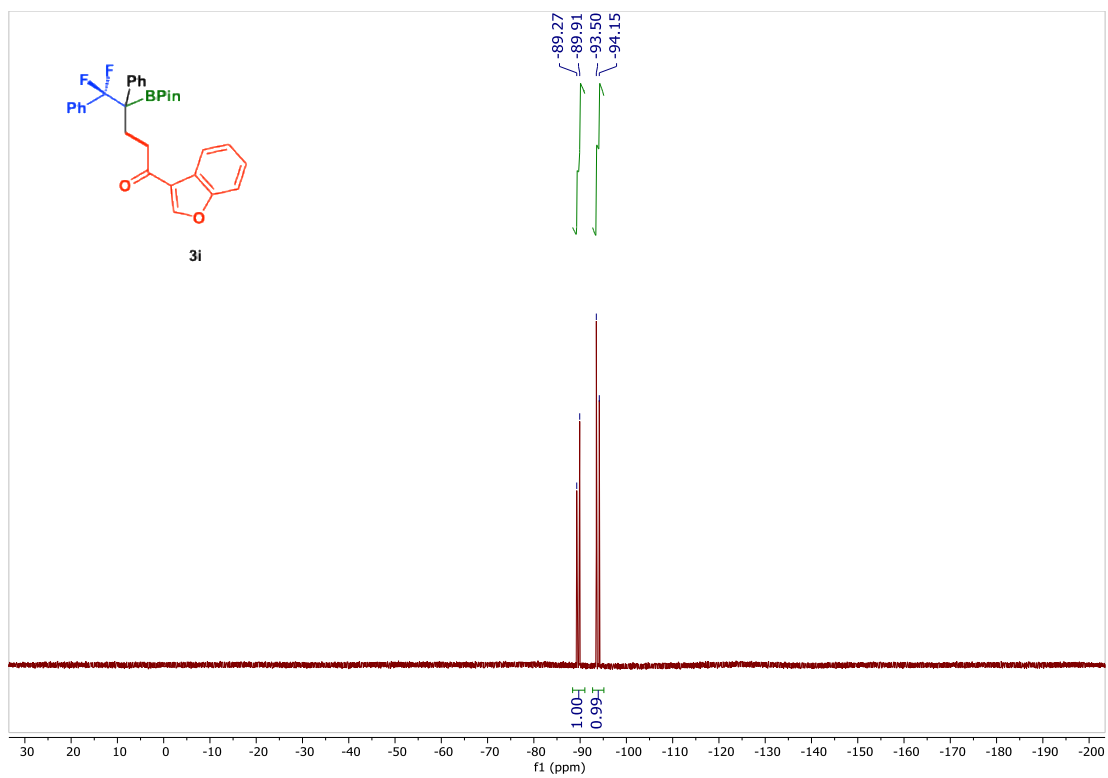


Fig. S53. ^{19}F NMR spectrum (CDCl₃, 25 °C) of **3i**.

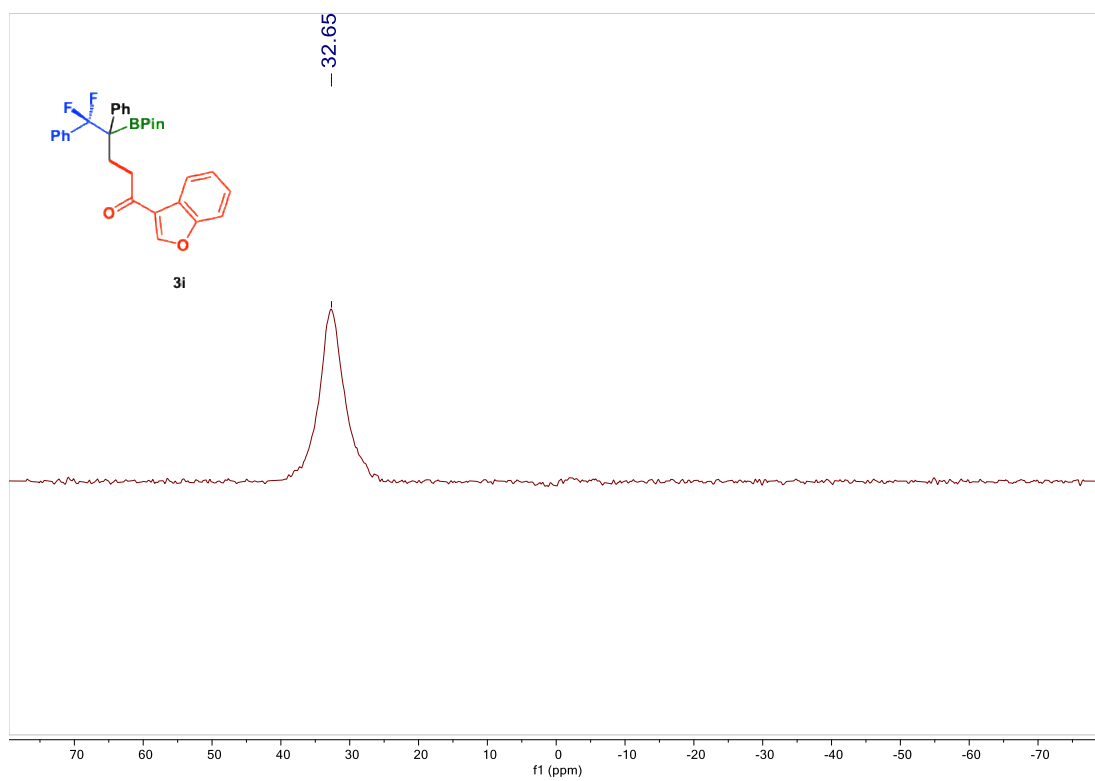


Fig. S54. ^{11}B NMR spectrum (CDCl₃, 25 °C) of **3i**.

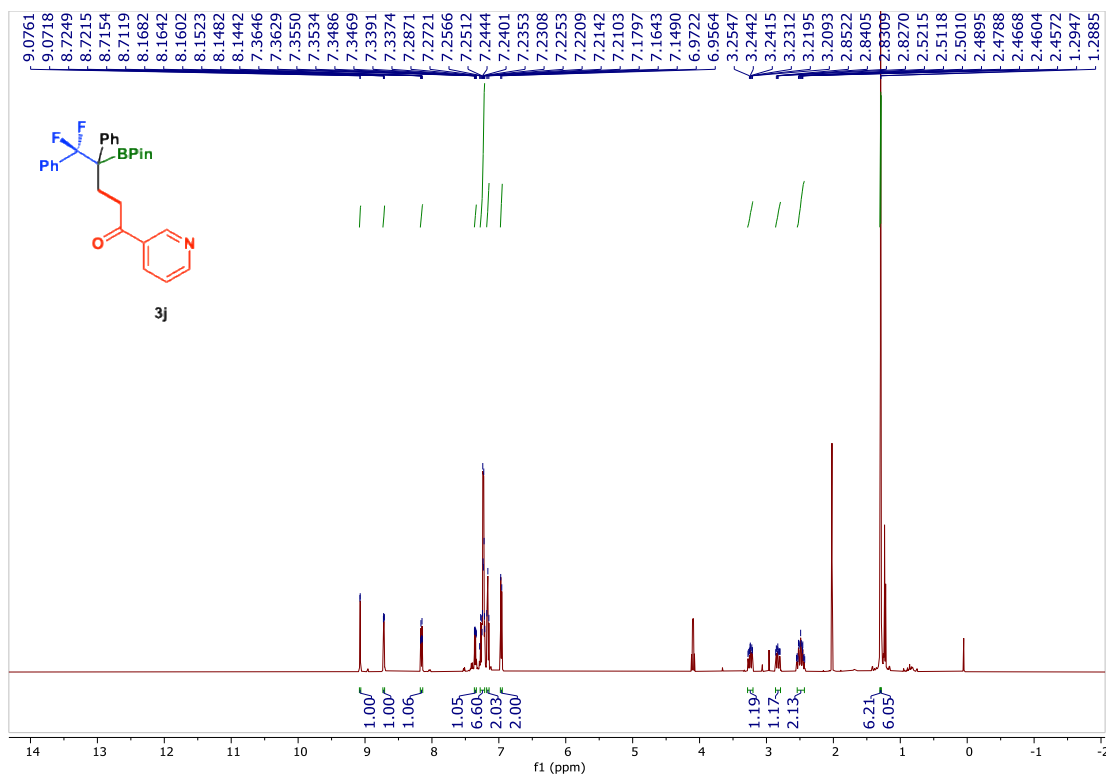


Fig. S55. ¹H NMR spectrum (CDCl₃, 25 °C) of **3j**.

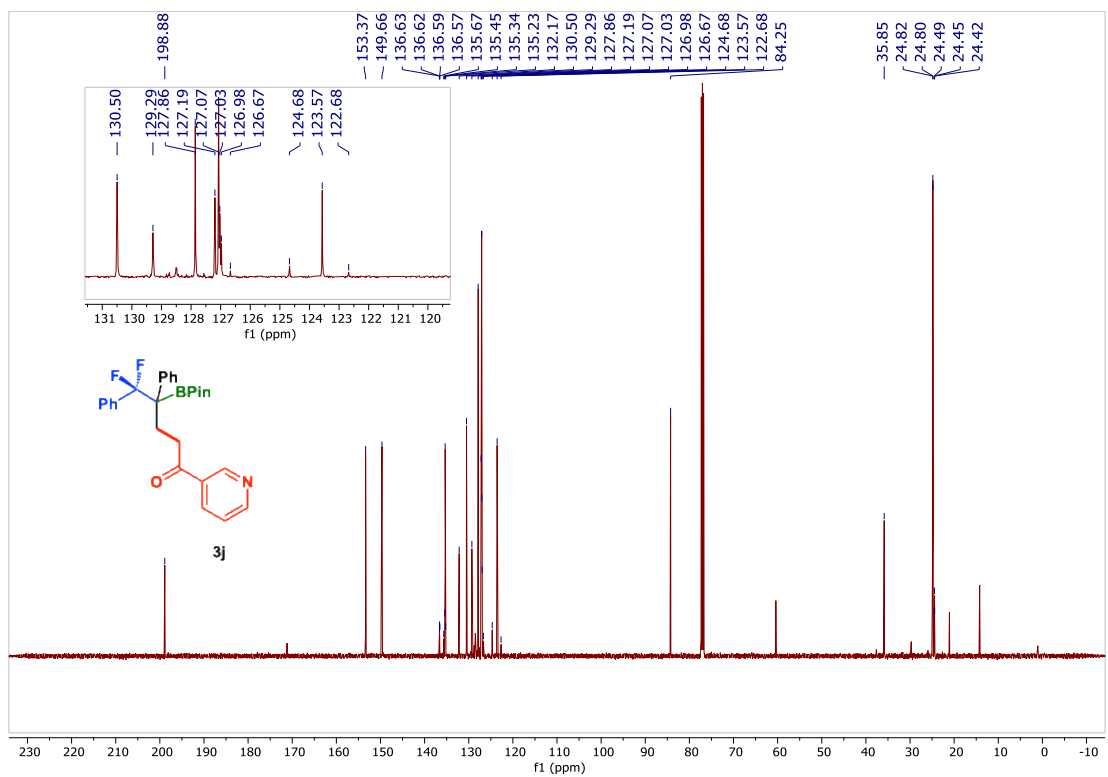


Fig. S56. ¹³C NMR spectrum (CDCl₃, 25 °C) of **3j**.

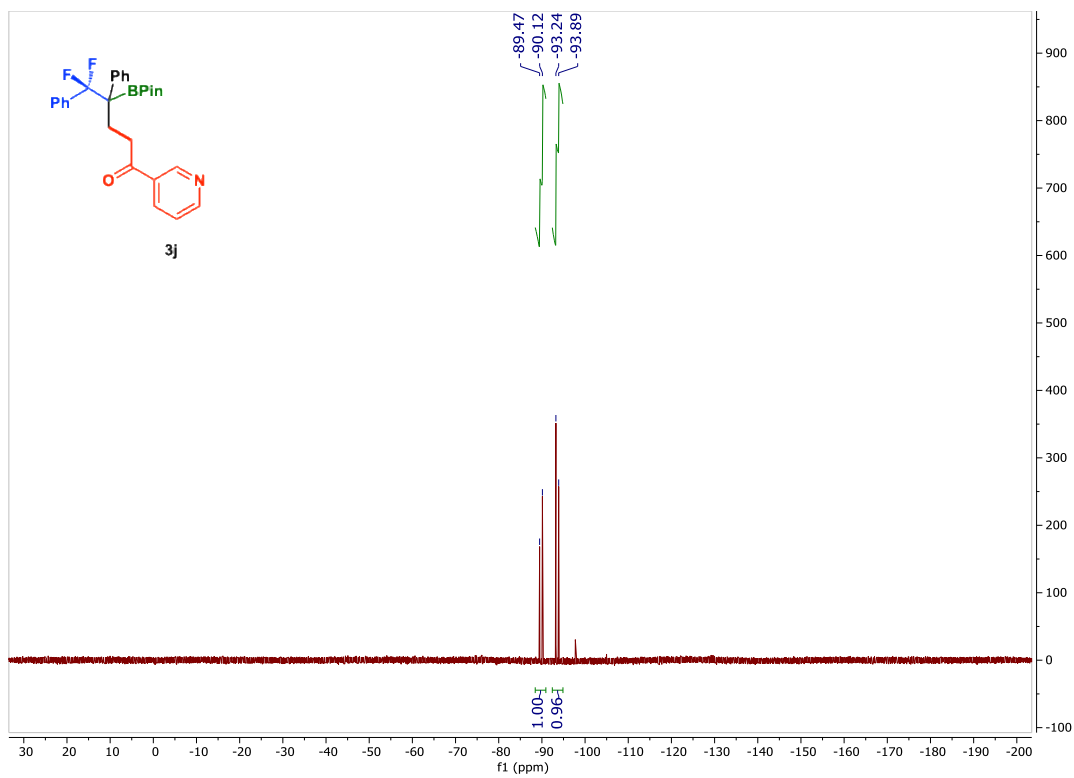


Fig. S57. ^{19}F NMR spectrum (CDCl_3 , 25 $^\circ\text{C}$) of **3j**.

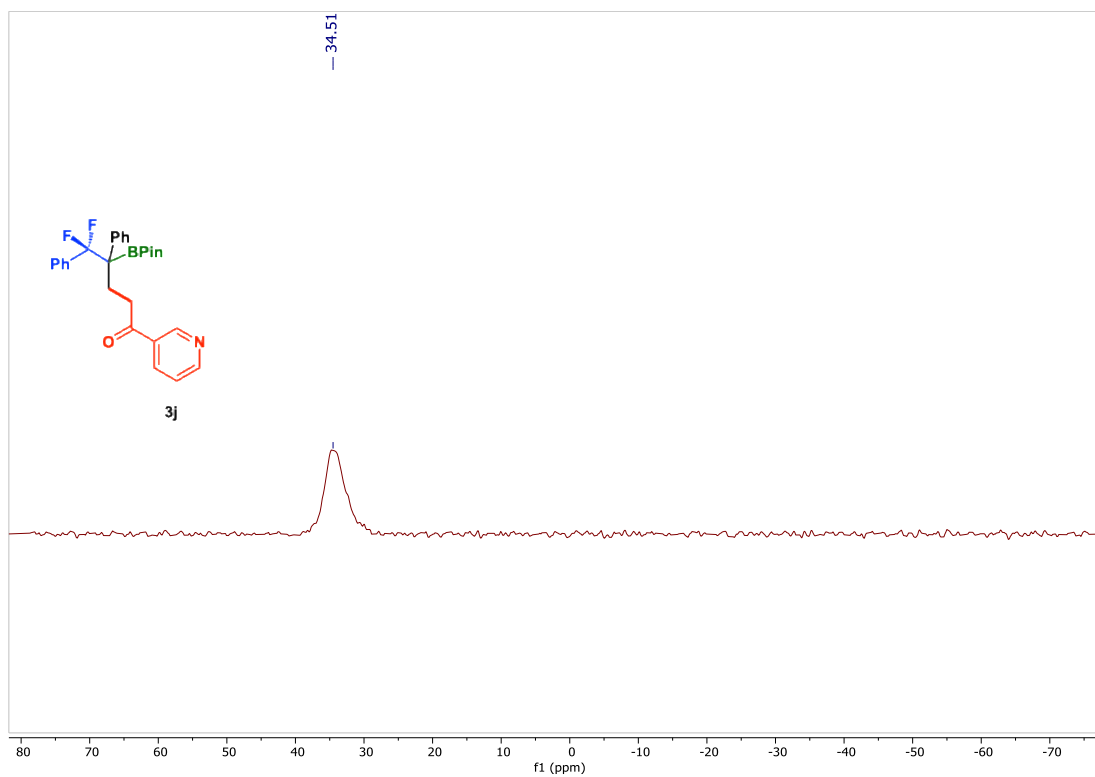


Fig. S58. ^{11}B NMR spectrum (CDCl_3 , 25 $^\circ\text{C}$) of **3j**.

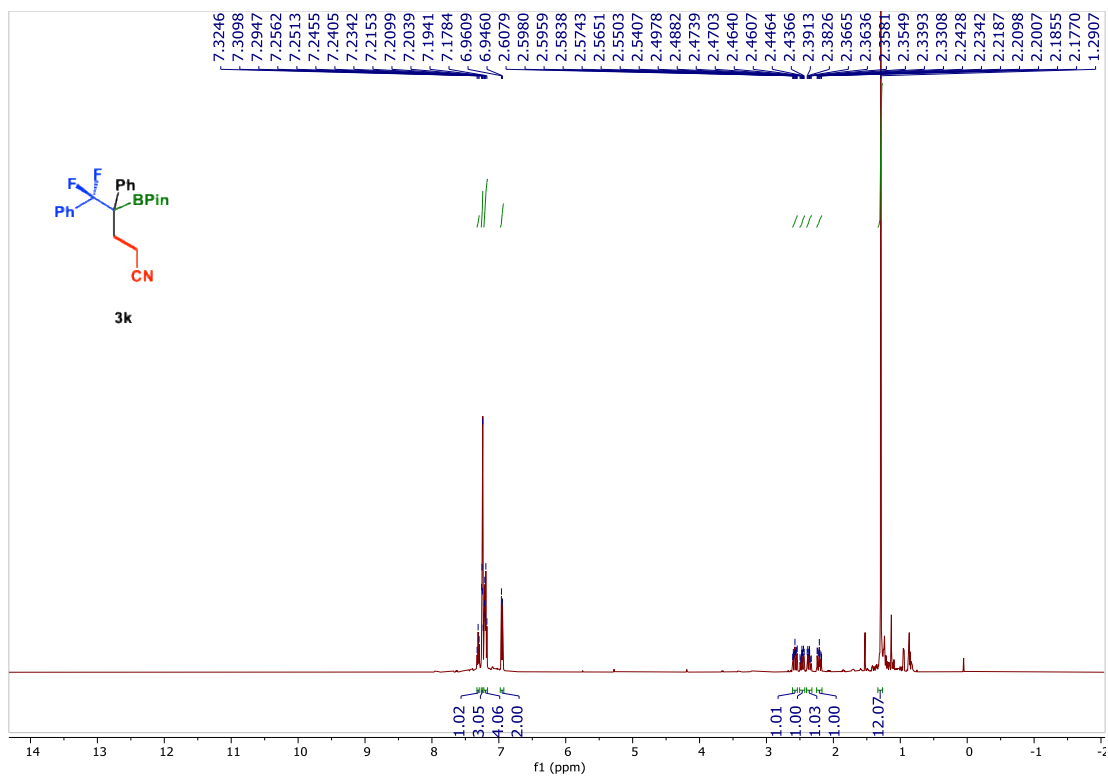


Fig. S59. ¹H NMR spectrum (CDCl₃, 25 °C) of **3k**.

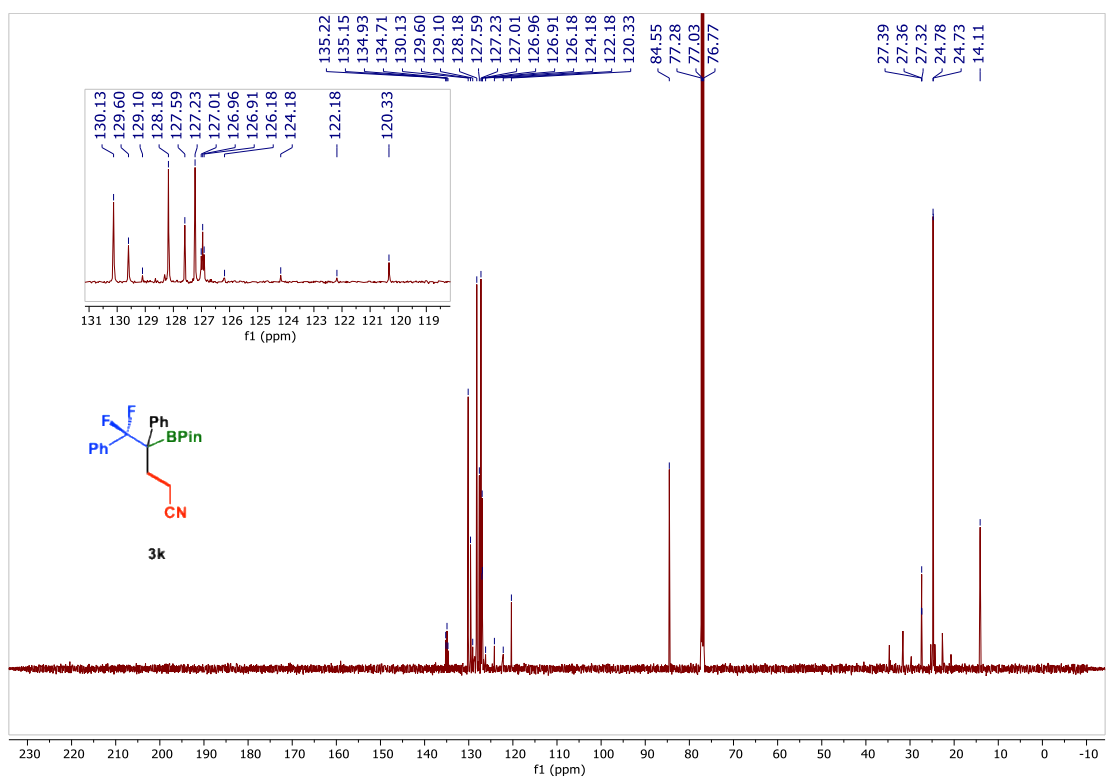


Fig. S60. ¹³C NMR spectrum (CDCl₃, 25 °C) of **3k**.

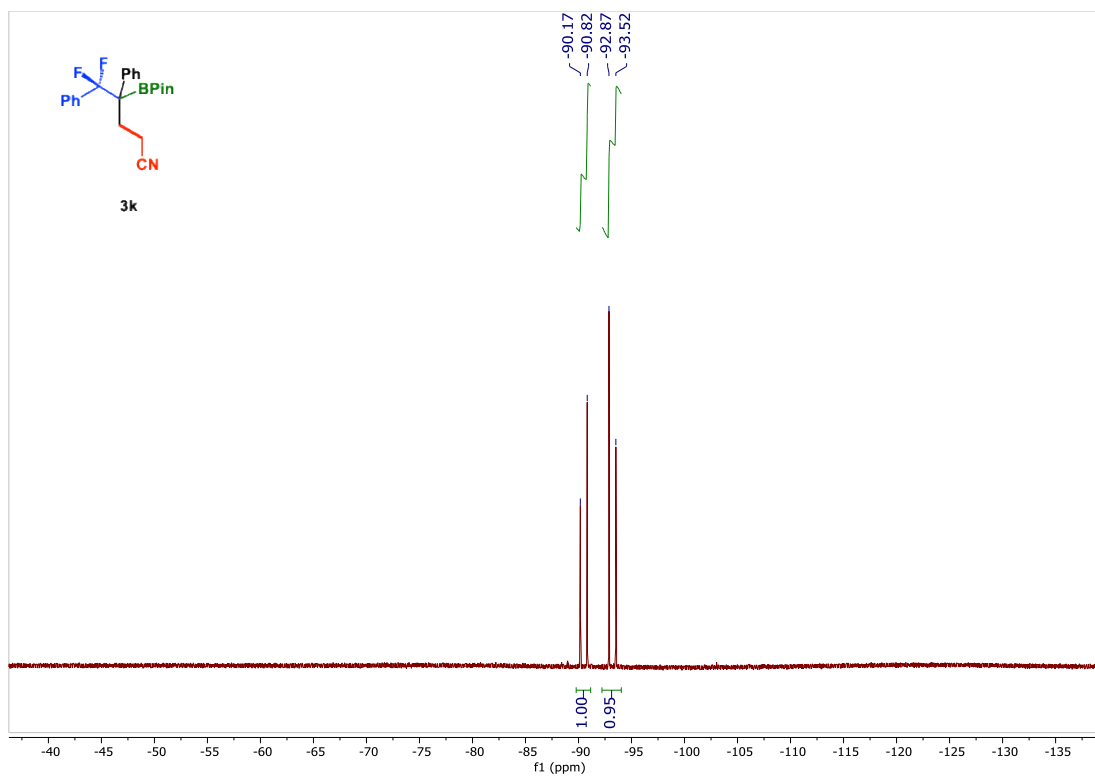


Fig. S61. ^{19}F NMR spectrum (CDCl_3 , 25°C) of **3k**.

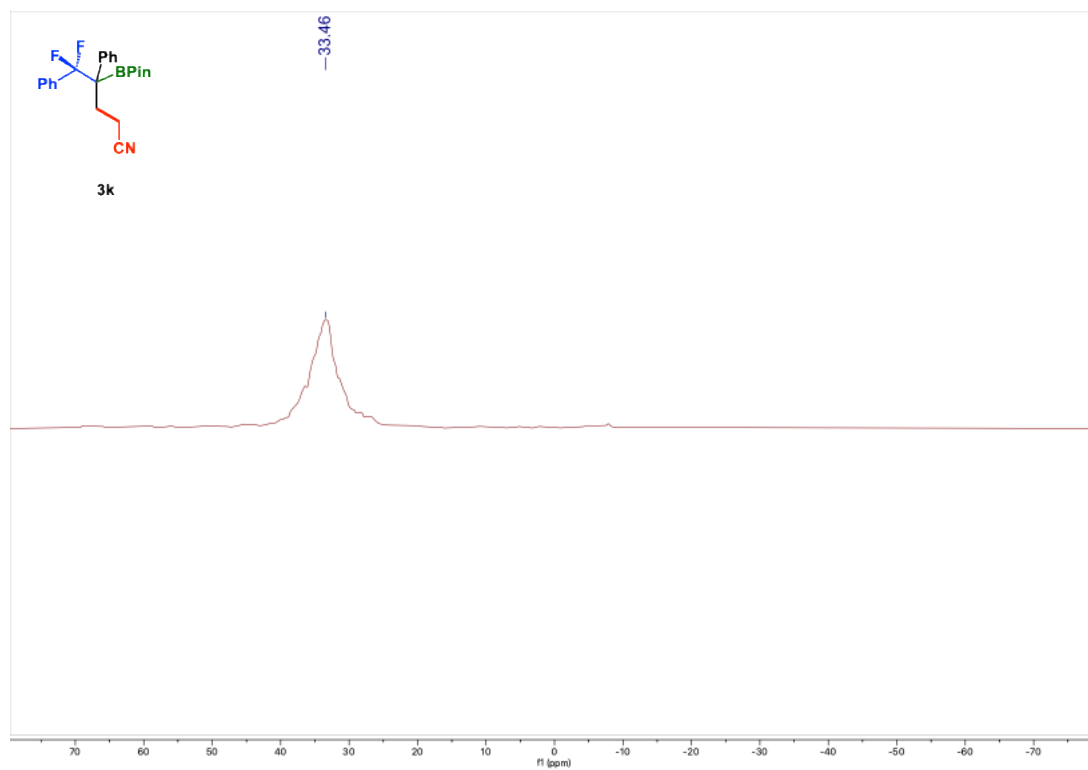


Fig. S62. ^{11}B NMR spectrum (CDCl_3 , 25°C) of **3k**.

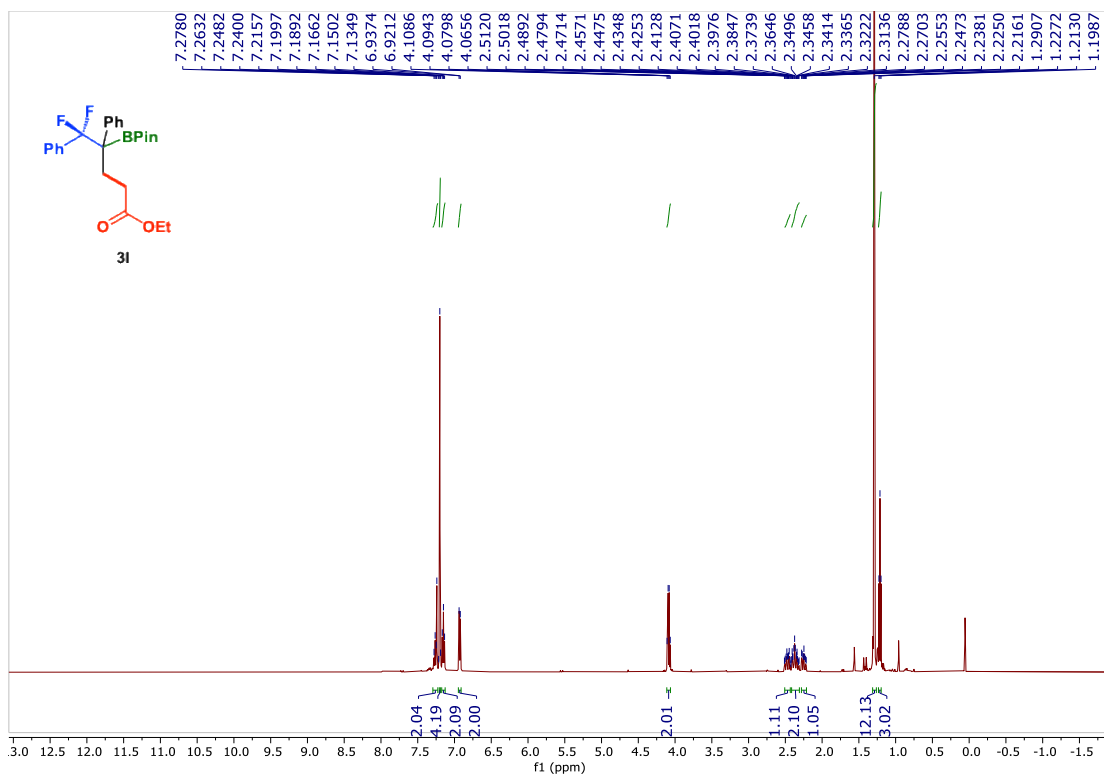


Fig. S63. ¹H NMR spectrum (CDCl₃, 25 °C) of **3l**.

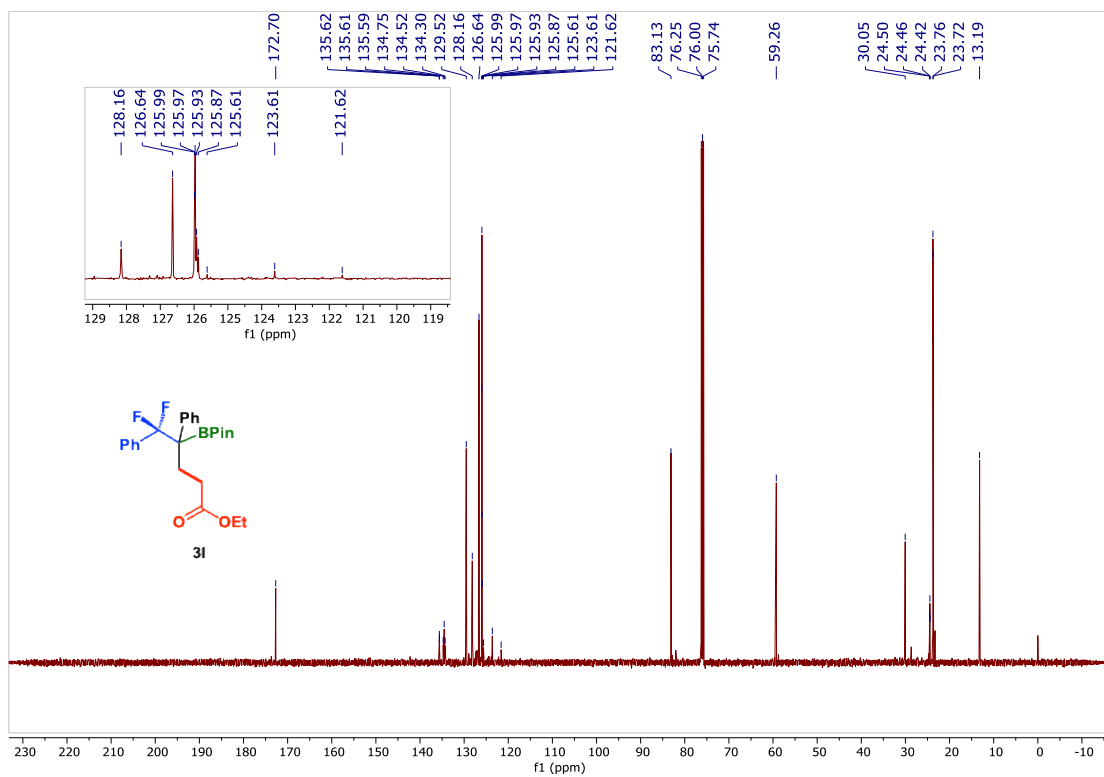


Fig. S64. ¹³C NMR spectrum (CDCl₃, 25 °C) of **3l**.

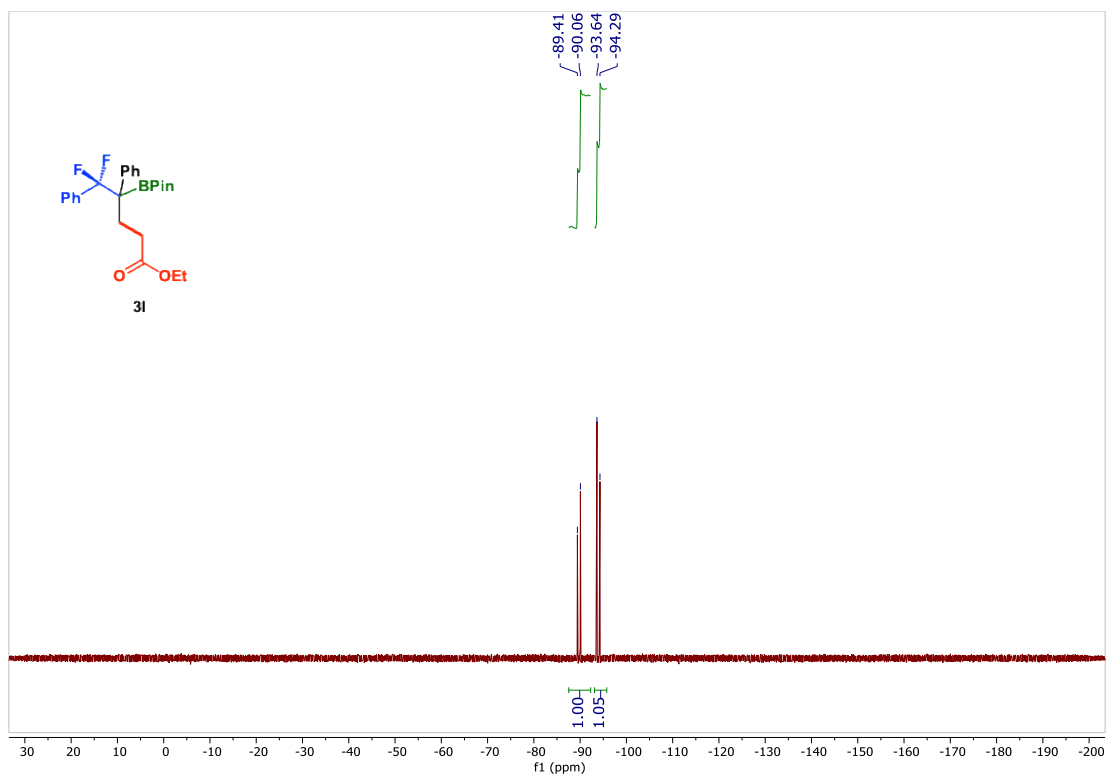


Fig. S65. ¹⁹F NMR spectrum (CDCl₃, 25 °C) of **3I**.

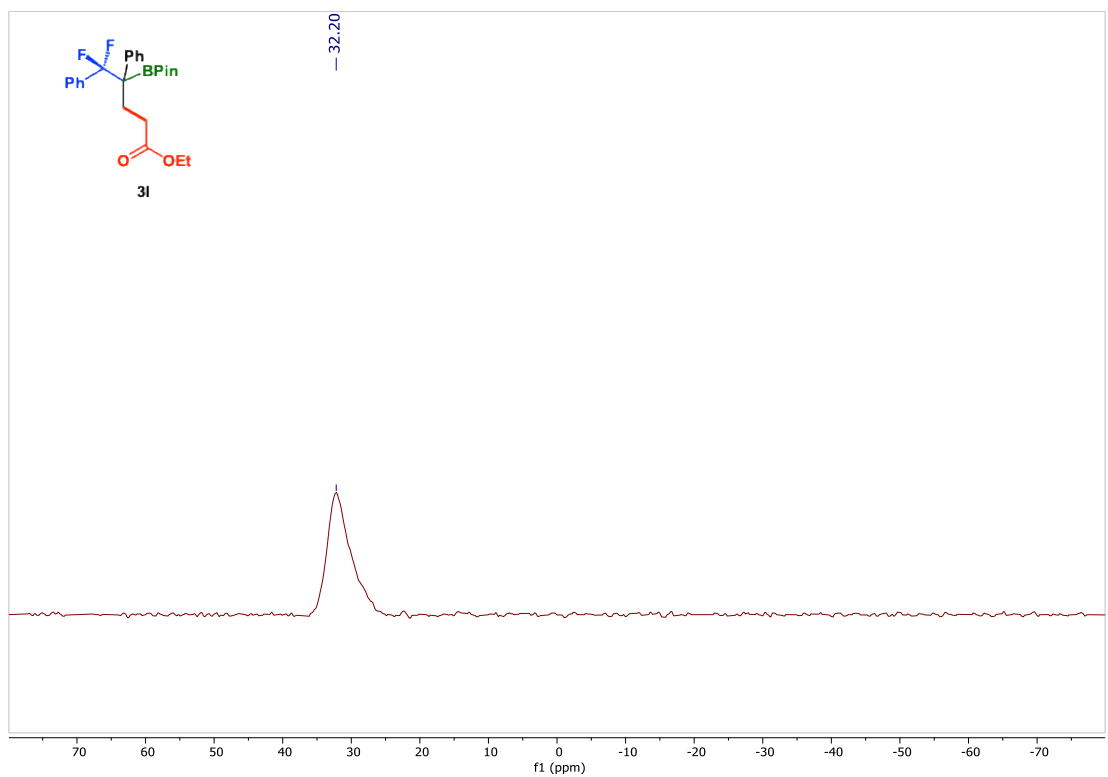


Fig. S66. ¹¹B NMR spectrum (CDCl₃, 25 °C) of **3I**.

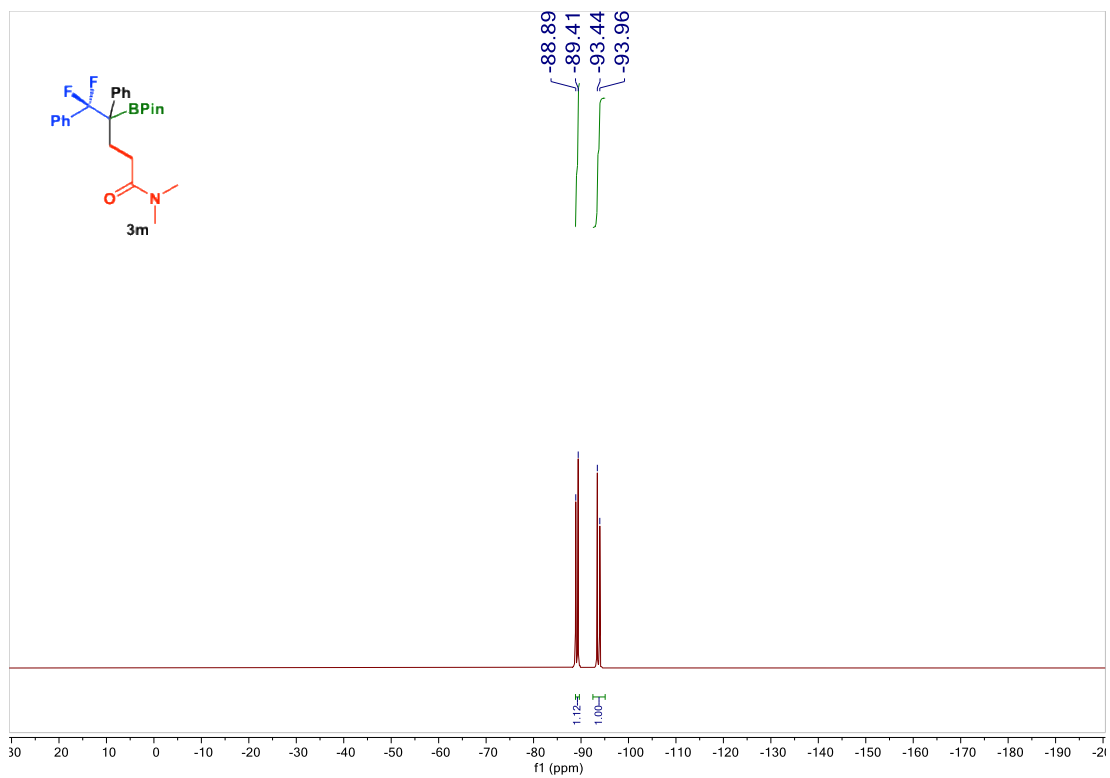


Fig. S67. ^{19}F NMR spectrum (CDCl₃, 25 °C) of **3m**.

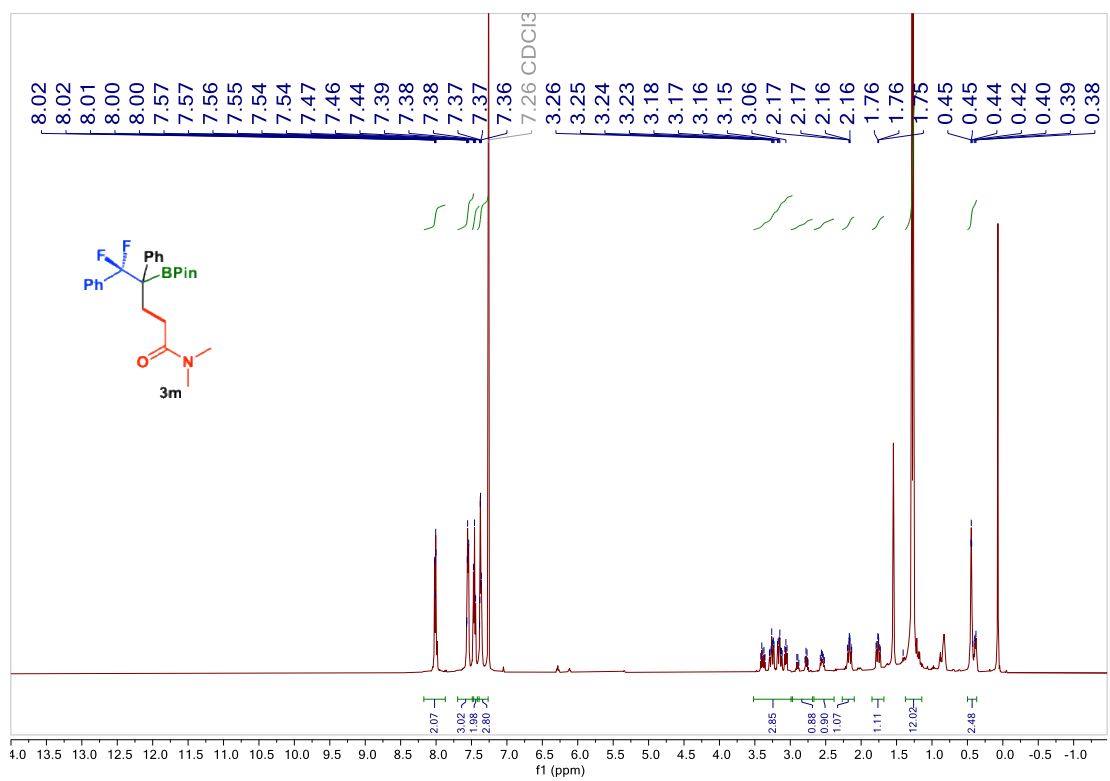


Fig. S68. ^1H NMR spectrum (CDCl₃, 25 °C) of **3m**.

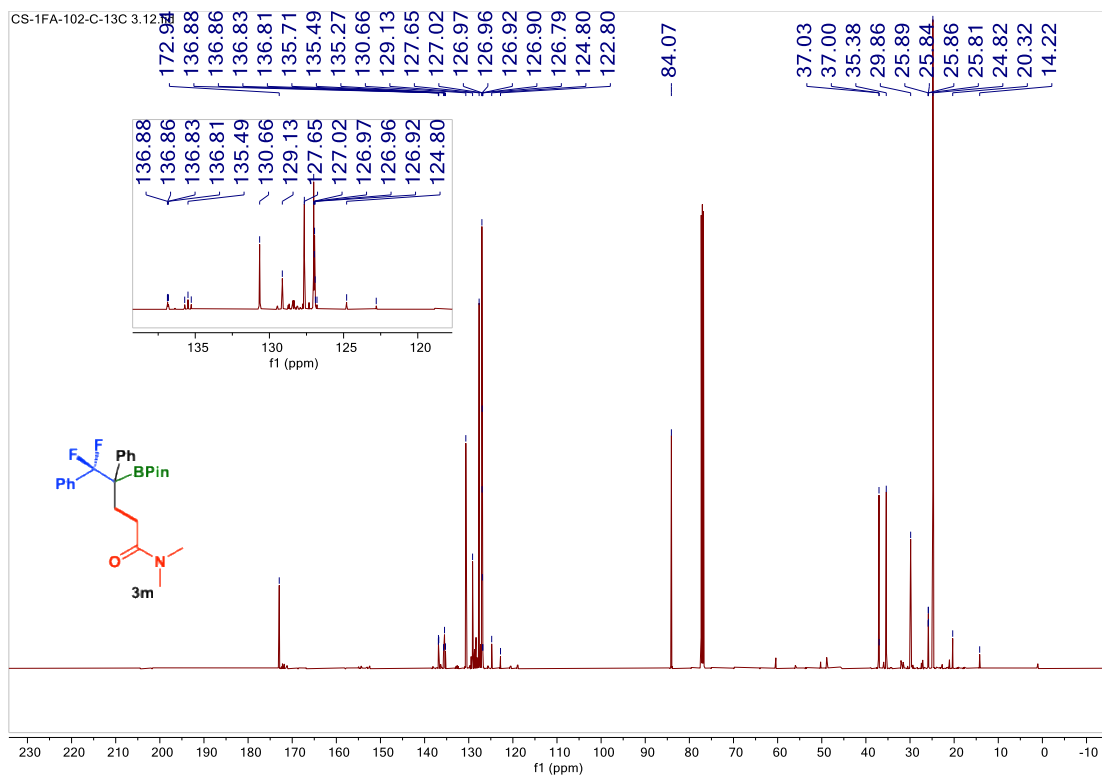


Fig. S69. ^{13}C NMR spectrum (CDCl_3 , 25 $^\circ\text{C}$) of **3m**.

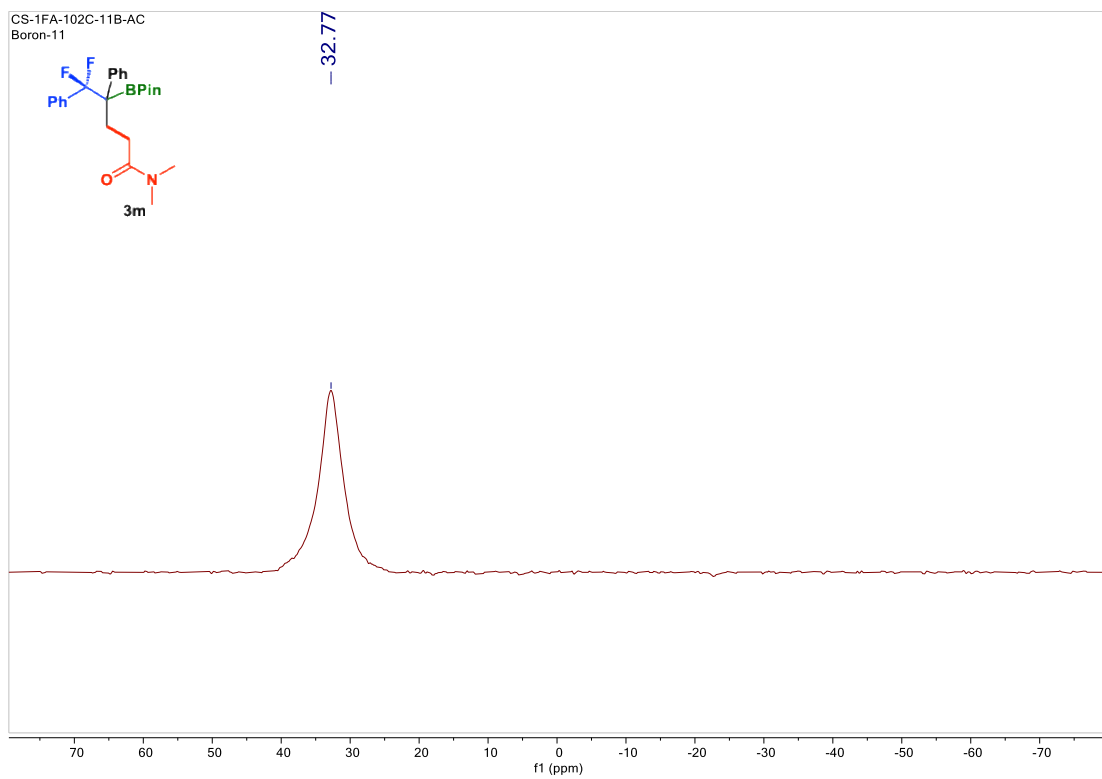


Fig. S70. ^{11}B NMR spectrum (CDCl_3 , 25 $^\circ\text{C}$) of **3m**.

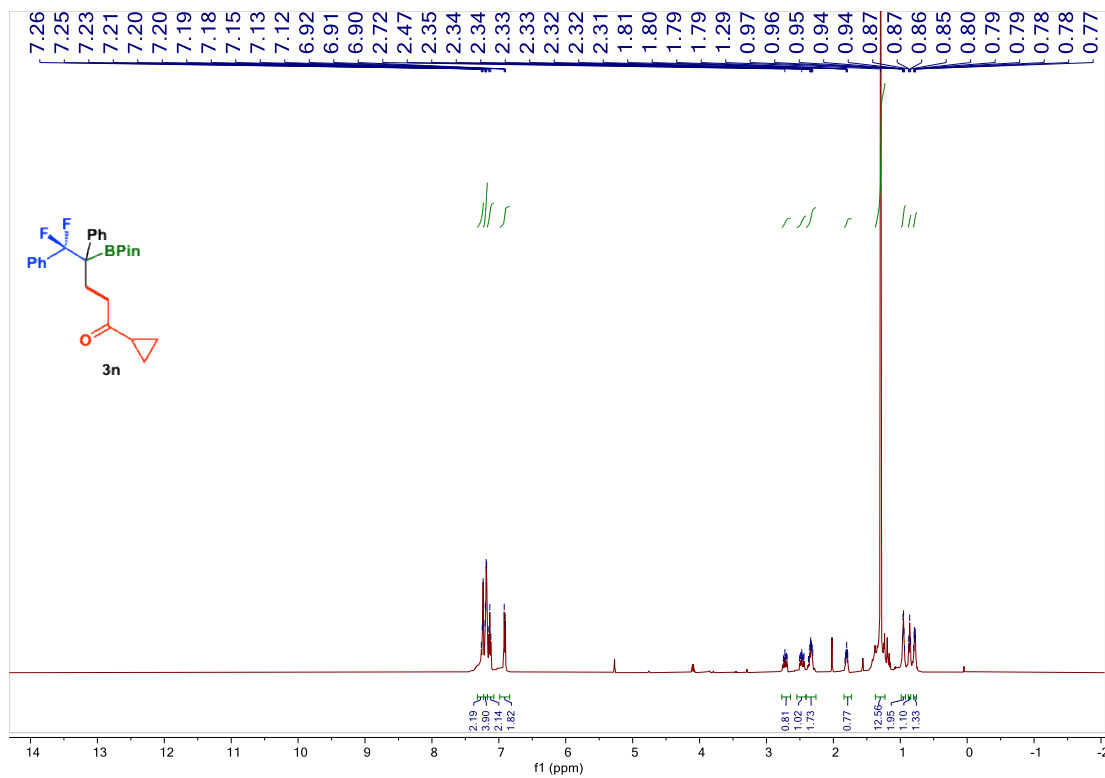


Fig. S71. ¹H NMR spectrum (CDCl₃, 25 °C) of **3n**.

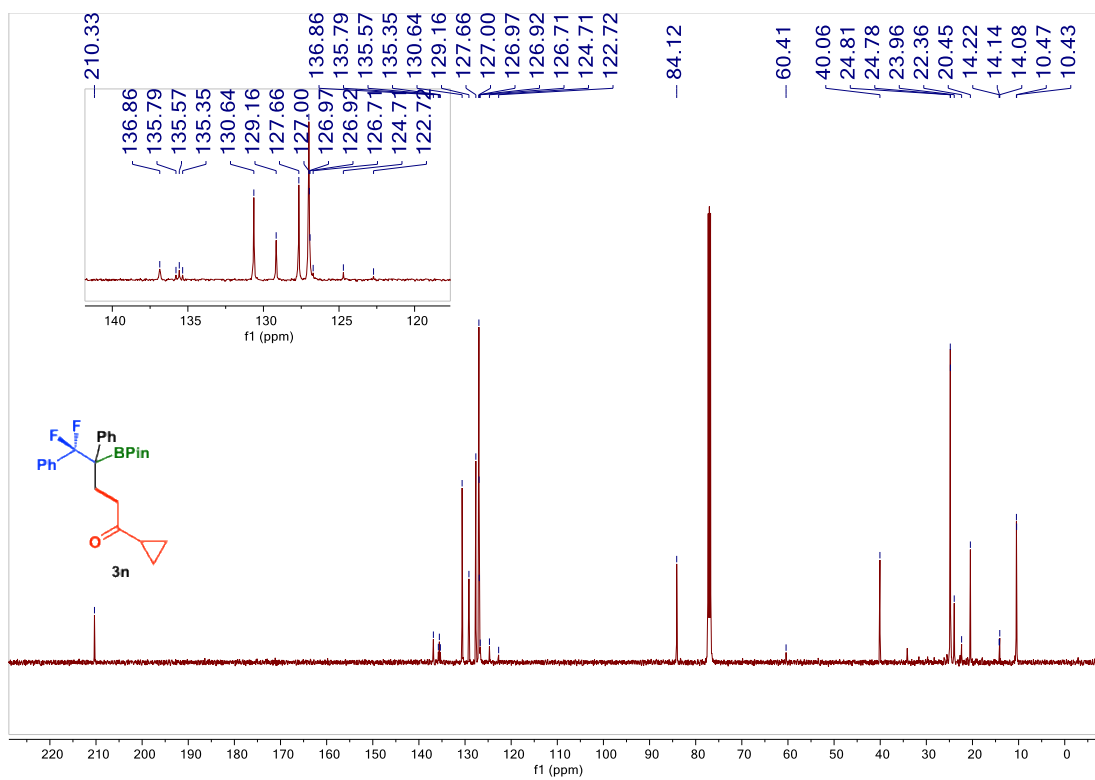


Fig. S72. ¹³C NMR spectrum (CDCl₃, 25 °C) of **3n**.

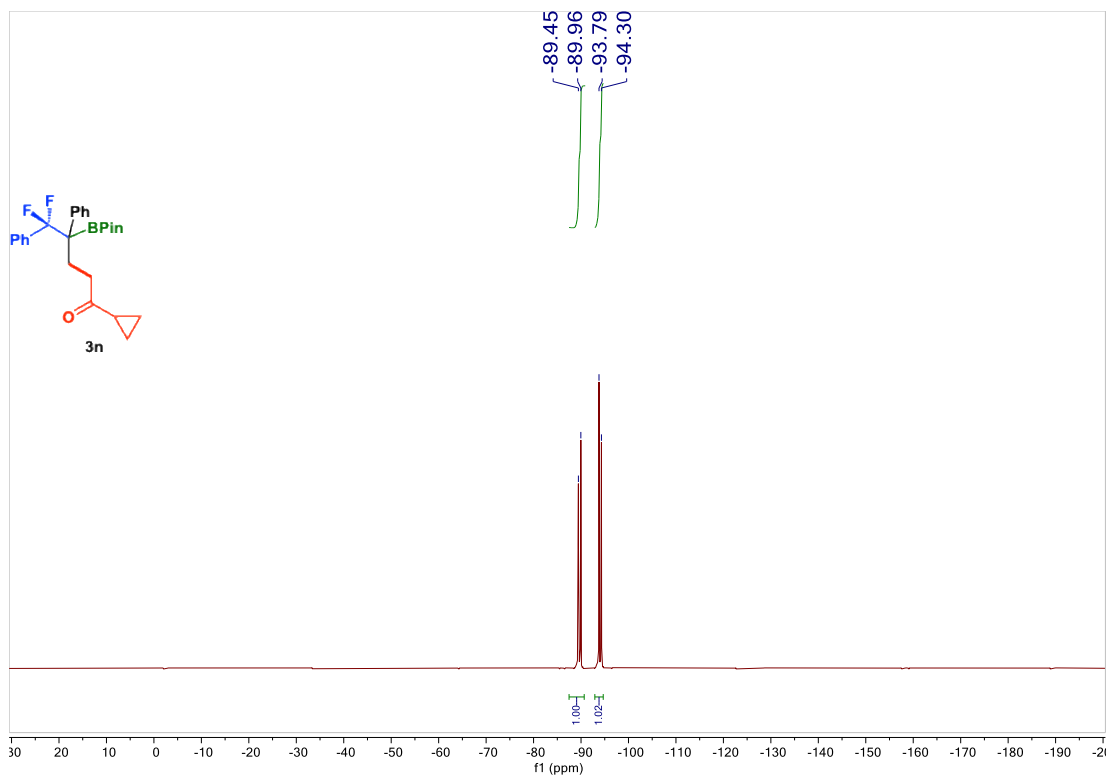


Fig. S73. ¹⁹F NMR spectrum (CDCl₃, 25 °C) of **3n**.

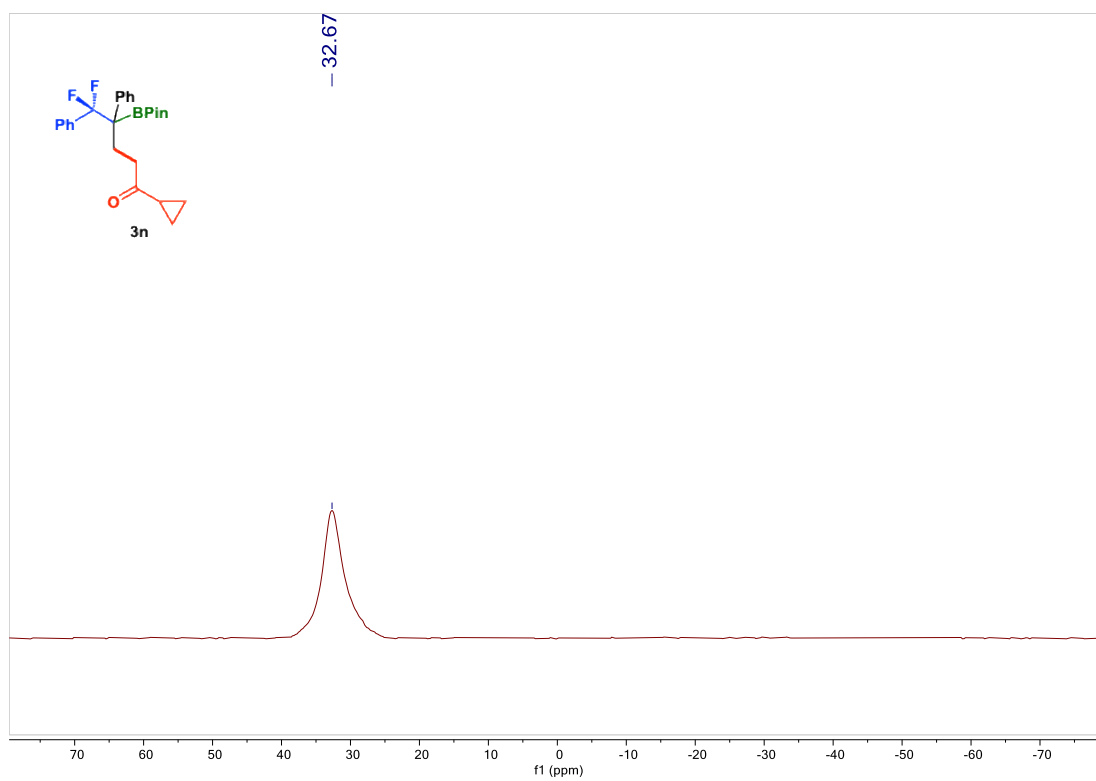


Fig. S74. ¹¹B NMR spectrum (CDCl₃, 25 °C) of **3n**.

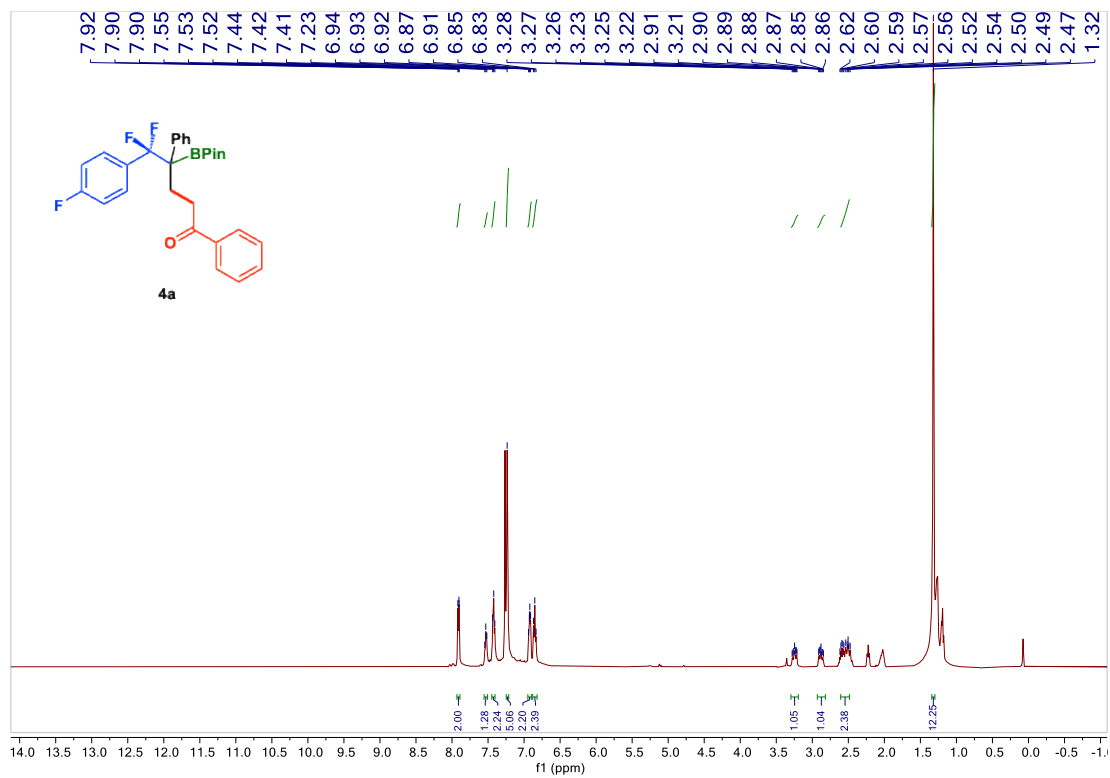


Fig. S75. ¹H NMR spectrum (CDCl₃, 25 °C) of 4a.

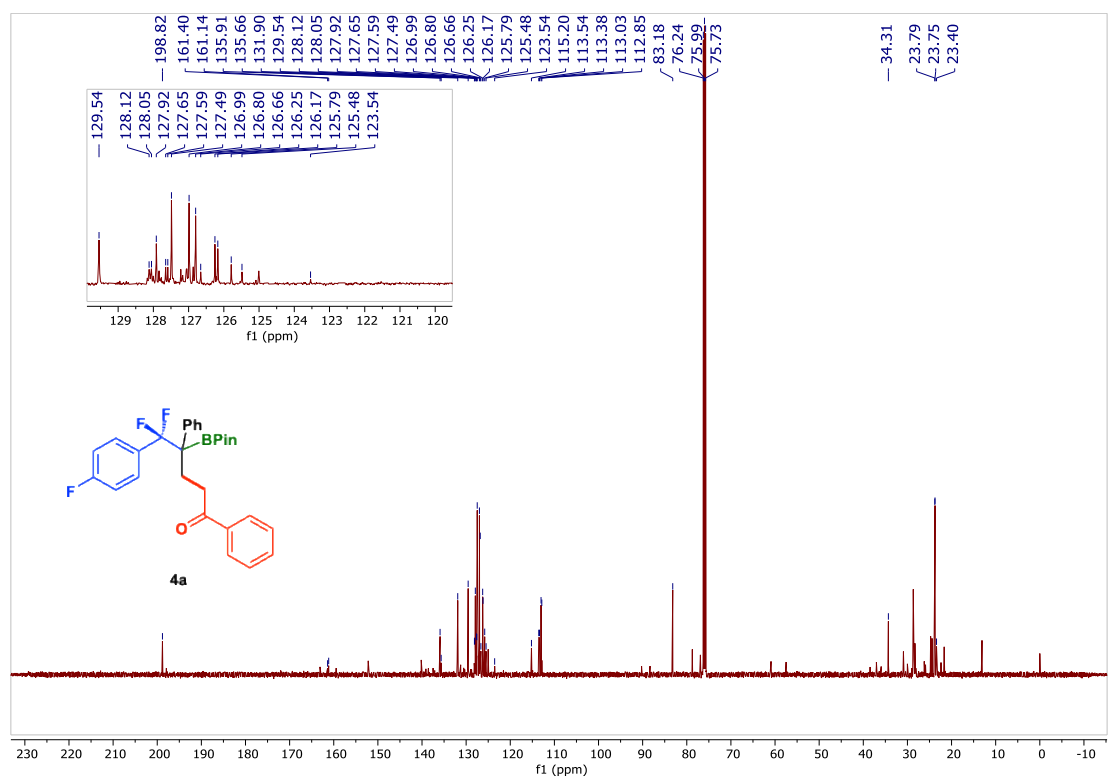


Fig. S76. ¹³C NMR spectrum (CDCl₃, 25 °C) of 4a.

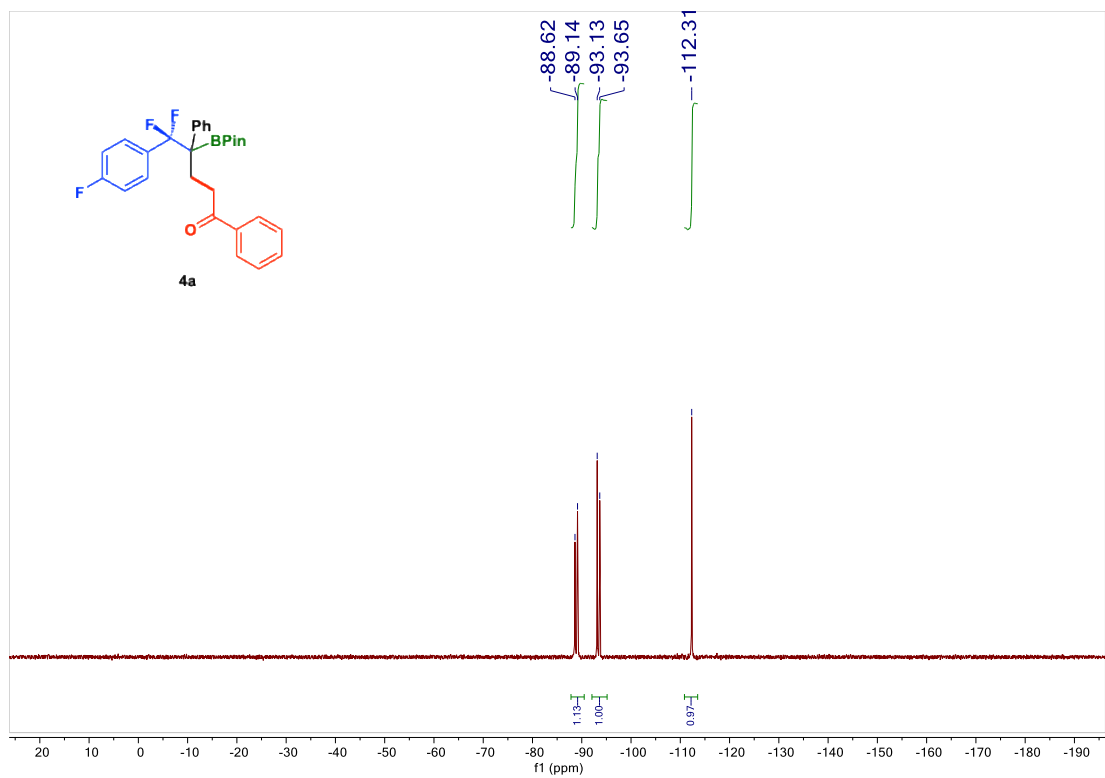


Fig. S77. ^{19}F NMR spectrum (CDCl_3 , 25 °C) of 4a.

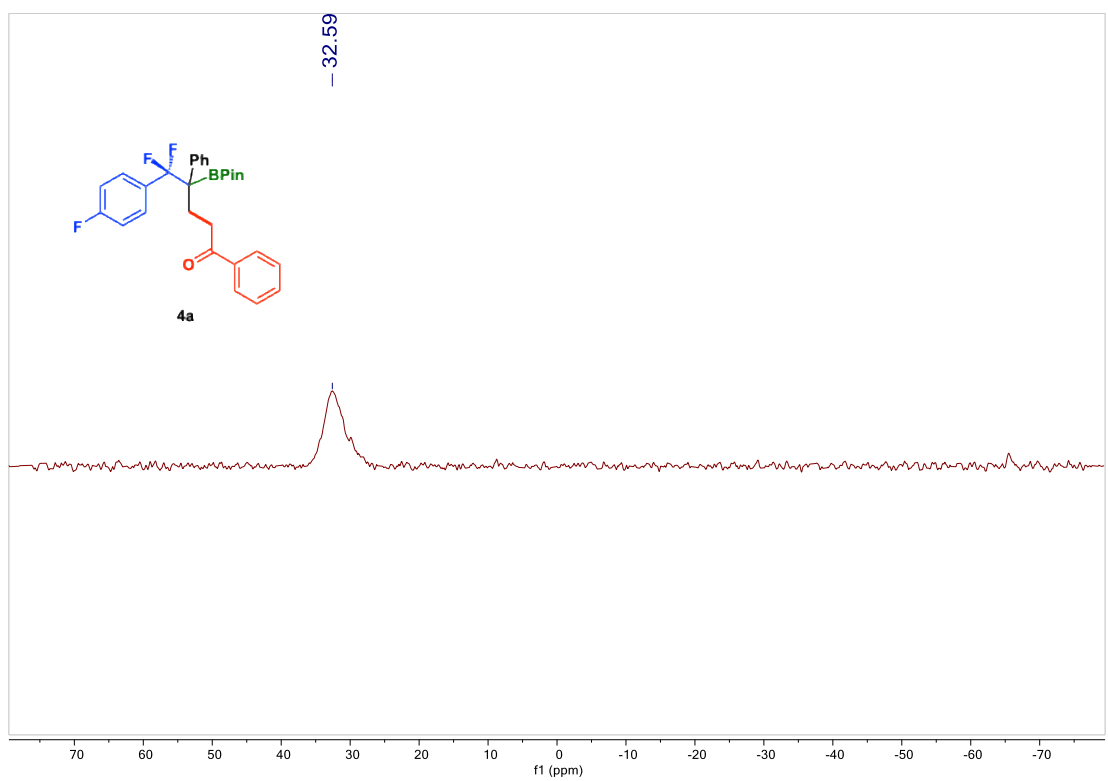


Fig. S78. ^{11}B NMR spectrum (CDCl_3 , 25 °C) of 4a.

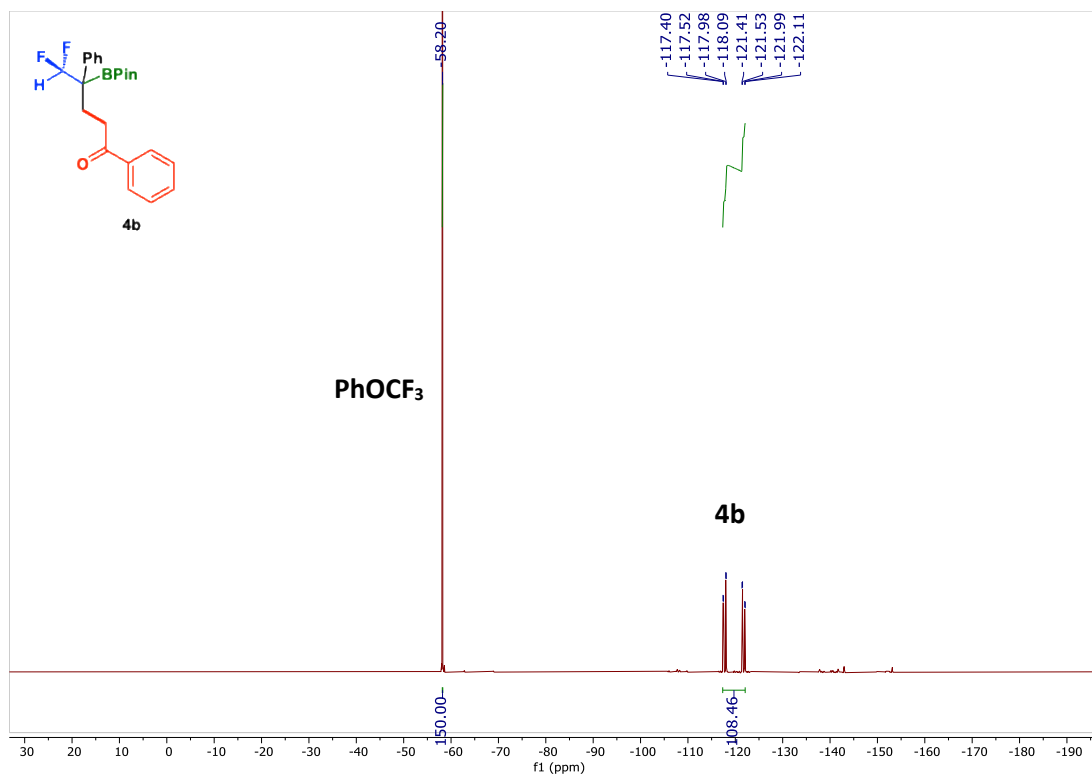


Fig. S79. ¹⁹F NMR spectrum (CDCl₃, 25 °C) of **4b**.

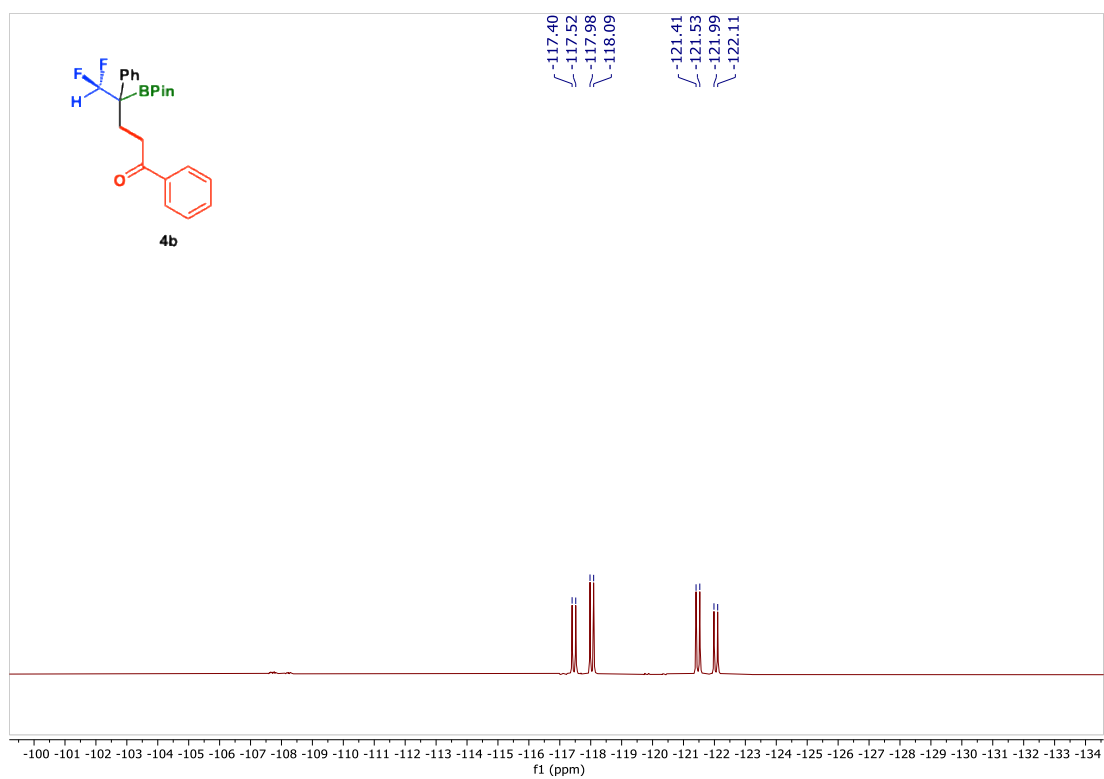


Fig. S80. ¹⁹F NMR spectrum (THF-H₈, 25 °C) of **4b** highlighting product peak.

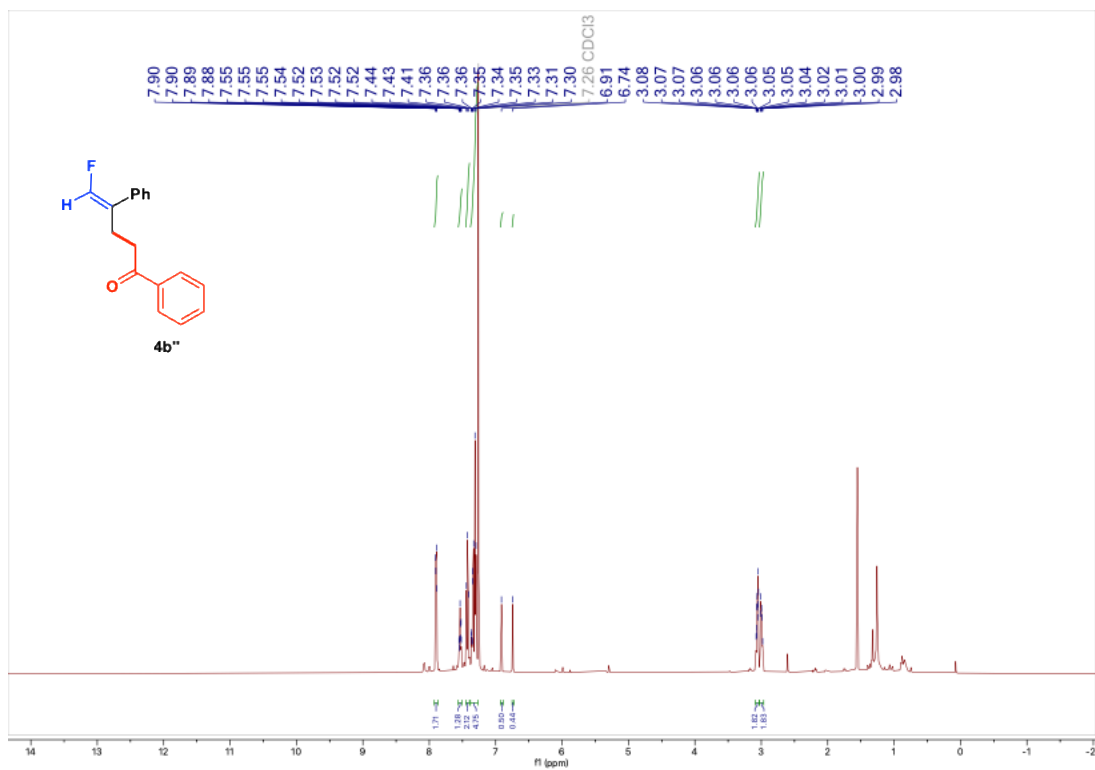


Fig. S81. ¹H NMR spectrum (CDCl₃, 25 °C) of **4b''**

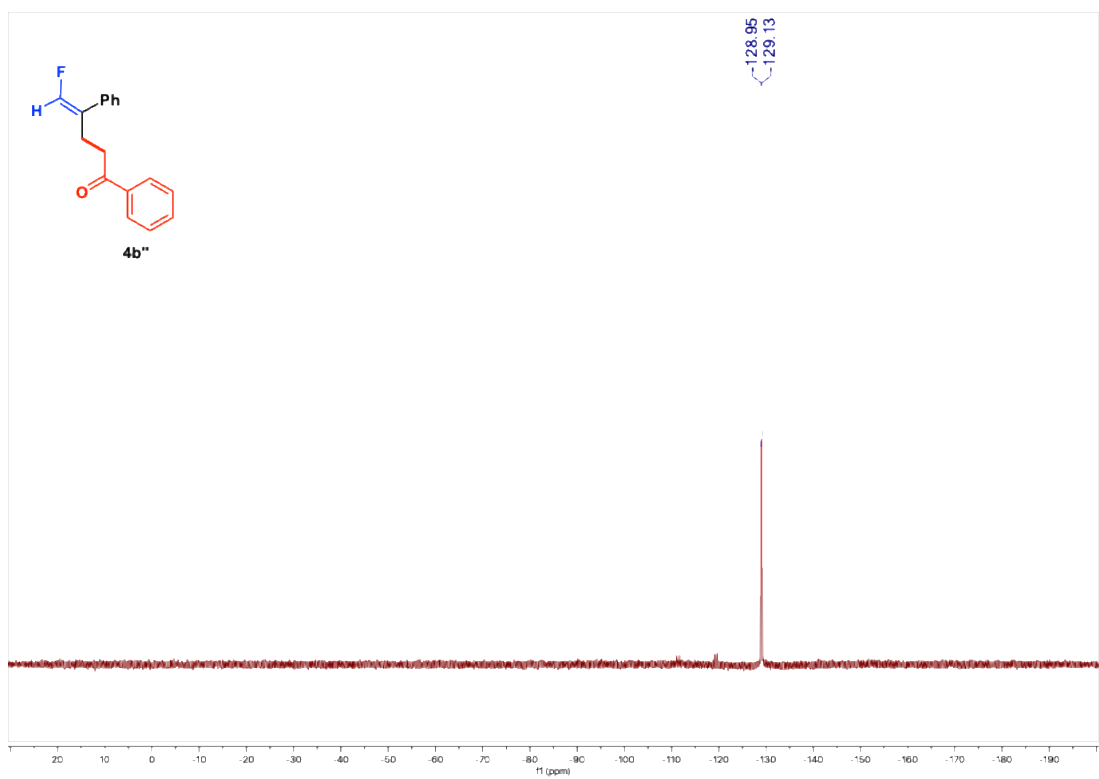


Fig. S82. ¹⁹F NMR spectrum (CDCl₃, 25 °C) of **4b''**

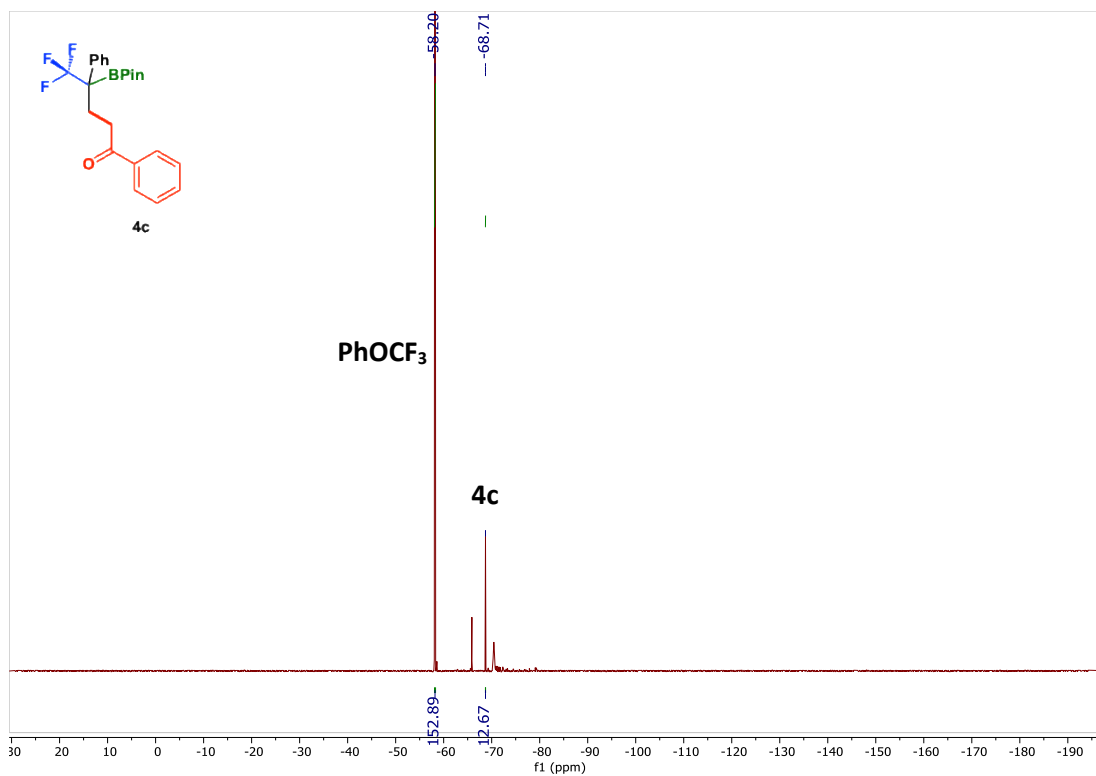
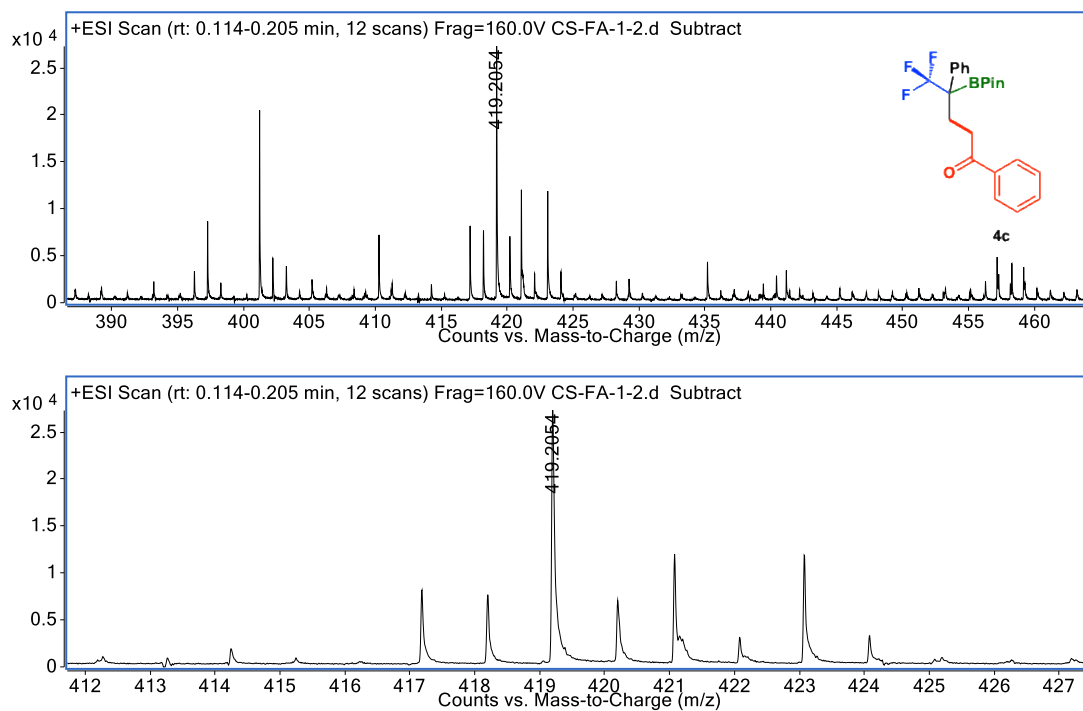


Fig. S83. ^{19}F NMR spectrum (THF- H_8 , 25 °C) of **4c**.



ESI-MS: calcd for $\text{C}_{23}\text{H}_{27}\text{BF}_3\text{O}_3$ (($\text{M}+\text{H}$)⁺): 419.2005, found: 419.2054.

Fig. S84. ESI-MS spectrum of **4c**.

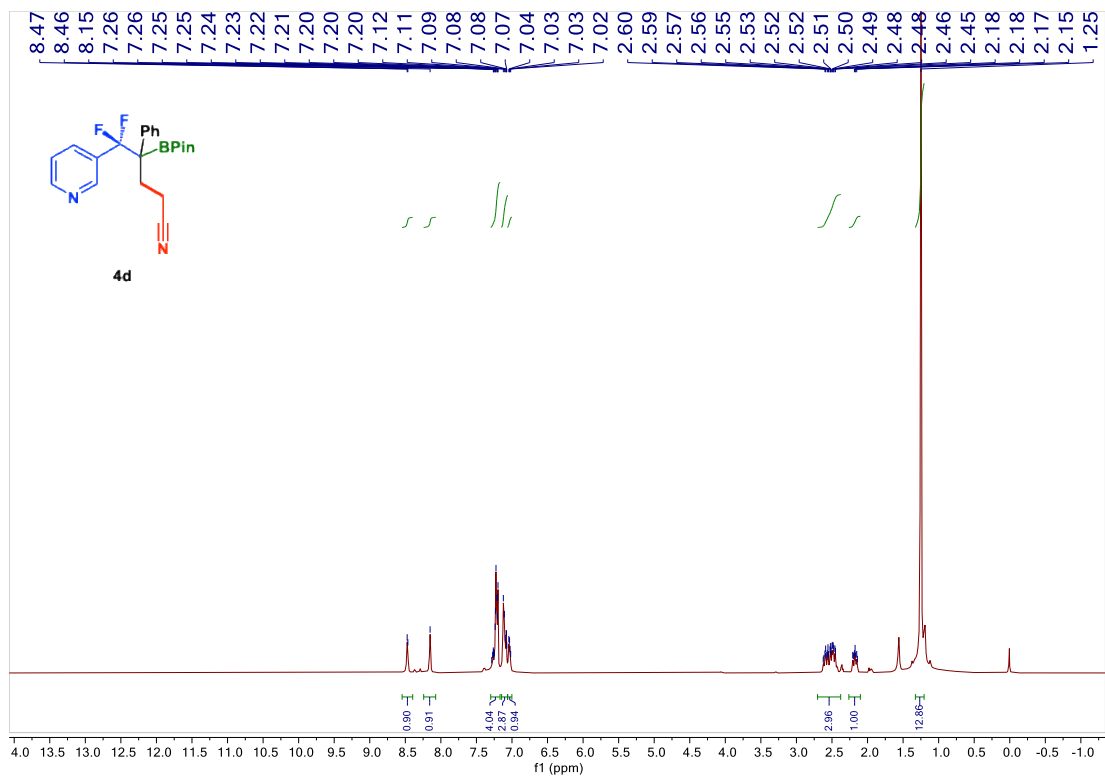


Fig. S85. ¹H NMR spectrum (CDCl₃, 25 °C) of 4d

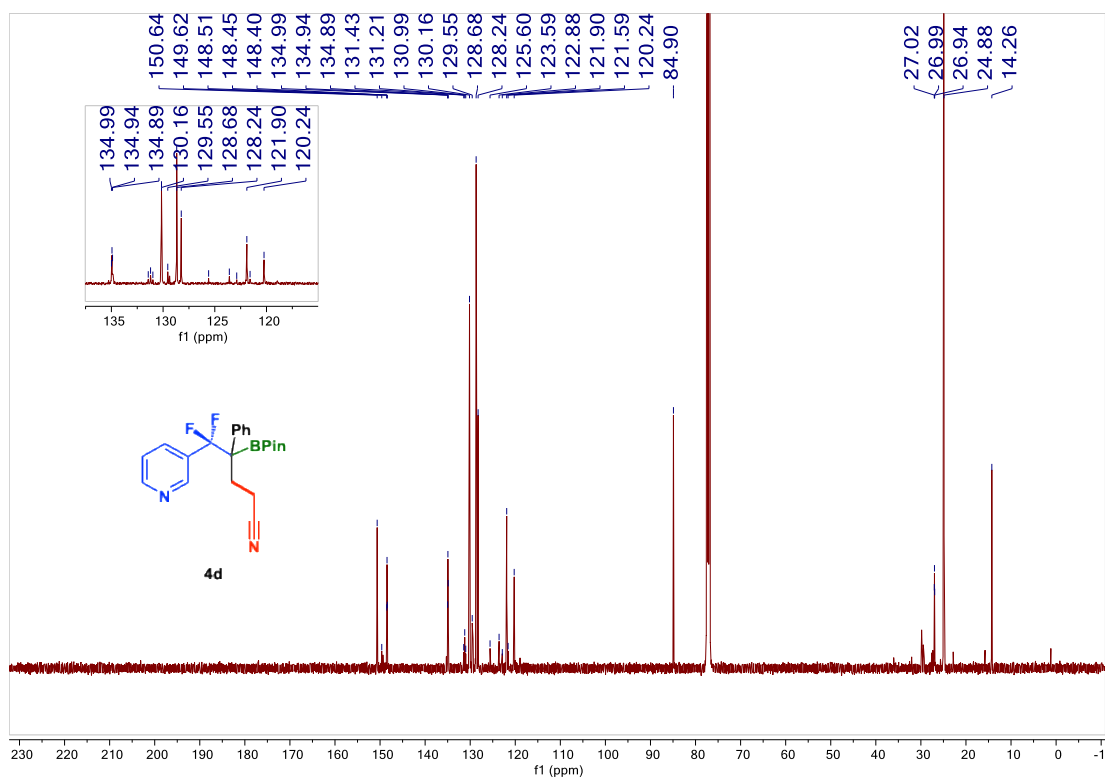


Fig. S86. ¹³C NMR spectrum (CDCl₃, 25 °C) of 4d

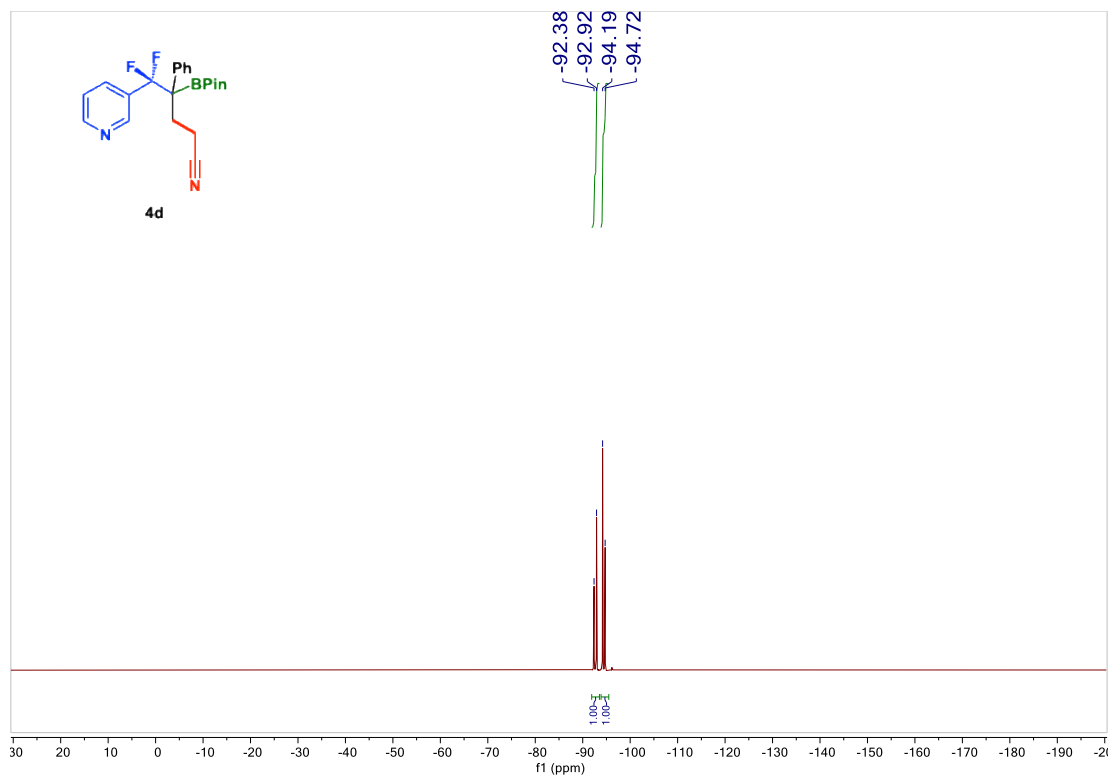


Fig. S87. ¹⁹F NMR spectrum (CDCl₃, 25 °C) of **4d**

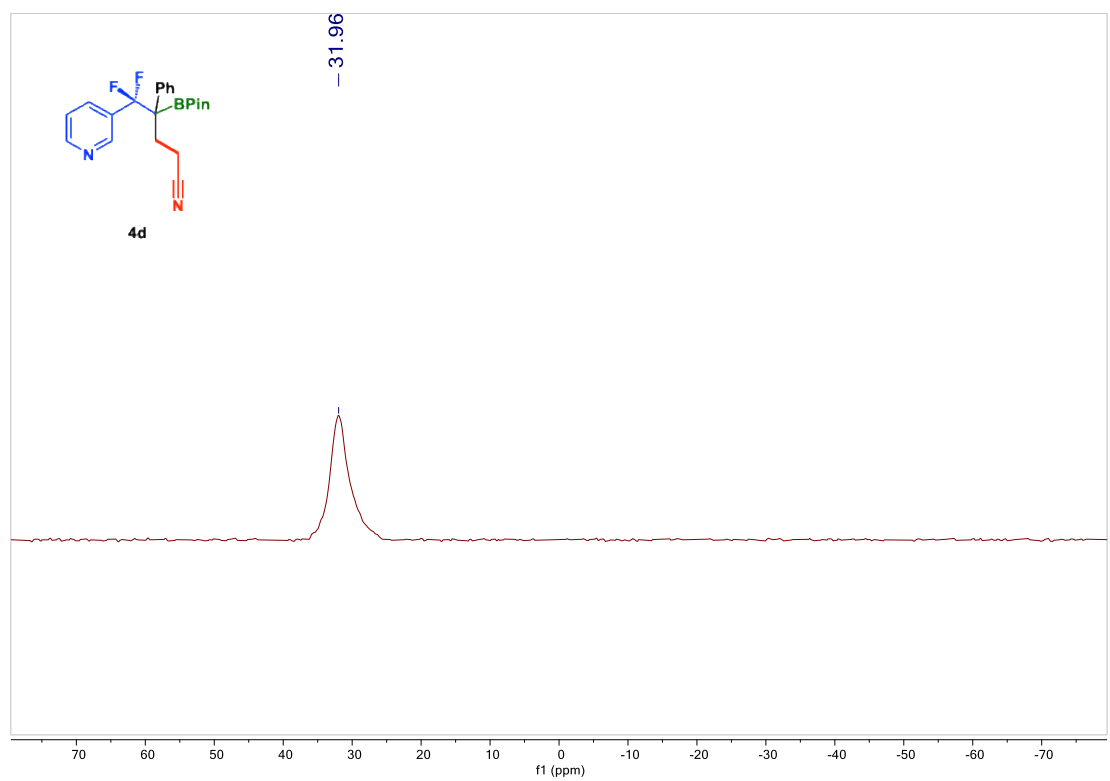


Fig. S88. ¹¹B NMR spectrum (CDCl₃, 25 °C) of **4d**

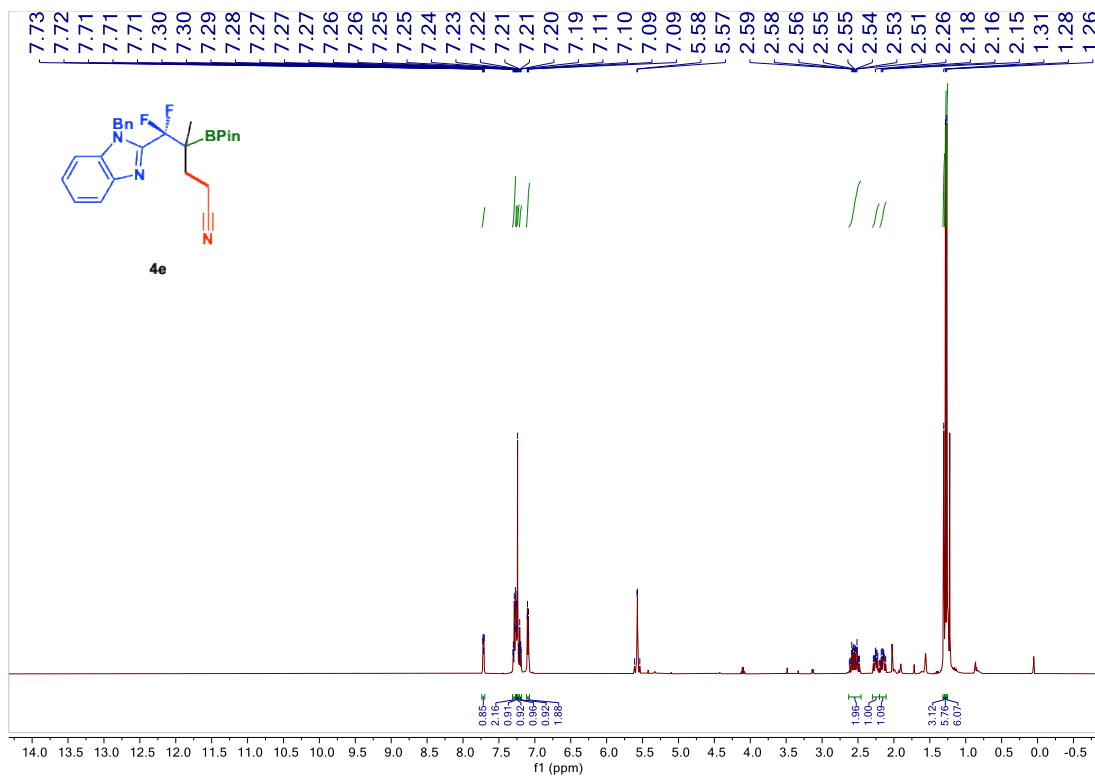


Fig. S89. ¹H NMR spectrum (CDCl₃, 25 °C) of 4e

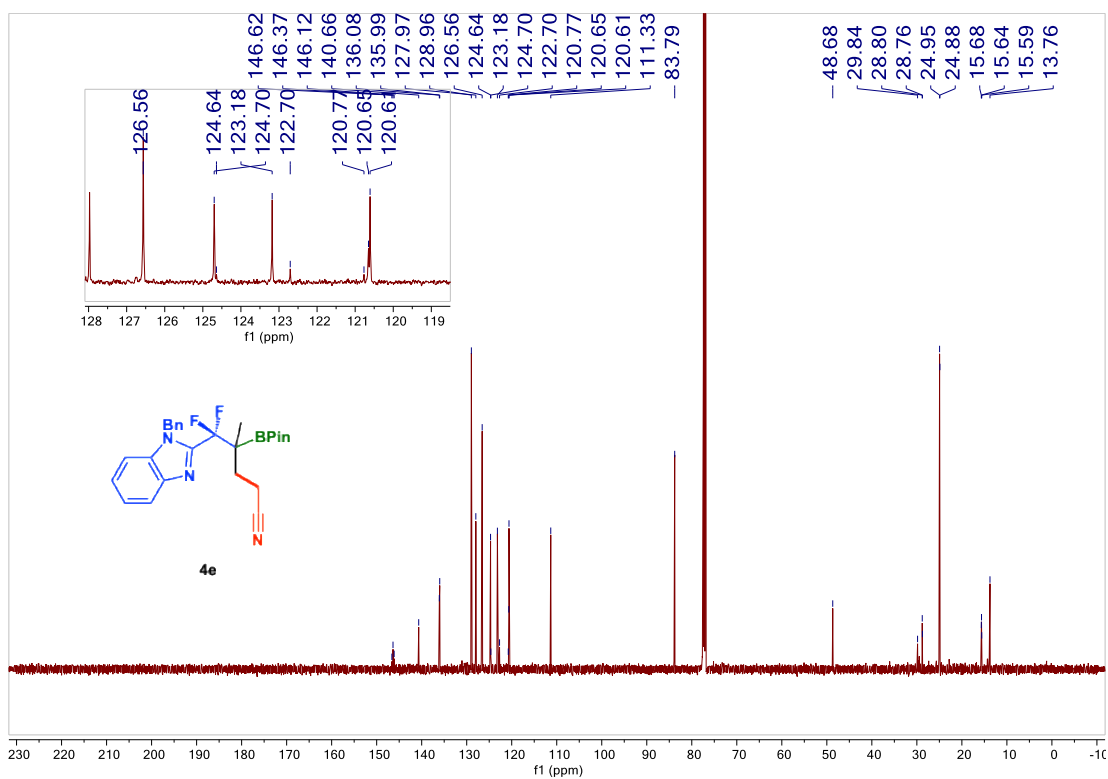


Fig. S90. ¹³C NMR spectrum (CDCl₃, 25 °C) of 4e

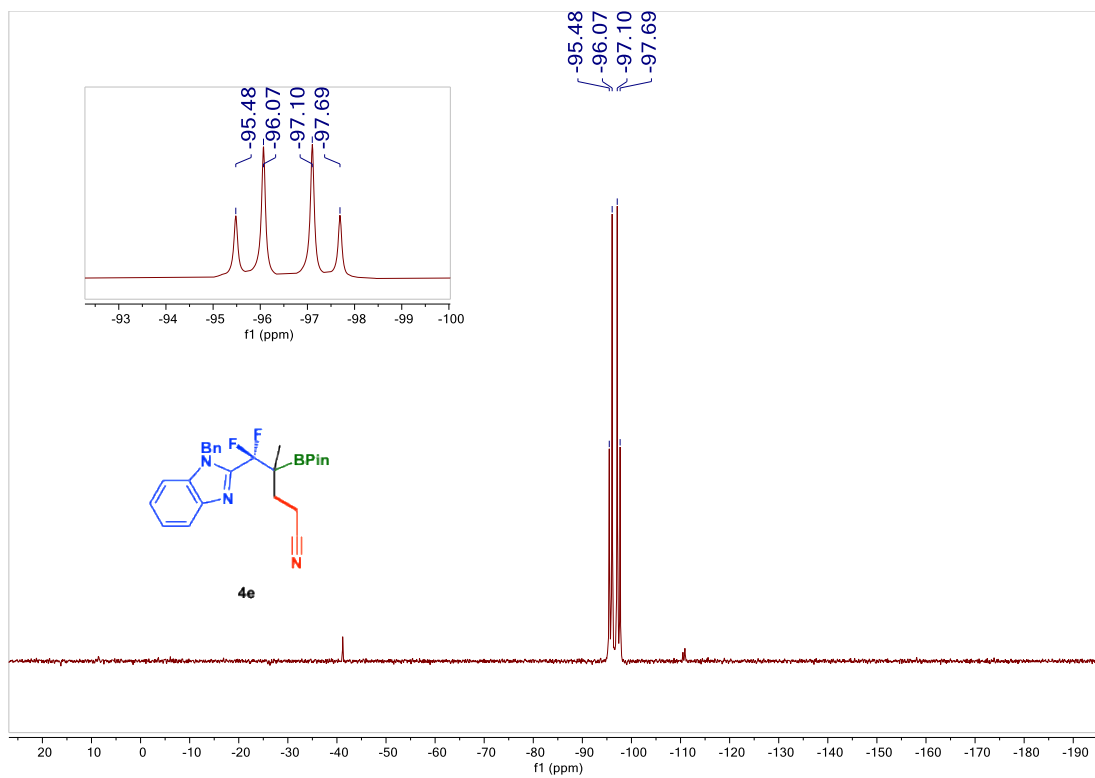


Fig. S91. ^{19}F NMR spectrum (CDCl₃, 25 °C) of **4e**

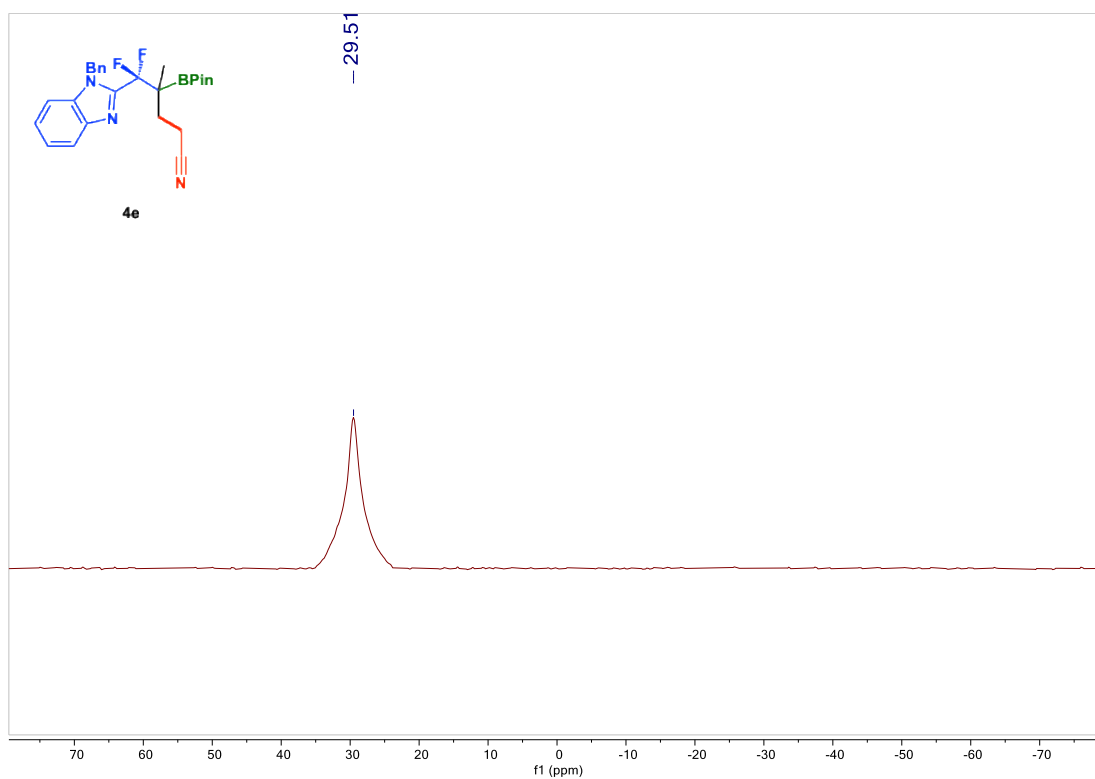


Fig. S92. ^{11}B NMR spectrum (CDCl₃, 25 °C) of **4e**

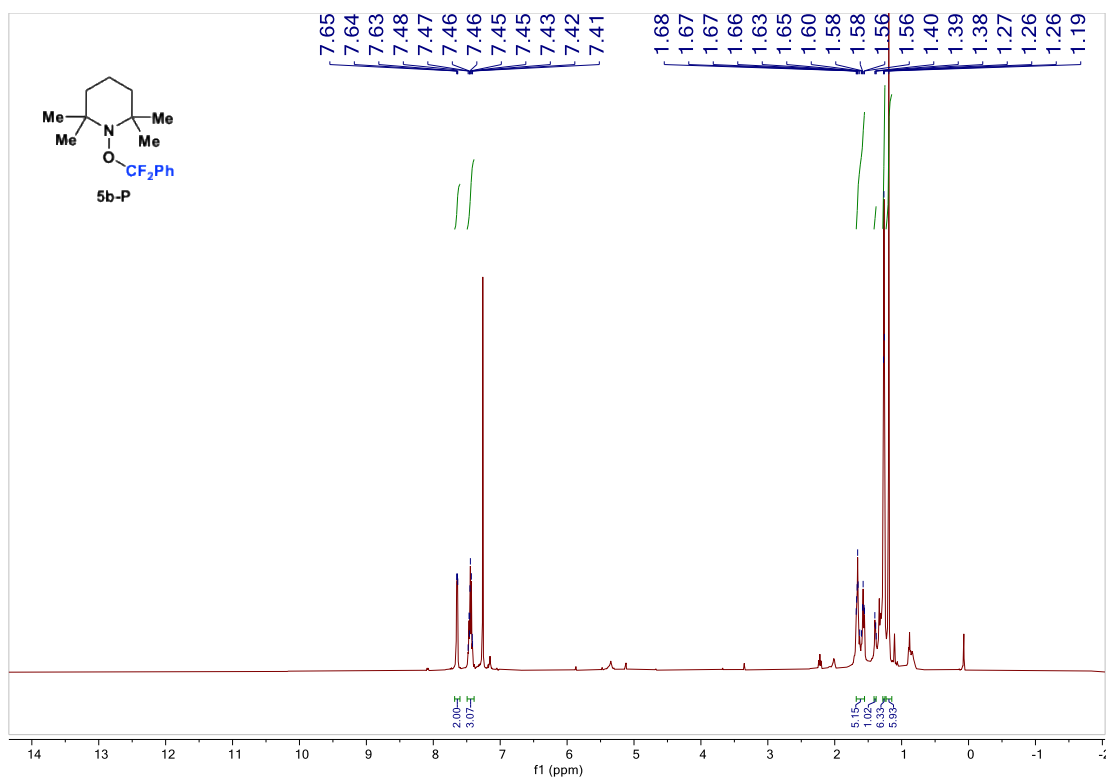


Fig. S93. ¹H NMR spectrum (CDCl₃, 25 °C) of 5b-P.

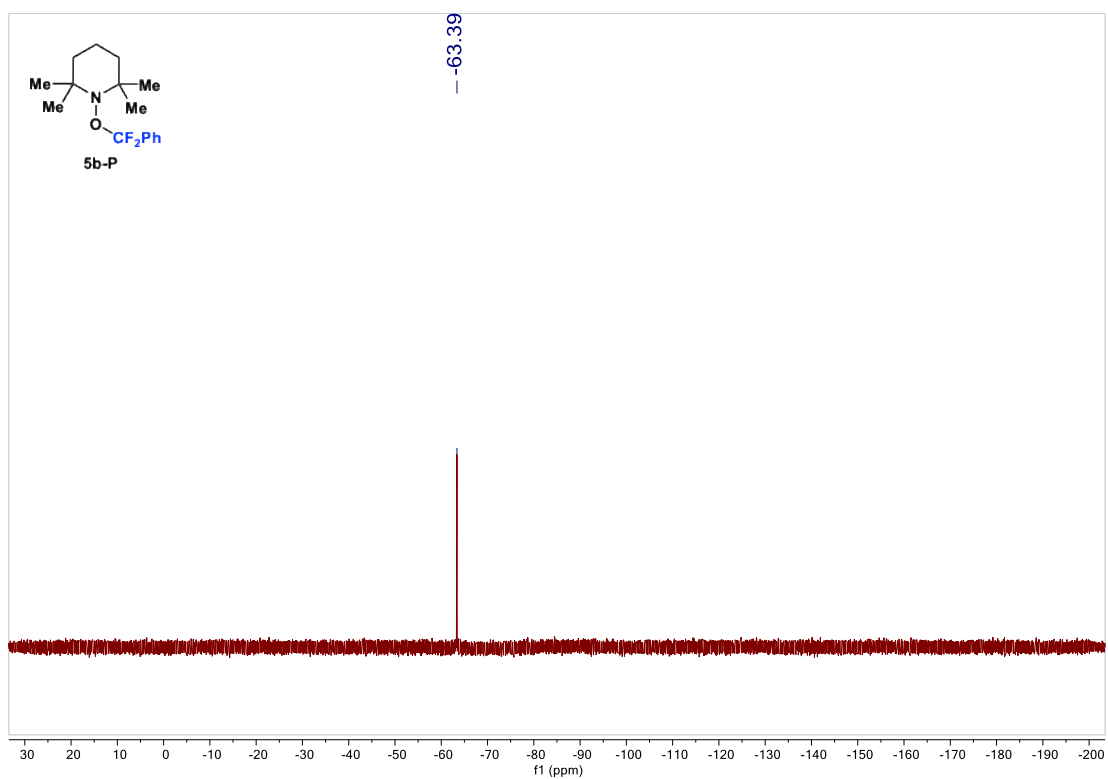


Fig. S94. ¹⁹F NMR spectrum (CDCl₃, 25 °C) of 5b-P.

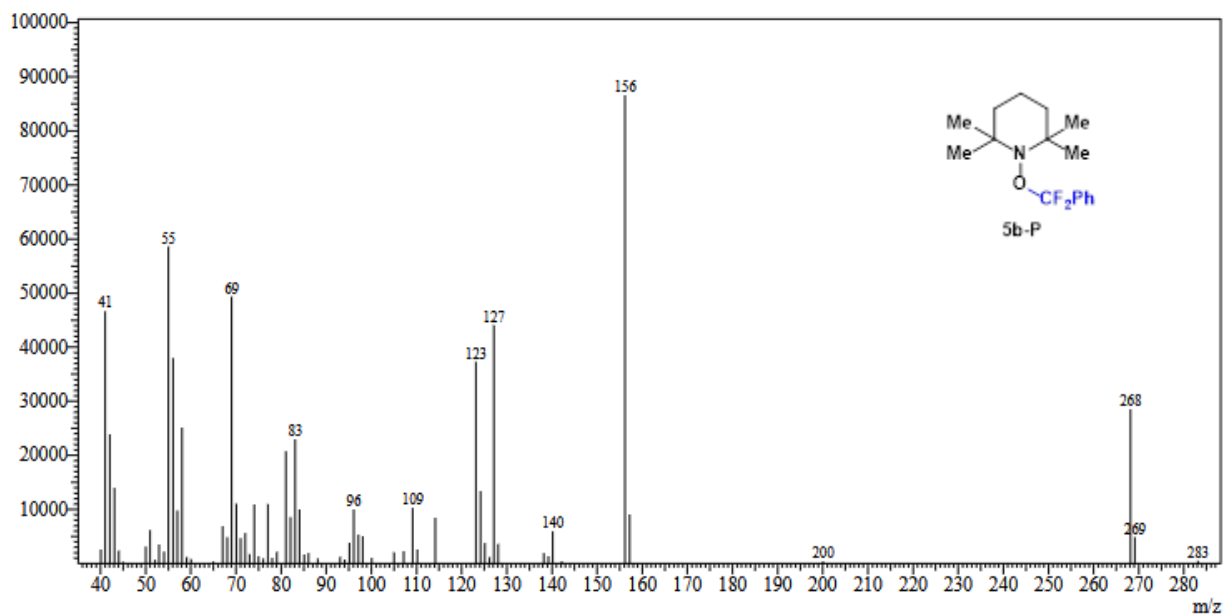


Fig. S95. GC-MS spectrum of 5b-P.

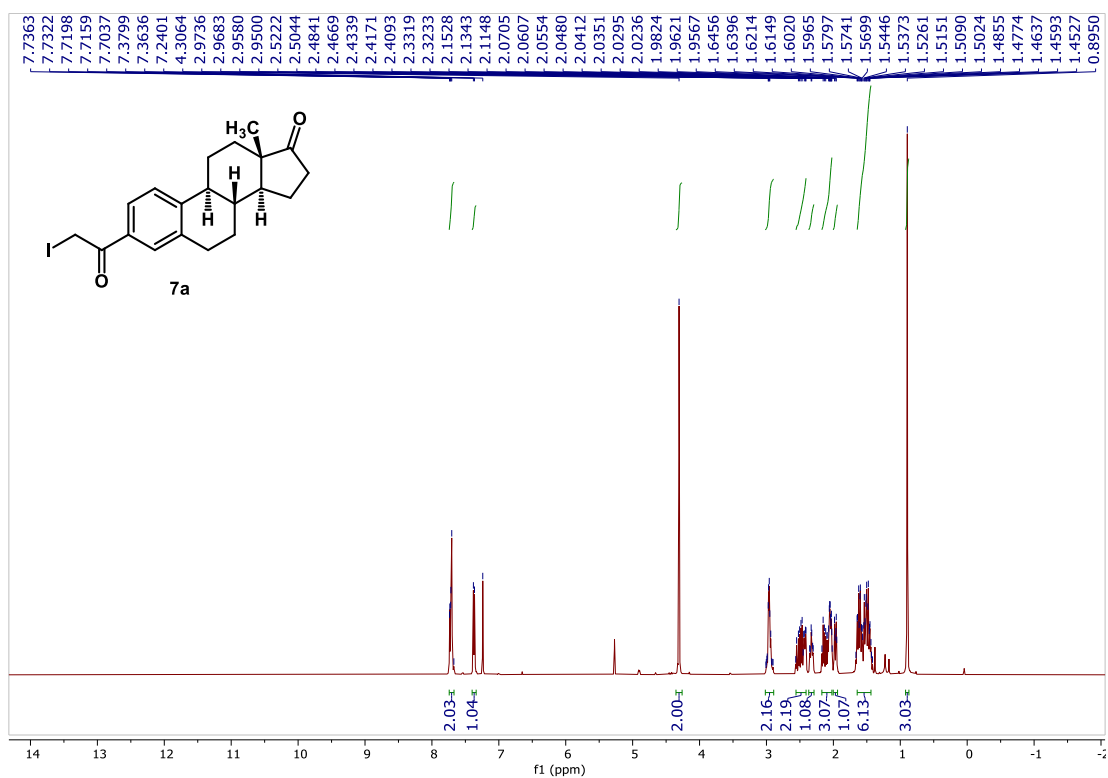


Fig. S96. ¹H NMR spectrum (CDCl₃, 25 °C) of 7a.

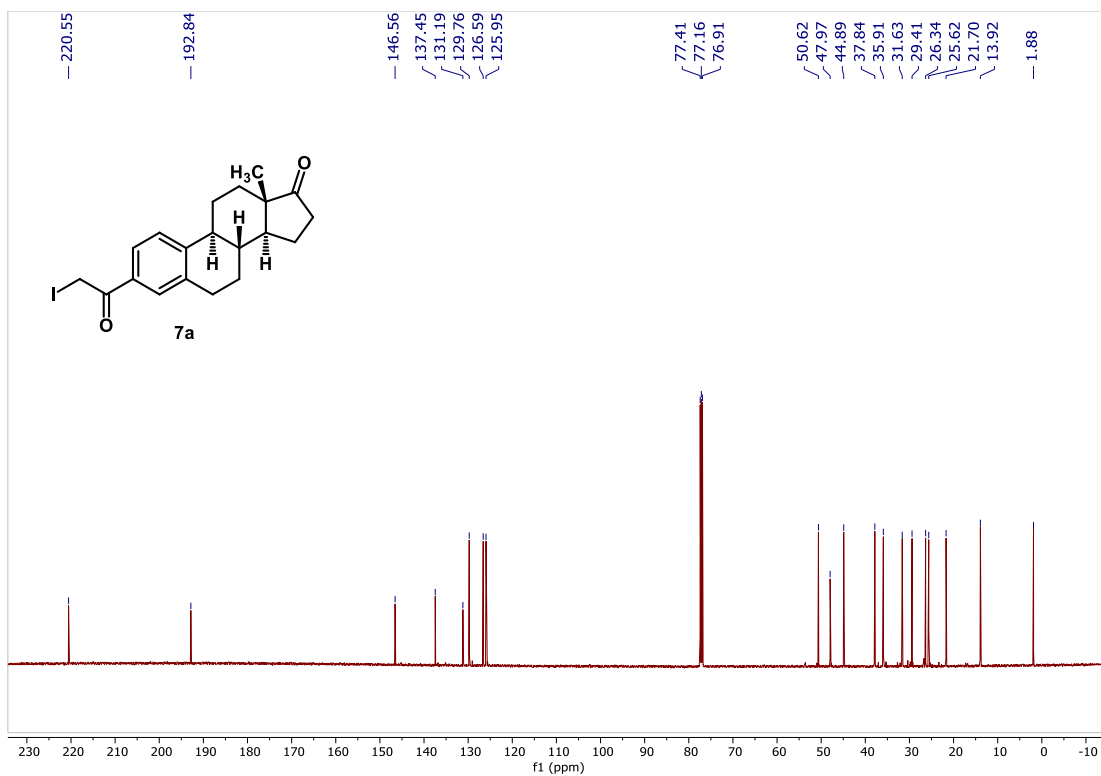


Fig. S97. ^{13}C NMR spectrum (CDCl_3 , 25 $^\circ\text{C}$) of **7a**.

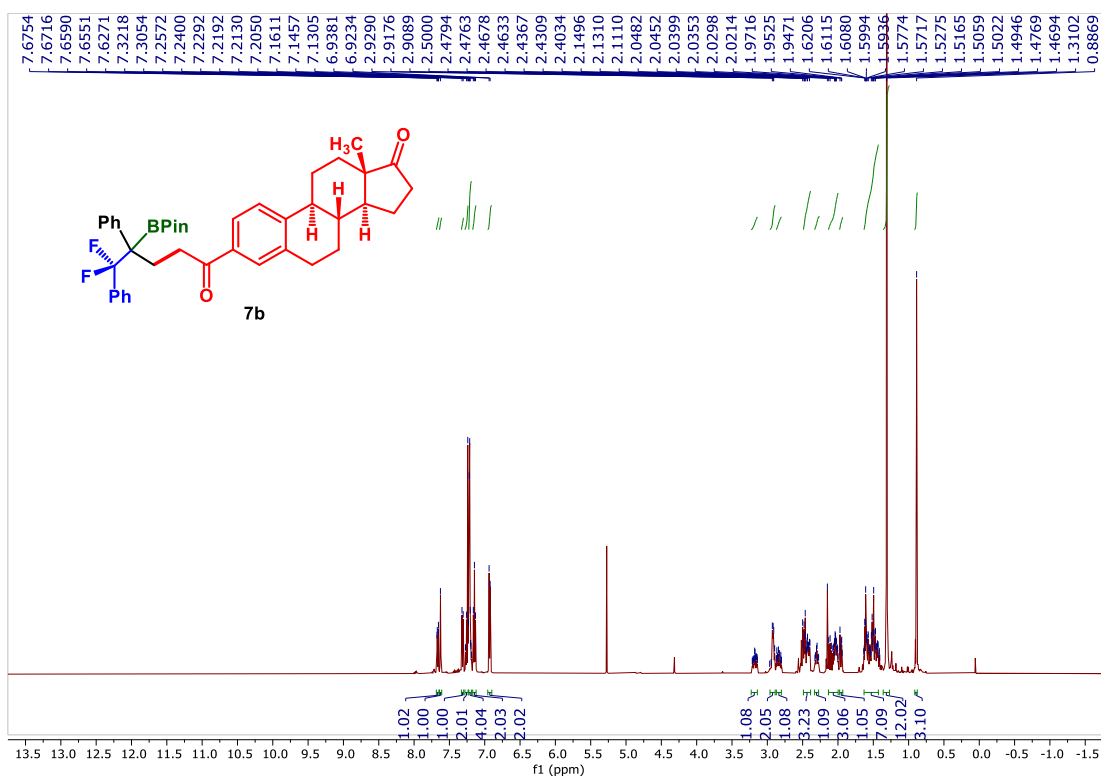


Fig. S98. ^1H NMR spectrum (CDCl_3 , 25 $^\circ\text{C}$) of **7b**.

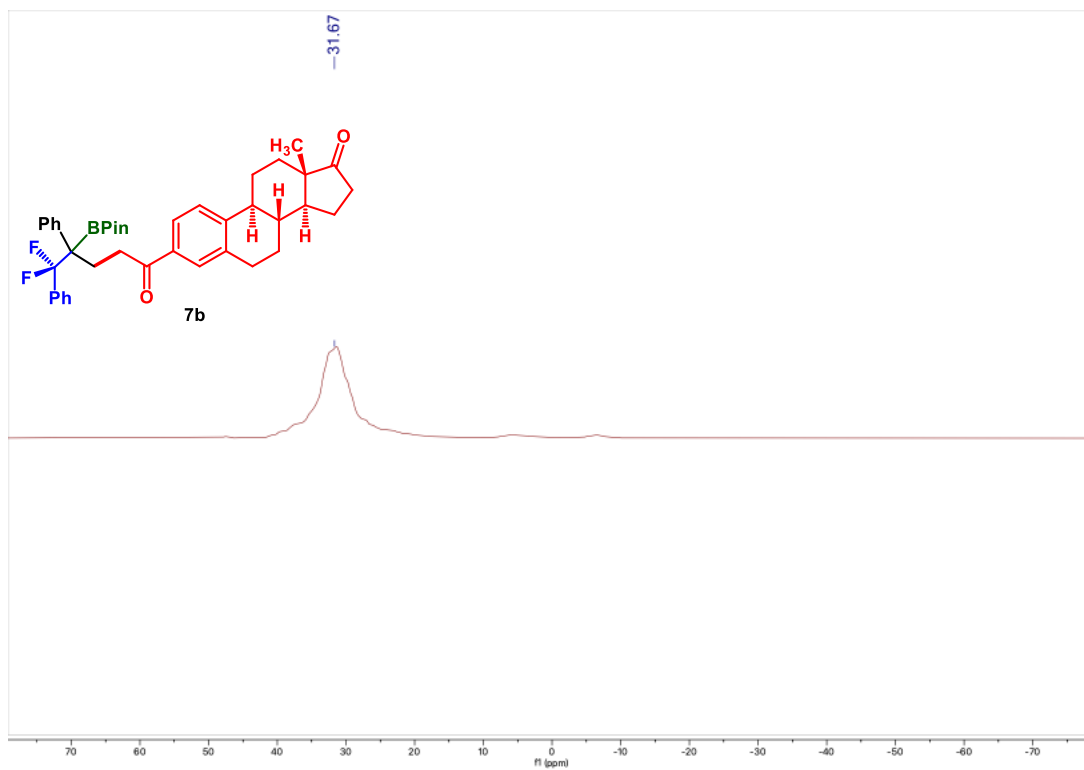


Fig. S101. ^{11}B NMR spectrum (CDCl_3 , 25 °C) of **7b**.

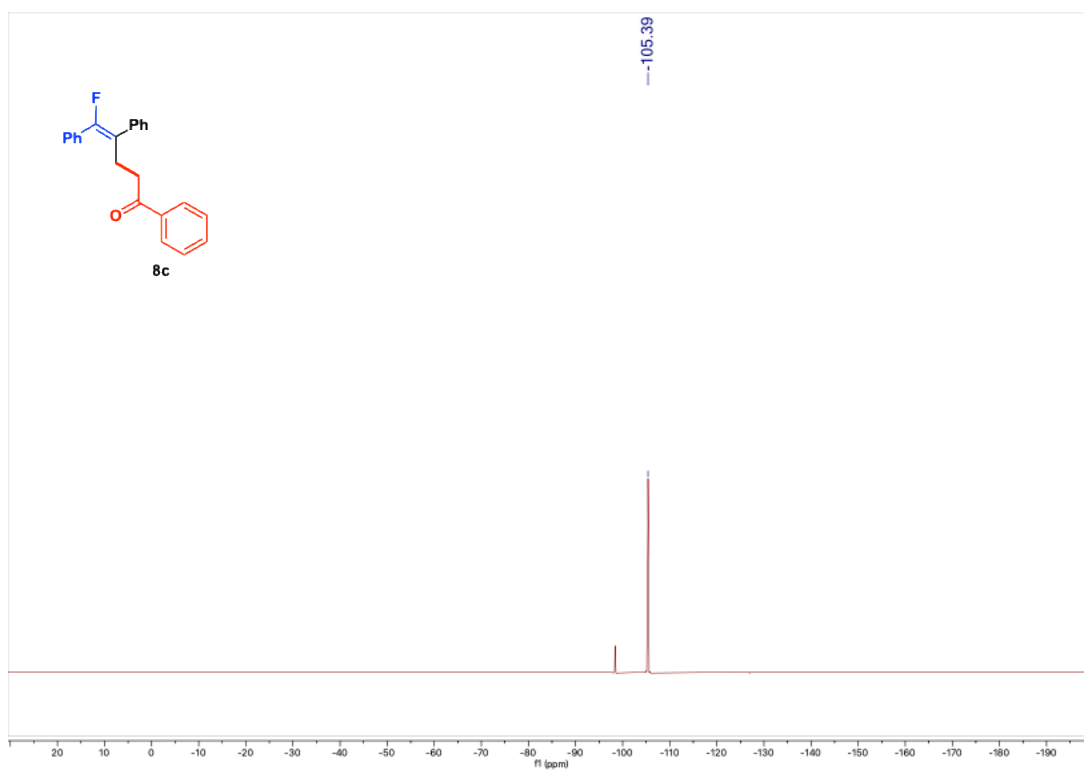


Fig. S102. ^{19}F NMR spectrum (CD_3OD , 25 °C) of **8c**.

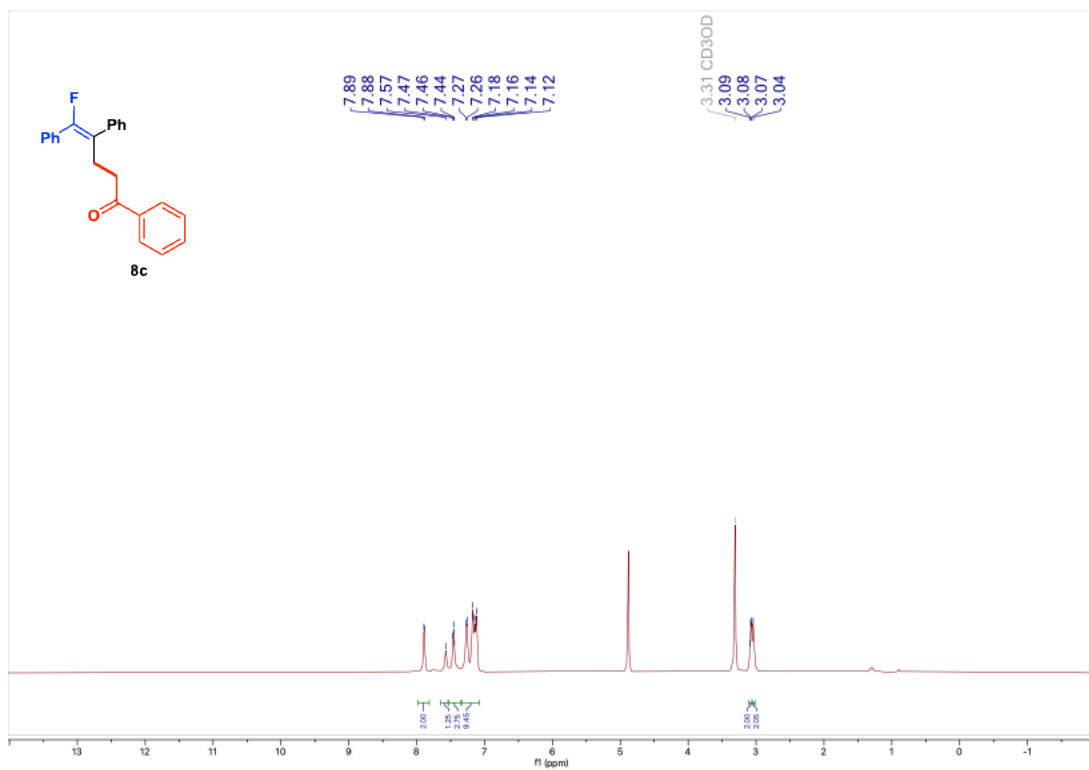


Fig. S103. ¹H NMR spectrum (CD₃OD, 25 °C) of **8c**.

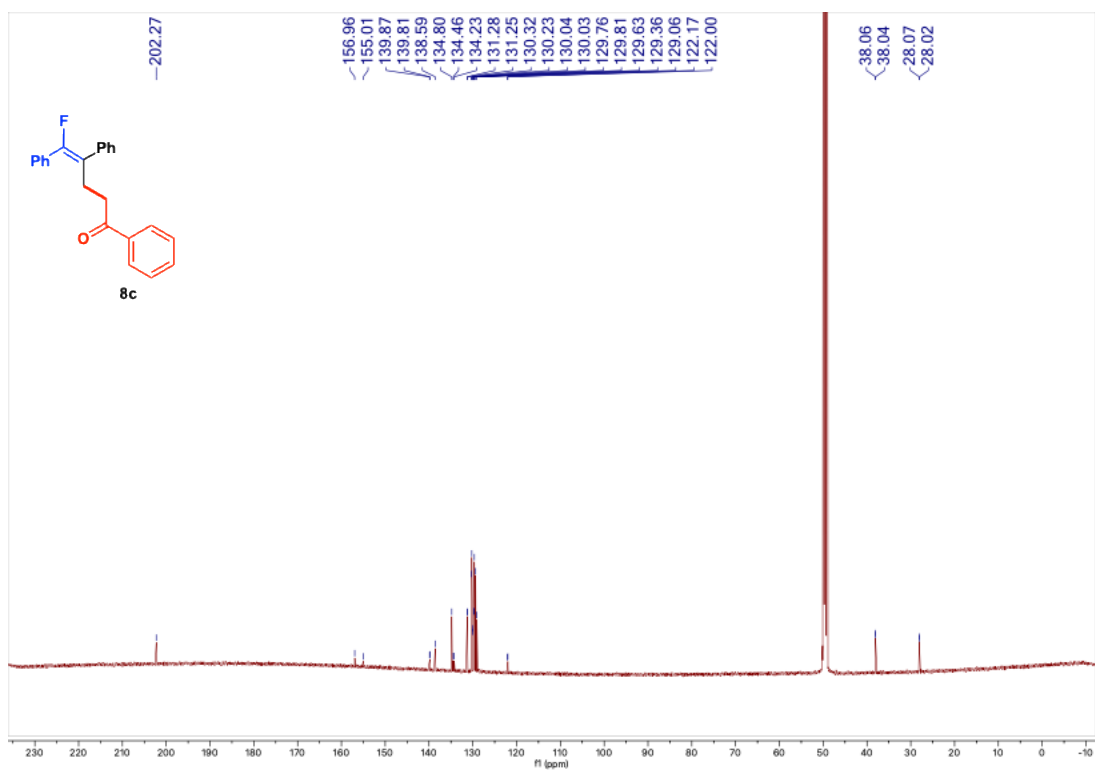


Fig. S104. ¹³C NMR spectrum (CD₃OD, 25 °C) of **8c**.

O) References

- (1) Geri, J. B.; Wade Wolfe, M. M.; Szymczak, N. K. The Difluoromethyl Group as a Masked Nucleophile: A Lewis Acid/Base Approach. *J. Am. Chem. Soc.* **2018**, *140* (30), 9404-9408. DOI: 10.1021/jacs.8b06093.
- (2) Geri, J. B.; Aguilera, E. Y.; Szymczak, N. K. Difluoromethane as a precursor to difluoromethyl borates. *Chemical Communications* **2019**, *55* (35), 5119-5122, 10.1039/C9CC01565E. DOI: 10.1039/C9CC01565E.
- (3) Geri, J. B.; Wade Wolfe, M. M.; Szymczak, N. K. Borazine-CF₃- Adducts for Rapid, Room Temperature, and Broad Scope Trifluoromethylation. *Angewandte Chemie International Edition* **2018**, *57* (5), 1381-1385. DOI: <https://doi.org/10.1002/anie.201711316>.
- (4) Zhang, X.; Zhang, Y.; Li, X.; Li, B.; Xiao, S.; Tang, Y.; Xie, P.; Loh, T.-P. Fluoroalkylation of Activated Allylic Acetates through Radical-Radical Coupling: Organophotoredox/DABCO Catalytic System. *Organic Letters* **2023**, *25* (37), 6863-6868. DOI: 10.1021/acs.orglett.3c02456.
- (5) Jereb, M.; Stavber, S.; Zupan, M. Direct α -Iodination of Aryl Alkyl Ketones by Elemental Iodine Activated by 1-Chloromethyl-4-fluoro-1,4-diazoniabicyclo[2.2.2]octane Bis(tetrafluoroborate). *Synthesis* **2003**, *2003* (06), 0853-0858. DOI: 10.1055/s-2003-38689. Wang, T.; Stein, P. M.; Shi, H.; Hu, C.; Rudolph, M.; Hashmi, A. S. K. Hydroxylamine-mediated C-C amination via an aza-hock rearrangement. *Nature Communications* **2021**, *12* (1), 7029. DOI: 10.1038/s41467-021-27271-y. Leese, M. P.; Hejaz, H. A. M.; Mahon, M. F.; Newman, S. P.; Purohit, A.; Reed, M. J.; Potter, B. V. L. A-Ring-Substituted Estrogen-3-O-sulfamates: Potent Multitargeted Anticancer Agents. *Journal of Medicinal Chemistry* **2005**, *48* (16), 5243-5256. DOI: 10.1021/jm050066a.
- (6) Silvi, M.; Sandford, C.; Aggarwal, V. K. Merging Photoredox with 1,2-Metallate Rearrangements: The Photochemical Alkylation of Vinyl Boronate Complexes. *Journal of the American Chemical Society* **2017**, *139* (16), 5736-5739. DOI: 10.1021/jacs.7b02569.
- (7) M. J. Frisch, G. W. T., H. B. Schlegel, G. E. Scuseria, M. A. Robb, J. R. Cheeseman, G. Scalmani, V. Barone, G. A. Petersson, H. Nakatsuji, X. Li, M. Caricato, A. V. Marenich, J. Bloino, B. G. Janesko, R. Gomperts, B. Mennucci, H. P. Hratchian, J. V. Ortiz, A. F. Izmaylov, J. L. Sonnenberg, D. Williams-Young, F. Ding, F. Lipparini, F. Egidi, J. Goings, B. Peng, A. Petrone, T. Henderson, D. Ranasinghe, V. G. Zakrzewski, J. Gao, N. Rega, G. Zheng, W. Liang, M. Hada, M. Ehara, K. Toyota, R. Fukuda, J. Hasegawa, M. Ishida, T. Nakajima, Y. Honda, O. Kitao, H. Nakai, T. Vreven, K. Throssell, J. A. Montgomery, Jr., J. E. Peralta, F. Ogliaro, M. J. Bearpark, J. J. Heyd, E. N. Brothers, K. N. Kudin, V. N. Staroverov, T. A. Keith, R. Kobayashi, J. Normand, K. Raghavachari, A. P. Rendell, J. C. Burant, S. S. Iyengar, J. Tomasi, M. Cossi, J. M. Millam, M. Klene, C. Adamo, R. Cammi, J. W. Ochterski, R. L. Martin, K. Morokuma, O. Farkas, J. B. Foresman, and D. J. Fox. Gaussian 16, Revision C.01. Gaussian, Inc.: Wallingford CT, 2016.
- (8) Zhao, Y.; Truhlar, D. G. The M06 suite of density functionals for main group thermochemistry, thermochemical kinetics, noncovalent interactions, excited states, and transition elements: two new functionals and systematic testing of four M06-class functionals and 12 other functionals. *Theoretical Chemistry Accounts* **2008**, *120* (1), 215-241. DOI: 10.1007/s00214-007-0310-x.
- (9) Grimme, S.; Antony, J.; Ehrlich, S.; Krieg, H. A consistent and accurate ab initio parametrization of density functional dispersion correction (DFT-D) for the 94 elements H-Pu. *The Journal of Chemical Physics* **2010**, *132* (15), 154104. DOI: 10.1063/1.3382344 (accessed 3/4/2024).
- (10) Marenich, A. V.; Cramer, C. J.; Truhlar, D. G. Universal Solvation Model Based on Solute Electron Density and on a Continuum Model of the Solvent Defined by the Bulk Dielectric Constant and Atomic Surface Tensions. *The Journal of Physical Chemistry B* **2009**, *113* (18), 6378-6396. DOI: 10.1021/jp810292n.
- (11) de la Cruz, C.; Molina, A.; Patil, N.; Ventosa, E.; Marcilla, R.; Mavrandonakis, A. New insights into phenazine-based organic redox flow batteries by using high-throughput DFT modelling. *Sustainable Energy & Fuels* **2020**, *4* (11), 5513-5521, 10.1039/D0SE00687D. DOI: 10.1039/D0SE00687D.

- (12) Hay, P. J.; Wadt, W. R. Ab initio effective core potentials for molecular calculations. Potentials for K to Au including the outermost core orbitals. *The Journal of Chemical Physics* **1985**, *82* (1), 299-310. DOI: 10.1063/1.448975 (accessed 4/22/2024).
- (13) Krishnan, R.; Binkley, J. S.; Seeger, R.; Pople, J. A. Self-consistent molecular orbital methods. XX. A basis set for correlated wave functions. *The Journal of Chemical Physics* **1980**, *72* (1), 650-654. DOI: 10.1063/1.438955 (accessed 3/4/2024). Clark, T.; Chandrasekhar, J.; Spitznagel, G. W.; Schleyer, P. V. R. Efficient diffuse function-augmented basis sets for anion calculations. III. The 3-21+G basis set for first-row elements, Li–F. *Journal of Computational Chemistry* **1983**, *4* (3), 294-301. DOI: <https://doi.org/10.1002/jcc.540040303>.
- (14) Fukui, K. The path of chemical reactions - the IRC approach. *Accounts of Chemical Research* **1981**, *14* (12), 363-368. DOI: 10.1021/ar00072a001. Hratchian, H. P.; Schlegel, H. B. In *Theory and Applications of Computational Chemistry: The First 40 Years*, Dykstra, C. E., Frenking, G., Kim, K. S., Scuseria, G. Eds.; Elsevier, 2005; pp 195-249.
- (15) M. Montalti, A. C., L. Prodi, T. Gandolfi. Chemical Actinometry. In *Handbook of Photochemistry*, 3rd ed.; CRC Press, 2006. Silvi, M.; Schrof, R.; Noble, A.; Aggarwal, V. K. Enantiospecific Three-Component Alkylation of Furan and Indole. *Chemistry – A European Journal* **2018**, *24* (17), 4279-4282. DOI: <https://doi.org/10.1002/chem.201800527> (accessed 2024/12/18).
- (16) Hatchard, C. G.; Parker, C. A.; Bowen, E. J. A new sensitive chemical actinometer - II. Potassium ferrioxalate as a standard chemical actinometer. *Proceedings of the Royal Society of London. Series A. Mathematical and Physical Sciences* **1997**, *235* (1203), 518-536. DOI: 10.1098/rspa.1956.0102 (accessed 2024/12/18).
- (17) Cismesia, M. A.; Yoon, T. P. Characterizing chain processes in visible light photoredox catalysis. *Chemical Science* **2015**, *6* (10), 5426-5434, 10.1039/C5SC02185E. DOI: 10.1039/C5SC02185E.